

# Gelfand-Levitan-Marchenko and model order reduction methods in inverse scattering

Andreas Tataris

Copyright ©2023 by Andreas Tataris

ISBN: 978-90-393-7604-1

DOI: [HTTPS://DOI.ORG/10.33540/2026](https://doi.org/10.33540/2026)

# **Gelfand-Levitan-Marchenko and model order reduction methods in inverse scattering**

## **Gelfand-Levitan-Marchenko en modelorderreductie methoden in inverse scattering**

(met een samenvatting in het Nederlands)

### **Proefschrift**

ter verkrijging van de graad van doctor aan de  
Universiteit Utrecht  
op gezag van de  
rector magnificus, prof.dr. H.R.B.M. Kummeling,  
ingevolge het besluit van het college voor promoties  
in het openbaar te verdedigen op

vrijdag 15 december 2023 des ochtends te 10:15 uur

door

**Andreas Tataris**

geboren op 16 december 1994  
te Athene, Griekenland

**Promotoren:**

Prof. dr. T. van Leeuwen

Prof. dr. S.M. Verduyn Lunel

**Copromotor:**

Dr. I. Pires de Vasconcelos

**Beoordelingscommissie:**

Prof. dr. C. Brune

Prof. dr. H.T. Koelink

Dr. ir. R.F. Remis

Prof. dr. J.A. Trampert

Prof. dr. K.P. Veroy Grepl

# Contents

<b>1</b>	<b>Introduction</b>	<b>5</b>
1.1	Direct Methods . . . . .	8
1.2	Indirect Methods . . . . .	9
1.3	Outline of the Thesis . . . . .	10
<b>2</b>	<b>A Regularised Total Least Squares Approach for 1D Inverse Scattering</b>	<b>13</b>
2.1	Introduction . . . . .	14
2.2	Preliminaries . . . . .	15
2.2.1	Formulation of the Forward Problem . . . . .	16
2.2.2	Classical Results from Scattering Theory . . . . .	17
2.2.3	The Inverse Scattering Problem and the Gelfand–Levitan–Marchenko Inversion Method . . . . .	18
2.3	Main Results . . . . .	20
2.3.1	Stability Estimates . . . . .	20
2.3.2	Variational Regularisation . . . . .	22
2.4	Numerical Results . . . . .	28
2.4.1	Numerical Implementation . . . . .	28
2.5	Numerical Examples . . . . .	31
2.5.1	Example 1: The Plasma Wave-Equation with a Smooth Potential . . . . .	32
2.5.2	Example 2: Data from the Wave Equation . . . . .	34
2.6	Discussion and Conclusions . . . . .	36
<b>3</b>	<b>A Distributional Gelfand-Levitan-Marchenko Equation For The Helmholtz Scat- tering Problem On The Line</b>	<b>39</b>
3.1	Introduction . . . . .	40
3.2	Preliminaries . . . . .	41
3.2.1	Forward Scattering Problem . . . . .	42
3.2.2	Basic Properties of the Solutions of the Forward Problem . . . . .	43

3.3	Main Result . . . . .	45
3.3.1	Generalised Povzner-Levitán Representation . . . . .	46
3.3.2	Properties of the GLM Kernel and of the Scattering Data . . . . .	50
3.3.3	Proof of Theorem 3.3.1 . . . . .	53
3.4	Inversion . . . . .	55
3.5	Discussion and Conclusions . . . . .	57
3.6	Appendix: Calculations with Distributions and Schwartz Functions . . . . .	57
<b>4</b>	<b>A Data-Driven Approach to Solving a 1D Inverse Scattering Problem</b>	<b>59</b>
4.1	Introduction . . . . .	60
4.1.1	Approach . . . . .	60
4.1.2	Contributions and Outline . . . . .	61
4.2	The Forward Problem . . . . .	61
4.2.1	A Reduced-Order Model . . . . .	61
4.3	The Inverse Problem . . . . .	63
4.3.1	Estimating the State . . . . .	63
4.3.2	Estimating the Scattering Potential . . . . .	64
4.4	Numerical Results . . . . .	65
4.4.1	Experimental Settings . . . . .	66
4.4.2	Benchmark Results . . . . .	66
4.4.3	Noiseless Data . . . . .	67
4.4.4	Noisy Data . . . . .	69
4.5	Discussion and Conclusions . . . . .	72
4.6	Appendix: Proofs and Regularization Parameter Selection . . . . .	74
4.6.1	Proofs . . . . .	74
4.6.2	Regularization Parameter Selection . . . . .	75
<b>5</b>	<b>Reduced Order Model Based Nonlinear Waveform Inversion for the 1D Helmholtz Equation</b>	<b>77</b>
5.1	Introduction . . . . .	78
5.2	Preliminaries . . . . .	79
5.3	Main Results . . . . .	81
5.3.1	ROM Matrices Construction Using Two-Sided Data . . . . .	81
5.3.2	Solving the Inverse Problem with Nonlinear Optimization . . . . .	83
5.4	Numerical Results . . . . .	87
5.4.1	Numerical Implementation: Discrete Optimality Condition . . . . .	88
5.4.2	Comparison with Conventional FWI: Convexity . . . . .	89

5.4.3	Comparison with conventional FWI: reconstruction of a smooth coefficient . . . . .	89
5.5	Discussion and Conclusions . . . . .	94
5.6	Appendix: Proofs . . . . .	95
5.6.1	Proof of Proposition 5.2.1 . . . . .	95
5.6.2	Proof of Lemma 5.3.1 . . . . .	96
5.6.3	Proof of Lemma 5.3.2 . . . . .	100
<b>6</b>	<b>Outlook and Conclusions</b>	<b>103</b>
6.1	Future Work on the Gelfand-Levitan-Marchenko Inversion . . . . .	104
6.2	Future Work on Reduced Order Model Inversion . . . . .	105
<b>7</b>	<b>Summary</b>	<b>107</b>
<b>8</b>	<b>Samenvatting</b>	<b>109</b>
<b>9</b>	<b>Acknowledgements</b>	<b>111</b>
<b>10</b>	<b>Curriculum Vitae</b>	<b>113</b>
	<b>Bibliography</b>	<b>114</b>





# Chapter 1

## Introduction

The study of inverse problems is an active area of research in applied mathematics that has attracted the attention of researchers both from mathematical and numerical analysis. The understanding of the theory of inverse problems and the development of tools aimed to study inverse boundary value problems have led to great advances in numerous areas of science, see [19, 5, 37] and the references therein. In seismology and subsurface imaging applications, changes in density and sound-speed of the earth are detected by solving highly ill-posed and nonlinear inverse problems based on reflection measurements, see figure 1.1. In medical applications such as ultrasound imaging, it is common to formulate an inverse problem of reconstructing the boundary of a scatterer or the change in material properties using reflections of known incident fields, see figure 1.2. Also, similar inverse problems can be found in astrophysics, and in particular in imaging of celestial and cosmic objects, see figure 1.3. Better understanding of the theory of inverse problems, can result in greater progress to other areas of science such as the aforementioned for example.

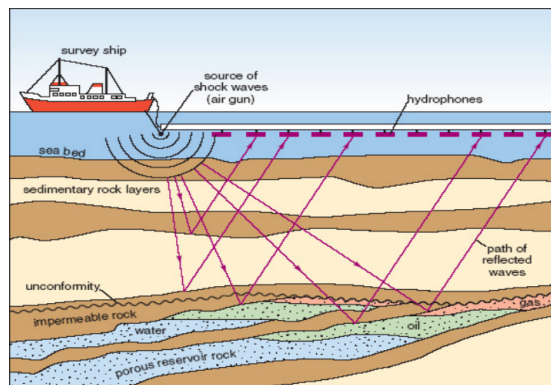


Figure 1.1: A simplified visual representation of a seismic survey



Figure 1.2: An ultrasound machine used to image internal organs. Nowadays, ultrasound machines keep getting a lot more portable.



Figure 1.3: Radio telescopes are used in collecting radio waves coming from outer space. Distant radio galaxies and quasars have been discovered using radio telescopes.

The writing of this thesis is motivated by the many applications of inverse problems in

science and the beauty of the related mathematics. Before elaborating more on the motivation, it is useful to explain two important terms/concepts of this thesis.

**Scattering.** Within this text, scattering refers to the interaction of an incoming wave with a scatterer (in acoustic scattering: change in sound-speed and/or density, in Schrödinger scattering: potential). Mathematically speaking, the Schrödinger equation is described as follows.

$$(-\Delta + q - k^2)u = f, \text{ on } D \subset \mathbb{R}^n, n = 1, 2, 3, \quad (1.1)$$

where  $\Delta$  being the Laplace operator,  $k \in \mathbb{C}$  is a wavenumber,  $q \in L^\infty(D)$  is a scattering potential and  $u$  is the solution. When  $D$  is unbounded, we use the Sommerfeld radiation condition. In case where  $D$  is bounded, we use an approximation of the radiation condition, often called impedance (Robin-type) boundary condition. The source term is denoted by  $f$  and it is responsible for causing an incident field inside the volume of the domain  $D$ . This incident field interacts with  $q$  by causing a scattered field. In cases where we study the full scattering problem ( $D = \mathbb{R}^n$ ) we can even assume that an incident plane wave or a spherical wave causes scattering. In this case, we even have an explicit formula for the incident field,  $u^i$ , and we have that  $u = u^i + u^s$  ( $u^s$  denotes scatterer field). Similarly, the Helmholtz equation is formulated as

$$(-\Delta - k^2 m)u = f, \text{ on } D \subset \mathbb{R}^n, \quad (1.2)$$

where the coefficient  $m \in L^\infty(D)$  describes the change in soundspeed. In both cases (Schrödinger and Helmholtz),  $u$  depends on  $k$ , and we usually write  $u = u(k)$ .

**Inverse scattering.** Within the boundaries of this thesis, inverse scattering refers to the reconstruction of an acoustic scatterer or a potential using measurements of scattered waves. Mathematically, we can formulate an inverse scattering problem of such kind as:

$$\begin{aligned} \text{given a set of frequencies } \Lambda = \{k_i\}_{i \in I} \text{ and measurements } \{u(k_i)|_{D_0}\}_{i \in I}, \text{ with } D_0 \subset D, \\ \text{estimate } q \text{ (or } m). \end{aligned} \quad (1.3)$$

The issues coming with inverse scattering problems of this type make on one hand inversion challenging, on the other hand they require special treatment that involves beautiful mathematical concepts. A major source of various issues when it comes to inversion, is the nonlinearity of the so-called coefficient to solution map. This makes the inversion process complicated because the nonlinear relations between coefficients of PDEs to their solutions, also transfer to the associated inverse scattering problems. Essentially, this means that the inverse problem is nonlinear. Another remarkable issue is the so-called ill-posedness of the inverse problem. This means that two different coefficients of a PDE can produce (nearly) the same measurements in the sense of the definition 1.3. Considering the nonlinearity and ill-posedness issues that come in pair with inverse problems, mathematicians have come up with several ways of solving them. In principle, there have been two main categories of methods for solving inverse scattering problems of

this kind. In general, we separate them in *direct* and *indirect* methods. A method is referred as *indirect*, when it is based on an implicit non-linear relation between data and coefficients that need to be solved iteratively. On the other hand, the inverse scattering problem can be solved using a *direct* method. Following a direct method, an explicit formula leads to the exact solution of the inverse problem. In the following two paragraphs, we elaborate on direct and indirect methods.

## 1.1 Direct Methods

Recently, in the context of seismic imaging, direct inversion methods based on inverse scattering theory have received attention. One of the most characteristic example of a direct method used in imaging is the so-called Marchenko integral equation method. The idea behind the Marchenko imaging method is closely related to the Gelfand-Levitan-Marchenko integral equation that can be found in the classical Schrödinger scattering theory. Both the classical GLM method within the Schrödinger scattering framework, and the Marchenko method are alternative linear ways of solving highly nonlinear inverse scattering problems. In short, in both methods one tries to solve the inverse scattering problem first by obtaining the solution of the PDE. In both cases, the solution (or a Fourier transform of the solution) is recovered by solving an integral equation, see [22], [18]. The advantages of both the classical GLM method and the Marchenko imaging method, and their high level similarities created the need for the development of a framework that will help us understand their possible connections.

Also recently, inverse boundary value problems were studied based on methods originating from the so-called theory of reduced order models. Reduced order model techniques were originally developed for solving numerically boundary value problems (as alternative to conventional finite elements) [46]. Within the context of inverse problems, the use of reduced order models was initially introduced in the inverse medium/coefficient problem for diffusion type PDEs or time-domain wave problems [8, 10]. In short, using reduced order models one can approximate the state of a PDE and subsequently solve the inverse problem using linear steps, in the same spirit as in the GLM method.

Over the previous years there have been great advances in both traditional inverse scattering techniques based on the GLM approach and on the ROM based inversion methods. Between the sixties and the eighties there have been great developments in the area of classical inverse scattering theory based on the GLM point of view. First of all, worth noting are the classic books [28, 17] and the paper [21] that develop both forward inverse scattering theory for the 1D Schrödinger equation. In the context of solving the inverse medium problem using the classic GLM approach, there were the innovative works by Ware and Aki [66] and Burridge et al. [15]. In these papers one can find elaborate discussion on how and why one can solve the inverse

scattering problem for the acoustic wave equation using the GLM integral equation. The key feature that allows the use of the GLM method for the Helmholtz equation is the equivalence between the 1D Helmholtz/acoustic and 1D Schrödinger equation through a coordinate transform. There have been notable attempts to extend this inversion approach to higher dimensions under some assumptions on the acoustic parameters. Though, for the general case it is still not known how the acoustic/Helmholtz equation can be transformed to the Schrödinger equation.

Now, regarding the ROM based inversion approach, there have been great advances and developments the past recent years. First of all, as it was mentioned above, reduced basis approximations were initially used in numerical analysis of PDEs, since, compared to conventional finite elements, they are computationally cheap. In the context of inverse problems, the ROM approach has been used primarily in combination with the so-called Lanczos method to obtain a linearized problem. The main idea in the ROM inversion method, is that one can use the Lanczos algorithm to orthogonalize the reduced order basis consisting of exact solutions corresponding to different frequencies. Interestingly, the new set of orthogonalized functions are localized compared to the original basis. Moreover, the localized basis functions seem to depend weakly on the coefficients of the PDE, therefore, one can approximate them using the set consisting of orthogonalized solutions corresponding to a background coefficient. This approach seems to produce better results than the conventional Born approximation. In high level, both the Born and the ROM inversion methods use a background model to estimate solutions of PDEs. Especially in time domain wave propagation and in diffusion, there are obvious improvements in the results using the ROM inversion method compared to classical approaches such as the Born inversion, see e.g. [26]. All of the above ideas on the ROM inversion in time domain wave propagation and in diffusion are elaborated in the following innovative works, [26, 8, 11, 27, 8]. All of these great developments and observations motivated us to apply these ideas of the ROM inversion in the frequency domain for a scattering framework.

## 1.2 Indirect Methods

The standard way of solving inverse scattering problems (since the early 2000's) is surprisingly an indirect method. It is the so-called full waveform inversion (FWI) that has been proposed in 1984 [58]. In short, using FWI, the inverse scattering problem is solved by formulating a PDE-constrained optimization problem. In particular, the unknown coefficient and the corresponding solution of the PDE are jointly recovered by matching observed data to modelled data. The full waveform inversion has been the standard approach for imaging purposes due to its many advantages. Apart from being a straightforward method to implement, the FWI method offers great detail in the solution of the inverse problem. Since the PDE-constrained problem is solved iteratively, one has the option to increase even more the detail in the reconstruction of the

minimizer through spatial grid refinement and strategic increases in the use of high frequency data in each iteration. Also, the FWI approach can be useful in cases where there are more than one PDE coefficients that need to be estimated. Moreover, the FWI method is a robust method when it comes to handling noise in the data. However, there is the big shortcoming of convexity due to the highly nonlinear coefficient to solution map. This makes the FWI method sensitive when it comes to choosing a coefficient as the initial iterate. For that reason, the FWI method is notorious for getting stuck in local minimizers. Also, due to the iterative approaches for solving the PDE-constrained problem that require multiple solutions of large linear systems, there is an increased need for computational power. Great sources for studying the FWI method are the classic papers [58, 64]. Also, for an introduction to optimal control for PDEs, the standard sources are [44, 35, 61].

### 1.3 Outline of the Thesis

So far, we have seen and discussed the main challenges one faces in the study of inverse problems. As we discussed above, the majority of the issues in the study of inverse problems have roots in the nonlinearity and also the ill-posedness of the coefficient to state map. For that reason, the contributions made in this thesis are mostly in the area of direct inversion methods, and in particular in the GLM inversion and in the ROM based inversion. The contributions will be highlighted in the next few following paragraphs describing the outline of the thesis.

The following two chapters (2-3) deal with developments on the classical Gelfand-Levitan-Marchenko inversion method in one spatial dimension. In particular, new results regarding variational Total Least Squares regularization and extension of the classical GLM equation to the Helmholtz scattering problem are presented. In chapters (4-5) we present the extension of the conventional ROM inversion method to a frequency domain scattering framework. We conclude this dissertation with an outlook and conclusions chapter.

In chapter 2 we study the inverse scattering problem for a Schrödinger operator related to a static wave operator with variable velocity, using the GLM integral equation. Assuming noise in the data, we derive a stability estimate for the error of the solution of the GLM integral equation by showing the invertibility of the GLM operator between suitable function spaces. To regularise the problem, we formulate a variational total least squares problem, and we show that, under certain regularity assumptions, the optimization problem admits minimizers. Finally, we compute numerically the regularised solution of the GLM equation using the total least squares method in a discrete sense.

In chapter 3 we study an inverse scattering problem for the Helmholtz equation on the whole line and we obtain a GLM type equation for the Jost solution that corresponds to the 1D Helmholtz differential operator. Using the asymptotic behaviour of the Jost solutions with

respect to the wave-number we derived a generalized Povzner-Levitan representation in the space of tempered distributions. We finally derive a generalized Gelfand-Levitan-Marchenko equation by applying the Fourier transform on the scattering relation that describes the solutions of the Helmholtz scattering problem.

In chapter 4, we extend the conventional ROM-based approach for inverse scattering with Neumann boundary conditions to the 1D Schrödinger equation with impedance (Robin) boundary conditions. We also propose a novel data-assimilation (DA) inversion method based on the ROM approach, thereby avoiding the need for a Lanczos-orthogonalization (LO). Furthermore, we present a detailed numerical study and comparison of the accuracy and stability of the DA and LO methods.

In chapter 5 we study a reduced order model (ROM) based waveform inversion method applied to a Helmholtz problem with impedance boundary conditions and variable refractive index. We first obtain relations that allow the reconstruction of the Galerkin projection of the continuous problem onto the space spanned by solutions of the Helmholtz equation. We also introduce and study a nonlinear optimization method based on the ROM aimed to estimate the refractive index from reflection and transmission data. Finally, we compare numerically our method to the conventional full waveform inversion method.

In the last chapter of the thesis we give the conclusions and outlook of the thesis.





## Chapter 2

# A Regularised Total Least Squares Approach for 1D Inverse Scattering

**Abstract:** We study the inverse scattering problem for a Schrödinger operator related to a static wave operator with variable velocity, using the GLM (Gelfand-Levitan-Marchenko) integral equation. We assume to have noisy scattering data, and we derive a stability estimate for the error of the solution of the GLM integral equation by showing the invertibility of the GLM operator between suitable function spaces. To regularise the problem, we formulate a variational total least squares problem, and we show that, under certain regularity assumptions, the optimization problem admits minimizers. Finally, we compute numerically the regularised solution of the GLM equation using the total least squares method in a discrete sense. This chapter is based on our paper [60].

## 2.1 Introduction

In many scientific, medical and industrial problems, one has to retrieve unknown coefficients of a governing differential equation (PDE) from (partial) measurements of its solution. This way, properties of materials can be studied in a medium that we do not have direct physical access to. In geophysics, for example, a well-known problem is estimating the elastic parameters of the subsurface from surface measurements. The governing PDE is a wave equation, and the measurements consist of a trace of its solution on the boundary of the domain. See, for example, [5] for an overview.

In particular, we focus on the inverse problem for the 1D static wave/Helmholtz equation

$$-\frac{d}{dy} \left\{ c^2(y) \frac{d}{dy} v(k, y) \right\} = k^2 v(k, y), \quad y \in \mathbb{R}, \quad (2.1)$$

with  $v = v^i + v^s$  and (asymptotic) boundary conditions

$$\lim_{y \rightarrow \pm\infty} \left\{ \frac{dv^s(k, y)}{dy} \mp ikv^s(k, y) \right\} = 0 \quad (2.2)$$

We let  $v^i(k, y) = e^{-iky}$ , which corresponds to an incoming plane wave from the right ( $+\infty$ ). The measurements at  $y = 0$  are given by

$$K(t) = \int_{\mathbb{R}} v^s(k, 0) e^{2ikt} dk,$$

for  $t \in [0, T]$ . The goal is now to retrieve  $c$  from these measurements.

Various methods for solving the inverse coefficient problem for the wave equation have been developed. A well-known method is full waveform inversion, which poses the inverse problem as a PDE-constrained optimization problem [58, 64]. Other variational formulations for the inverse problem have been proposed as well; see, for example, [56, 57]. We refer to such methods as *indirect*, as they are based on an implicit non-linear relation between data and coefficients that need to be solved iteratively. On the other hand, the inverse problem can be solved using a *direct* method. Here, an explicit formula leads to the exact solution of the inverse problem (for noiseless data). A classical direct method is given by the Gelfand-Levitan-Marchenko (GLM) integral equation [18, 66, 15]. This method has its roots in inverse scattering theory, and has recently attracted renewed attention [2, 45, 13, 53]. In [14], for example, a GLM-like approach for wavefield redatuming was proposed. Here, boundary measurements are used to estimate the wavefield in the entire domain. Subsequently, such a wavefield can be used to estimate medium parameters by solving the Lippmann-Schwinger integral equation [23].

One advantage of the indirect (variational) methods over the direct ones is that they can handle better situations where there is noise in the data. In direct methods, noise in the data

likely gets amplified. To counter such instabilities, one typically adds regularisation. In particular, the GLM approach with noisy data requires a total least squares (TLS) approach, and was studied numerically by [55]. Other regularised approaches for similar integral equations in seismic imaging are discussed in [62].

In this chapter, we revisit the classical GLM approach for the 1D inverse medium problem and consider in particular the infinite dimensional case with noisy measurements. To regularise the problem, we formulate a regularised (TLS) approach for it. To solve the resulting variational problem, we use an alternating iterative method [7]. Some numerical examples complete the chapter.

Our main contributions are as follows:

- We extend the stability estimates that can be found in [16] to the classical GLM integral equation.
- We show that the variational TLS formulation of the GLM method admits minimizers.

This chapter is organised as follows. In Section 2.2, we state the forward scattering problem and we review some classical results from scattering theory. We also review basic properties of the GLM integral operator. In Section 2.3, we include our new findings, namely the stability estimate for the GLM inversion assuming having access to noisy scattering data. We then continue studying the variational total least squares problem of reconstructing the solution of the inverse problem from noisy scattering data, and we show the well-posedness of it. We also discuss its analytical limitations. In Section 2.4 we implement numerically the proposed total least squares regularisation method. In Section 2.5 we show a number of numerical examples and conclude the chapter with a discussion section.

## 2.2 Preliminaries

This section summarises mostly known and well-established results in 1D scattering theory. In Section 2.2.1, we use the travel time coordinate transform to derive the equivalence of the static wave equation with variable velocity to the Schrödinger equation and we formulate the forward scattering problem. In Section 2.2.2, we repeat the classical procedure of using the Jost solutions to construct the solution of the forward scattering problem. In Section 2.2.3, we briefly discuss the derivation of the GLM integral equation and we review some basic properties of the GLM integral operator.

### 2.2.1 Formulation of the Forward Problem

It has been well-established (see, for example, [66, 15]) that the inverse problem for the 1D static wave/ Helmholtz equation may equivalently be stated in terms of the 1D Schrödinger equation

$$\left\{ -\frac{d^2}{dx^2} + q(x) \right\} u(k, x) = k^2 u(k, x), \quad x \in \mathbb{R}, \quad (2.3)$$

with boundary conditions

$$\lim_{x \rightarrow +\infty} \left\{ \frac{du^s(k, x)}{dx} - iku^s(k, x) \right\} = 0, \quad (2.4)$$

$$\lim_{x \rightarrow -\infty} \left\{ \frac{du^s(k, x)}{dx} + iku^s(k, x) \right\} = 0, \quad (2.5)$$

where

$$u(k, \cdot) = u^i(k, \cdot) + u^s(k, \cdot) \quad (2.6)$$

with  $u^i(k, x) = e^{-ikx}$ ,  $x \in \mathbb{R}$ . The quantities are related via

$$u(k, x) = \eta(x)v(k, y(x)), \quad x \in \mathbb{R}, \quad (2.7)$$

$$q(x) = \frac{1}{\eta(x)} \frac{d^2 \eta(x)}{dx^2}, \quad x \in \mathbb{R}. \quad (2.8)$$

where

$$\eta(x) = \{c(y(x))\}^{1/2}, \quad (2.9)$$

and

$$y(x) = \int_0^x \eta^2(r) dr, \quad x \in \mathbb{R}. \quad (2.10)$$

We assume that the velocity is  $c > 0$  is bounded and sufficiently smooth to apply the coordinate transform. We also assume that  $c'$  is bounded and has a compact support and that  $c''$  is a bounded function. Therefore,  $q$  is bounded and compactly supported since  $\eta''$  is bounded and compactly supported. We refer to [60] for more details on this transformation. Furthermore, we note that we seek for an element of  $H_{loc}^2(\mathbb{R})$  as the solution of the differential equation since the scattering potential can be discontinuous in general, and thus, we cannot necessarily obtain a solution of  $C^2$ -regularity.

A key result that we will need later on is the absence of bound states.

**Theorem 2.2.1.** *Let the Schrödinger operator*

$$S = -\frac{d^2}{dx^2} + q : H^2(\mathbb{R}) \rightarrow L^2(\mathbb{R}), \quad (2.11)$$

where  $q$  is given by relation (2.8). Then the discrete spectrum of  $S$  is empty.

For the proof of the result of the absence of bound states for this particular Schrödinger operator see [66, 60].

## 2.2.2 Classical Results from Scattering Theory

It is well known that the Schrödinger differential equation can be reduced to the following Schrödinger integral equations at  $\pm\infty$ .

$$f^+(k, x) = e^{ikx} - \int_x^\infty \frac{\sin(k(x-y))}{k} q(y) f^+(k, y) dy, x \in \mathbb{R},$$

and

$$f^-(k, x) = e^{-ikx} + \int_{-\infty}^x \frac{\sin(k(x-y))}{k} q(y) f^-(k, y) dy, x \in \mathbb{R}.$$

Such Volterra-type integral equations can be derived using the variation of constants and we refer to [39] for a discussion about the existence and uniqueness of solutions of these integral equations. The functions  $f^\pm(\pm k, \cdot)$  are called the Jost solutions, and the solution of the forward scattering problem can be decomposed as a sum of these functions as

$$u(k, x) = T(k) f^-(k, x) = f^+(-k, x) + R(k) f^+(k, x), x \in \mathbb{R}, \quad (2.12)$$

where the functions  $T, R$  are called the transmission and reflection coefficients respectively. The transmission and reflection coefficients, as functions of the wavenumber  $k$ , satisfy the following relations

$$\begin{aligned} T(k) &= 1 + \frac{1}{2ik} \int_{\mathbb{R}} u(k, y) q(y) e^{iky} dy, \\ R(k) &= \frac{1}{2ik} \int_{\mathbb{R}} u(k, y) q(y) e^{-iky} dy, \end{aligned} \quad (2.13)$$

for  $k \in \mathbb{R} \setminus \{0\}$  and the conservation of energy

$$|T(k)|^2 + |R(k)|^2 = 1, k \in \mathbb{R} \setminus \{0\}. \quad (2.14)$$

The scattering theory for the Schrödinger equation is a classical mathematical subject that dates back to the 1960s. We refer, for example, to [24, 39, 52] and the references therein for introduction and extensive analysis of the quantum scattering problem.

### 2.2.3 The Inverse Scattering Problem and the Gelfand–Levitan–Marchenko Inversion Method

The inverse scattering problem is now to retrieve the scattering potential,  $q$ , from the reflection coefficient  $R$ . The GLM integral equation is the key for solving this inverse scattering problem. In this section, we review the classical inverse scattering problem of the determination of the scattering potential from scattering data, using the GLM integral equation. In Section 2.2.3, we study the integral operator defined by the GLM equation in order to derive properties that will help us to construct an inequality for the error of the solution of the GLM equation as we show in Section 2.3.1.

#### Derivation of the GLM Equation

The key ingredient for deriving the GLM integral equation is the scattering identity (2.12). For fixed  $x$ , we get that  $\mathbb{C}_{Im>0} \ni k \mapsto f^+(k, x)e^{-ikx} - 1$  is an element of the Hardy class  $\mathcal{H}_2^+$ . Using the Paley–Wiener theorem, we obtain that  $f^+(\cdot, x)$  satisfies the following relation

$$e^{-ikx} f^+(k, x) = 1 + \int_0^\infty B(x, t) e^{2ikt} dt, \quad \forall k \in \mathbb{R} \setminus \{0\}, \quad (2.15)$$

where  $B(x, \cdot) \in L^2(0, \infty)$  satisfies

$$-\frac{dB(x, 0)}{dx} = q(x). \quad (2.16)$$

The calculation of the Fourier transform of relation (2.12) gives the classical GLM integral equation. For more details on the application of the Paley-Wiener theorem to the Jost function  $f^+(\cdot, \cdot)$ , we refer to [39]. Below, we give the GLM integral equation. For a detailed proof, we refer again to [39], which gives a very detailed exposition of the quantum scattering problem on the line using analytical methods.

**Theorem 2.2.2.** *Let  $x \in \mathbb{R}$ . Then the function  $B(x, \cdot)$  satisfies the GLM integral equation*

$$K(x+t) + \int_0^\infty B(x, z) K(x+t+z) dz + B(x, t) = 0, \quad a.e. \text{ for } t \in [0, \infty), \quad (2.17)$$

where the scattering data  $K = K_c + K_d$  are given by

$$K_c(t) = \frac{1}{\pi} \int_{\mathbb{R}} R(k) e^{2ikt} dk, \quad t \in [0, \infty), \quad (2.18)$$

$$K_d(t) = 2 \sum_{n=1}^N \rho_n e^{-2p_n t}, \quad t \in [0, \infty), \quad (2.19)$$

where  $(-\rho_n)_{n=1}^N$  are the eigenvalues of the Schrödinger operator  $S = -\frac{d^2}{dx^2} + q$  and  $(-p_n = -\frac{1}{\|f_n\|_{L^2(\mathbb{R})}})_{n=1}^N$ ,  $(f_n)_{n=1}^N$  are the eigenfunctions corresponding to the eigenvalues.

### Analysing the GLM Operator

In this subsection, we study the GLM integral operator and we review some of its properties. In particular, we use these properties in Section 2.3.1 for deriving an upper bound for the error of the noisy inverse problem. Since we assume that the scattering potential  $q$  is compactly supported, we obtain that for every fixed  $x \in \mathbb{R}$ , the solution of the GLM equation  $B(x, \cdot)$  is compactly supported. In particular, this is justified using the following inequality,

$$|B(x, t)| \leq \int_{x+t}^{\infty} |q(z)| dz \exp\left(\int_x^{\infty} (z-x)|q(z)| dz\right), \quad (2.20)$$

for  $x \in \mathbb{R}$  and  $t > 0$ , see [39]. Consequently, the domain of integration in the GLM integral equation can be reduced to an integration over a finite interval. For a fixed potential  $q$ , we assume that the interval of integration is  $(0, T_x)$ , where  $T_x$  depends on the fixed value of  $x \in \mathbb{R}$ . In addition, since we are interested in reconstructing  $B(\cdot, \cdot)$  for the values of  $x$  where the scattering potential is supported, it is reasonable to consider the following. Since the set  $\{T_x : x \in \text{supp}(q)\}$  is bounded from above, we denote with  $T$  its supremum. We assume without loss of generality that  $(0, T) \supset \text{supp}(q)$ . We define

$$\mathcal{Y} = \{f \in L^2(\mathbb{R}) : \text{supp}(f) \subset (0, T)\}. \quad (2.21)$$

We also define the set  $\mathcal{B}(\mathcal{Y}) = \{L : \mathcal{Y} \rightarrow \mathcal{Y} : \text{bounded and linear}\}$ . Additionally, for a fixed  $x \in (0, T)$  and  $f \in \mathcal{Y}$  we define

$$\{A(K)f\}(x, t) := \int_0^T \chi_{(0, T)}(t) K(x+t+z) f(z) dz, \quad t \in \mathbb{R}. \quad (2.22)$$

Since we fix  $K \in L^2(\mathbb{R})$ , we write for simplicity

$$\{A(K)f\}(x, \cdot) = A_x f. \quad (2.23)$$

With  $\chi_{\omega}(\cdot)$ , we denote the characteristic function which is 1 in  $\omega$  and 0 in  $\mathbb{R} \setminus \omega$ . Since the reflection coefficient  $R \in L^2(\mathbb{R})$ , thus  $K \in L^2(\mathbb{R})$ , see [39], we find the following.

**Lemma 2.2.1.** *For fixed  $x$ , the operator*

$$A_x : \mathcal{Y} \rightarrow \mathcal{Y} \quad (2.24)$$

*is compact and self-adjoint.*

**Lemma 2.2.2.** *The numbers  $\lambda = \pm 1$  are not eigenvalues of  $A_x$ .*

Considering the previous lemmas, the following result follows.

**Proposition 2.2.1.** *The operator  $I + A_x \in \mathcal{B}(\mathcal{Y})$  is invertible and its inverse is given by the Neumann series expansion in  $\mathcal{B}(\mathcal{Y})$ .*

## 2.3 Main Results

So far, we have summarised mainly known results for the scattering problem of our study. In the following subsection, we provide the reader with a new result regarding the stability of the reconstruction of the GLM kernel from noisy scattering data. In Section 2.3.2, we show the existence of minimizers for the variational total least squares regularisation of the GLM inversion.

### 2.3.1 Stability Estimates

Assuming now that there is an error  $\varepsilon \in L^2(\mathbb{R})$  in the measurements of the scattering data  $K$  (due to noise, measuring errors, etc.); we are then dealing with the following problem.

$$\text{Given } K^* = K + \varepsilon \in L^2(\mathbb{R}), \text{ find } B_x^* \in L^2(0, T) : \quad (2.25)$$

$$B_x^*(t) + \int_0^T \chi_{(0,T)}(t) K^*(x+t+z) B_x^*(z) dz + K^*(x+t) = 0, \text{ a.e. for } t \text{ in } (0, T), \quad (2.26)$$

where we let  $B_x(\cdot) = B(x, \cdot)$  for ease of notation. We then want to bound  $\|B_x^* - B_x\|_{L^2(\mathbb{R})}$  in terms of  $\|\varepsilon\|_{L^2(\mathbb{R})}$ . A similar upper bound for the error for a similar GLM equation is given in [16], but not in  $L^2(\mathbb{R})$ . In addition, we refer to [1] for a discussion on a stability estimate of the Marchenko inversion where the bounds are on the scattering potential. In the application of recovering the scattering potential from scattering data, a pointwise estimate for the error is sufficient in view of relation (2.16). We denote

$$\Delta B_x = B_x^* - B_x. \quad (2.27)$$

and



$$\varepsilon_x(t) = K^*(x+t) - K(x+t), \text{ a.e for } t \in \mathbb{R}. \quad (2.28)$$

Assuming further that the error  $\varepsilon$  is real valued, we obtain, as before, that  $A_x^*$  is a compact and self-adjoint operator. We then find the following result.

**Lemma 2.3.1.** *Let the previous assumptions be true. The following inequality holds,*

$$\|A_x^* - A_x\|_{\mathcal{B}(\mathcal{Y})} \leq \sqrt{T} \|\varepsilon\|_{L^2(\mathbb{R})}. \quad (2.29)$$

*Proof.* Let  $f \in \mathcal{Y}$ . We obtain

$$|[(A_x^* - A_x)f](t)| = \left| \int_0^T \chi_{[0,T]}(z) \left\{ K^*(x+z+t) - K(x+z+t) \right\} f(z) dz \right| \leq \quad (2.30)$$

$$\|\varepsilon_{x+t}\|_{L^2(0,T)} \|f\|_{L^2(0,T)} \leq \|\varepsilon\|_{L^2(\mathbb{R})} \|f\|_{\mathcal{Y}} \text{ a.e. for } t \in (0, T) \Rightarrow \quad (2.31)$$

the operator  $(A_x^* - A_x)$  is well defined and

$$\|(A_x^* - A_x)f\|_{L^2(0,T)} \leq \sqrt{T} \|\varepsilon\|_{L^2(\mathbb{R})} \|f\|_{\mathcal{Y}}, \quad (2.32)$$

$\forall f \in \mathcal{Y}$ . □

With this, we are ready to present the error bound.

**Theorem 2.3.1.** *Under the previous assumptions, we obtain the following:*

$$\|\Delta B_x\|_{\mathcal{Y}} \leq \frac{\|\varepsilon\|_{L^2(\mathbb{R})} (1 + \sqrt{T} \|B_x^*\|_{\mathcal{Y}})}{1 - \|A_x\|_{\mathcal{B}(\mathcal{Y})}} \quad (2.33)$$

*Proof.* We subtract (2.26)–(2.17) to obtain

$$(I + A_x + \{A_x^* - A_x\})B_x^* - (I + A_x)B_x = -\varepsilon_x \iff \quad (2.34)$$

$$(I + A_x)\Delta B_x = -(A_x^* - A_x)B_x^* - \varepsilon_x \Rightarrow \quad (2.35)$$

since 1 is not an eigenvalue of  $A_x$

$$\Delta B_x = (I + A_x)^{-1} \{-\varepsilon_x - (A_x^* - A_x)B_x^*\} \Rightarrow \quad (2.36)$$

$$\|\Delta B_x\|_{\mathcal{Y}} \leq \|(I + A_x)^{-1}\|_{\mathcal{B}(\mathcal{Y})} \{\|\varepsilon_x\|_{\mathcal{Y}} + \|A_x^* - A_x\|_{\mathcal{Y}} \|B_x^*\|_{\mathcal{Y}}\} \leq \quad (2.37)$$

$$\frac{\|\varepsilon\|_{L^2(\mathbb{R})} (1 + \sqrt{T} \|B_x^*\|_{\mathcal{Y}})}{1 - \|A_x\|_{\mathcal{B}(\mathcal{Y})}}. \quad (2.38)$$

□

The previous stability estimate gives an upper bound for the error of the solution of the GLM equation, which is proportional to the  $L^2$ - norm of the error in the measurements,  $\varepsilon$ . Though, we cannot rule out the case where the operator norm of  $A_x$  is almost 1. In general, the operator norm of  $A_x$  is determined by  $K$ . However, what kind of potential produces scattering data that make the operator norm be closer to 1 is still something to investigate.

### 2.3.2 Variational Regularisation

In this section, we define and show well-posedness for the variational total least squares regularisation problem of determining the kernel  $B$  from inexact scattering data. Similar work on this subject was done in the finite dimensional setting by [55], where they considered discrete scattering data and they followed a data analytic way for studying the total least squares problem for regularizing the GLM equation. In our approach, we fill the theoretical gap of showing well-posedness of the total least squares regularisation method of the GLM inversion in the infinite dimensional setting.

Now, for a set  $\Omega \subset \mathbb{R}^N$ ,  $N = 1, 2$  and a generic function space  $\Psi(\Omega) = \{f : \Omega \rightarrow \mathbb{C}\}$ , we define the extension operator

$$E_0 : \Psi(\Omega) \rightarrow \Psi(\mathbb{R}^N), \quad (2.39)$$

as the map that extends a function to 0 if the argument is not included in  $\Omega$ . (This is a bounded operator if, for example,  $\Psi(\Omega) = L^2(0, T)$ .) Then, we consider the usual Lebesgue space

$$L^2((0, T)^2) = \{f : (0, T) \rightarrow L^2(0, T) : \int_0^T \|f(t, \cdot)\|_{L^2(0, T)}^2 dt < \infty\}.$$

The inner product is given by

$$\langle f, g \rangle_{L^2((0, T)^2)} = \int_0^T \langle f(t), g(t) \rangle_{L^2(0, T)} dt = \int_0^T \int_0^T f(x, t) \overline{g(x, t)} dx dt.$$

We also define

$$\Theta : L^2((0, T)^2) \rightarrow L^2((0, T), L^2(\mathbb{R})) \quad (2.40)$$

with

$$\Theta f = x \mapsto E_0 f(x, \cdot), \quad \text{for almost all } x \in (0, T). \quad (2.41)$$

**Lemma 2.3.2.**  $\Theta$  is a bounded linear operator.

*Proof.* The linearity is easy to show. Now, for the boundedness, let  $f \in L^2((0, T)^2)$

$$\|f\|_{L^2((0, T)^2)}^2 = \int_0^T \int_0^T |f(x, t)|^2 dt dx = \int_0^T \int_{\mathbb{R}} |E_0 f(x, t)|^2 dt dx = \|\Theta f\|_{L^2((0, T), L^2(\mathbb{R}))}^2.$$

□

We define  $G : L^2((0, T)^2) \times L^2(\mathbb{R}) \rightarrow L^2((0, T), L^2(\mathbb{R}))$  as

$$\begin{aligned} G(B, K) &= \{I + A(K)\} \Theta B = \\ x &\mapsto \left\{ t \mapsto \Theta B(x, t) + \int_0^T \chi_{(0, T)}(t) \Theta B(x, z) K(x + t + z) dz \right\} \end{aligned} \quad (2.42)$$

**Remark 2.3.1.** We need  $\Theta$  in order to have a well-defined convolution type relation in  $G$ . In addition, compare this with the setting of the previous section. By using  $\Theta$ , we avoid the use of the space  $\mathcal{Y}$  altogether.

**Proposition 2.3.1.**  $G : L^2((0, T)^2) \times L^2(\mathbb{R}) \rightarrow L^2((0, T), L^2(\mathbb{R}))$  is well defined.

*Proof.* Let  $(B, K) \in L^2((0, T)^2) \times L^2(\mathbb{R})$ . We want to show that  $G(B, K) \in L^2((0, T), L^2(\mathbb{R}))$ . For almost all  $x \in (0, T), t \in \mathbb{R}$ , we obtain that

$$\begin{aligned} |A(K) \Theta B(x, t)| &= \left| \int_0^T \chi_{(0, T)}(t) \Theta B(x, z) K(x + t + z) dz \right| \leq \\ &\|E_0 B(x, \cdot)\|_{L^2(\mathbb{R})} \|K\|_{L^2(\mathbb{R})} = \|B(x, \cdot)\|_{L^2(0, T)} \|K\|_{L^2(\mathbb{R})} \Rightarrow \\ &\int_0^T \left\{ \int_0^T \chi_{(0, T)}(t) \Theta B(x, z) K(x + t + z) dz \right\}^2 dt \leq T \|B(x, \cdot)\|_{L^2(0, T)}^2 \|K\|_{L^2(\mathbb{R})}^2. \end{aligned}$$

Therefore,

$$\left\| x \mapsto \left\{ t \mapsto \int_0^T \chi_{(0, T)}(t) \Theta B(x, z) K(x + t + z) dz \right\} \right\|_{L^2((0, T), L^2(\mathbb{R}))}^2 \leq T \|K\|_{L^2(\mathbb{R})}^2 \|B\|_{L^2((0, T)^2)}^2.$$

Finally,

$$\|G(B, K)\|_{L^2((0, T), L^2(\mathbb{R}))} \leq \sqrt{T} \|K\|_{L^2(\mathbb{R})} \|B\|_{L^2((0, T)^2)} + \|B\|_{L^2((0, T)^2)}.$$

□

Now, for a function  $g \in L^2(\mathbb{R})$ , we define for almost all  $x \in (0, T)$

$$S(g) : x \mapsto g(x + \cdot). \quad (2.43)$$

**Lemma 2.3.3.**  $S : L^2(\mathbb{R}) \rightarrow L^2((0, T), L^2(\mathbb{R}))$  is linear and bounded.

*Proof.* Let  $g, g_1, g_2 \in L^2(\mathbb{R})$ .

$$S(ag)(x, t) = ag(x + t) = aSg(x, t), \text{ a.e. in } (0, T) \times \mathbb{R}.$$

In addition,

$$S(g_1 + g_2)(x, t) = (g_1 + g_2)(x + t) = Sg_1(x, t) + Sg_2(x, t), \text{ a.e. in } (0, T) \times \mathbb{R}.$$

Now, we observe that

$$\|Sg\|_{L^2((0, T), L^2(\mathbb{R}))}^2 = \int_0^T \|g(x + \cdot)\|_{L^2(\mathbb{R})}^2 dx = \quad (2.44)$$

$$\int_0^T \|g\|_{L^2(\mathbb{R})}^2 dx = T \|g\|_{L^2(\mathbb{R})}^2 \Rightarrow \|Sg\|_{L^2((0, T), L^2(\mathbb{R}))} = \sqrt{T} \|g\|_{L^2(\mathbb{R})}. \quad (2.45)$$

□

Let  $K \in L^2(\mathbb{R})$  given. Let also  $\alpha, \beta > 0$ . We define the total least squares functional  $\phi_K : H^1((0, T)^2) \times H_0^1(0, 3T) \rightarrow [0, \infty]$  as

$$\phi_K(B, e) :=$$

$$\|G(B, K + E_0 e) + S(K + E_0 e)\|_{L^2((0, T), L^2(\mathbb{R}))}^2 + \alpha \|B\|_{L^2((0, T)^2)}^2 + \beta \|e\|_{L^2(0, 3T)}^2. \quad (2.46)$$

We assume that we have access to inexact scattering data  $K \in L^2(\mathbb{R})$ . We will define the solution of the inverse problem of finding the kernel  $B$  (in a region where the potential is supported) from  $K$ .

**Definition 2.3.1.** Let  $K \in L^2(\mathbb{R})$  inexact scattering data. Let  $\alpha, \beta > 0$ , and let that there exist functions  $\widehat{B} \in H^1((0, T)^2)$  and  $\widehat{e} \in H_0^1(0, 3T)$  such that

$$(\widehat{B}, \widehat{e}) \in \underset{B \in \mathcal{U}, e \in \mathcal{V}}{\operatorname{argmin}} \phi_K(B, e), \quad (2.47)$$

with  $\mathcal{U} \subset H^1((0, T)^2)$ ,  $\mathcal{V} \subset H_0^1(0, 3T)$ , both bounded convex and closed in the respective topologies. Then, we call  $\widehat{B}$  a regularised total least squares solution of the GLM integral equation.

**Remark 2.3.2.** *Ideally, we would like to find a perturbation  $e$  that will almost cancel out the noise  $\varepsilon$  which is included in  $K$ .*

We state some auxiliary results needed for showing well-posedness for the variational inverse problem (2.47).

**Lemma 2.3.4.** *Let  $K \in L^2(\mathbb{R})$  and let the strongly convergent sequences*

$$B_n \rightarrow B \text{ in } L^2((0, T)^2) \quad (2.48)$$

and

$$e_n \rightarrow e \text{ in } L^2(0, 3T). \quad (2.49)$$

Then

$$A(K + E_0 e_n) \Theta B_n \rightarrow A(K + E_0 e) \Theta B \text{ in } L^2((0, T), L^2(\mathbb{R})). \quad (2.50)$$

*Proof.* For almost all  $x \in (0, T), t \in \mathbb{R}$ , we take

$$\begin{aligned} & \int_0^T \chi_{(0, T)}(t) \Theta B_n(x, z) (K + E_0 e_n)(x + t + z) dz - \\ & \int_0^T \chi_{(0, T)}(t) \Theta B(x, z) (K + E_0 e)(x + t + z) dz = \\ & \int_0^T \chi_{(0, T)}(t) \Theta \{B_n(x, z) - B(x, z)\} (K + E_0 e_n)(x + t + z) dz + \end{aligned} \quad (2.51)$$

$$\int_0^T \chi_{(0, T)}(t) \Theta B(x, z) (K + E_0 e_n - K - E_0 e)(x + t + z) dz = \quad (2.52)$$

Using the triangular inequality and working similarly to proposition 2.3.1, we obtain

$$\|A(K + E_0 e_n) \Theta B_n - A(K + E_0 e) \Theta B\|_{L^2((0, T), L^2(\mathbb{R}))} \leq \quad (2.53)$$

$$\begin{aligned} & \sqrt{T} \|K + E_0 e_n\|_{L^2(\mathbb{R})} \|B_n - B\|_{L^2((0, T)^2)} + \sqrt{T} \|E_0 e_n - E_0 e\|_{L^2(\mathbb{R})} \|B\|_{L^2((0, T)^2)} \leq \\ & \sqrt{T} (\|K\|_{L^2(\mathbb{R})} + \|e_n\|_{L^2(0, 3T)}) \|B_n - B\|_{L^2((0, T)^2)} + \sqrt{T} \|e_n - e\|_{L^2(0, 3T)} \|B\|_{L^2((0, T)^2)}. \end{aligned} \quad (2.54)$$

As  $n \rightarrow \infty$ ,  $\|e_n\|_{L^2(0, 3T)}$  is bounded, so we conclude the result.  $\square$

Now, using the above auxiliary results, we find the following well-posedness result.

**Theorem 2.3.2.** *The optimization problem (2.47) admits minimizers.*

*Proof.* Since

$$0 \leq \phi_K(B, e), \forall (B, e) \in \mathcal{U} \times \mathcal{V}, \quad (2.55)$$

we can find a minimizing sequence  $(B_n, e_n) \subset \mathcal{U} \times \mathcal{V}$  with

$$\lim_n \phi_K(B_n, e_n) = \inf_{(e, B) \in \mathcal{U} \times \mathcal{V}} \phi_K(B, e) = \mathcal{M}. \quad (2.56)$$

Since  $\mathcal{U}, \mathcal{V}$ , are bounded in their respective spaces these two sequences are bounded. By reflexivity, see ([12, pages 67-68]), there exist weak limits  $B, e$  such that (passing to subsequences using the same indexing)

$$B_n \rightharpoonup B \text{ in } \sigma(H^1((0, T)^2), H^1((0, T)^2)') \quad (2.57)$$

and

$$e_n \rightharpoonup e \text{ in } \sigma(H_0^1(0, 3T), H^{-1}(0, 3T)). \quad (2.58)$$

Since  $\mathcal{U}, \mathcal{V}$  are strongly closed and convex subsets of reflexive spaces, they are also weakly closed; see ([12, page 60]). Therefore,

$$(B, e) \in \mathcal{U} \times \mathcal{V}. \quad (2.59)$$

Now, by the following compact embeddings,

$$H_0^1(0, 3T) \xhookrightarrow{c} L^2(0, 3T)$$

see [12, theorem 8.8] and

$$H^1((0, T)^2) \xhookrightarrow{c} L^2((0, T)^2)$$

we can conclude the strong convergence

$$B_n \rightarrow B \text{ in } L^2((0, T)^2) \quad (2.60)$$

and

$$e_n \rightarrow e \text{ in } L^2(0, 3T). \quad (2.61)$$

Using the above lemmas, we obtain that

$$\mathcal{M} = \lim_{n \rightarrow \infty} \phi_K(B_n, e_n) = \quad (2.62)$$

(continuity of the square function and the norm function)

$$\begin{aligned}
& \|\lim_n G(B_n, K + E_0 e_n) + S(K) + \lim_n S(E_0 e_n)\|_{L^2((0,T), L^2(\mathbb{R}))}^2 + \\
& \quad \alpha \|\lim_n B_n\|_{L^2((0,T)^2)}^2 + \beta \|\lim_n e_n\|_{L^2(0,3T)}^2 = \\
& \|\lim_n B_n + \lim_n A(K + E_0 e_n) \Theta B_n + S(K) + \lim_n S(E_0 e_n)\|_{L^2((0,T), L^2(\mathbb{R}))}^2 + \\
& \quad \alpha \|\lim_n B_n\|_{L^2((0,T)^2)}^2 + \beta \|\lim_n e_n\|_{L^2(0,3T)}^2 = \\
& \|G(B, K + E_0 e) + S(K) + S(E_0 e)\|_{L^2((0,T), L^2(\mathbb{R}))}^2 + \alpha \|B\|_{L^2((0,T)^2)}^2 + \beta \|e\|_{L^2(0,3T)}^2 \Rightarrow \phi_K(B, e) = \mathcal{M}
\end{aligned}$$

□

**Remark 2.3.3.** *The set  $(0, T)^2 \subset \mathbb{R}^2$  is a bounded Lipschitz domain. By the Rellich-Kondrachov theorem, we conclude the following compact embedding*

$$H^1((0, T)^2) \xrightarrow{c} L^2((0, T)^2),$$

see [29].

**Remark 2.3.4.** *Regarding the choice of  $H = H^1((0, T)^2)$  and the choice of  $H_0^1(0, 3T)$  as the space of the perturbations. We choose in particular these spaces for the space of the GLM kernels (in the total least squares sense) and the perturbations since we have the above compact embedding properties. Otherwise (working, for example, with the  $L^2((0, T)^2)$  and the  $L^2(0, 3T)$ ), we cannot pass to some further strongly convergent subsequences in the proof of existence of minimizers of our variational inverse problem and conclude the existence result. Similar work on this subject was done in [6]. However, the assumptions made in this paper are too strong to require in our application. In particular, the authors considered the existence of minimizers issue for a general class of total least squares problems. Assuming that the inverse problem is described by a bilinear operator with the property that weakly convergent sequences are mapped to strongly convergent sequences, they show existence. However, without working the way we did, the weak to strong continuity property of the forward operator is a very strong assumption to claim, and in general it does not hold. To see that, it is sufficient to pick a weakly convergent sequence of the form  $(B_n, 0)_n \subset L^2((0, \tau)^2) \times L^2(\mathbb{R})$  and then observe that  $(G(B_n, 0))_n$  is not necessarily norm convergent. Keep also in mind that  $G$  is not bilinear. In addition, the convolution type relation between  $K$  and  $B$  should be carefully studied under the convolution and the weak convergence.*

*To sum up our approach, we pick the spaces of interest so that we have a compact embedding property. This way, we do not need to make any assumptions on  $G$ .*

**Remark 2.3.5.** *Regarding the reasonability of the  $H^1$ -regularity assumption for the GLM kernels. Even though a GLM kernel naturally has an  $L^2$ -regularity at least in the box of interest, we know that it satisfies a Goursat-type hyperbolic PDE (see [39])*

$$\{\partial_x(\partial_x - \partial_t) - q(x)\}B(x,t) = 0, \quad x \in \mathbb{R}, \quad t > 0 \quad (2.63)$$

$$B(x,0) = \int_x^\infty q(z)dz, \quad x \in \mathbb{R} \quad (2.64)$$

$$\lim_{x \rightarrow \infty} \|B(x,0)\|_\infty = 0. \quad (2.65)$$

*So either we study the regularity of solutions of the above PDE, or we just view our proposed existence of minimizers result as a relaxed version of the problem of seeking kernels with  $L^2$ -regularity (and perturbations).*

**Remark 2.3.6.** *Finally, another thing to keep in mind is that it is possible to obtain multiple minimizers of the above optimization problem since the TLS functional,  $\phi_K$ , is not convex.*

## 2.4 Numerical Results

### 2.4.1 Numerical Implementation

In this section, we show the discrete form of the GLM equation and its numerical implementation. We also implement numerically the total least squares regularisation method of the GLM equation, using noisy scattering data.

#### Discretisation of the GLM Equation

We discretise the quantities  $K$  and  $B$  on a regular grid of samples  $t_i = i \cdot \Delta t$ . We then denote the discrete scattering data by  $\mathbf{k} \in \mathbb{R}^n$ . The discrete GLM kernel is denoted by  $\mathbf{B} \in \mathbb{R}^{(m+1) \times (m+1)}$ . The discrete counterpart to GLM equation is then given by

$$b_{ij} + \Delta t \sum_{l=0}^m b_{il} k_{i+j+l} = -k_{i+j}, \quad (2.66)$$

for  $i, j = 0, 1, \dots, m$ . We will assume that  $n = 3m$  to properly define these relations. The discrete GLM equation can be more compactly expressed using the map  $G : \mathbb{R}^{(m+1) \times (m+1)} \times \mathbb{R}^n \rightarrow \mathbb{R}^{(m+1)^2}$  and  $S : \mathbb{R}^n \rightarrow \mathbb{R}^{(m+1)^2}$ :

$$G(\mathbf{B}, \mathbf{k}) + S(\mathbf{k}) = \mathbf{0}. \quad (2.67)$$





where  $L$  represents a finite-difference approximation of the second derivative. Due to the special form of the equations for fixed  $\mathbf{k}$ , this problem separates in  $m$  separate least-squares problems for the columns of  $\mathbf{B}$ . These problems can be readily solved using standard iterative methods, such as LSQR.

The total least-squares (TLS) functional in the discrete setting is given by

$$\phi_{\mathbf{k}}(\mathbf{B}, \mathbf{e}) = \|G(\mathbf{B}, \mathbf{k} + \mathbf{e}) + S(\mathbf{k} + \mathbf{e})\|_2^2 + \alpha \|\mathbf{L}\mathbf{B}\|_F^2 + \beta \|\mathbf{e}\|_2^2. \quad (2.70)$$

To find a minimizer, we apply an alternating minimisation algorithm, as proposed by [7] we repeat for  $k = 0, 1, \dots$

$$\mathbf{B}^{(k+1)} = \underset{\mathbf{B}}{\operatorname{argmin}} \phi_{\mathbf{k}}(\mathbf{B}^{(k)}, \mathbf{e}^{(k)}) \quad (2.71)$$

$$\mathbf{e}^{(k+1)} = \underset{\mathbf{e}}{\operatorname{argmin}} \phi_{\mathbf{k}}(\mathbf{B}^{(k+1)}, \mathbf{e}^{(k)}). \quad (2.72)$$

As explained in the previous section, both steps involve a quadratic problem that can easily be solved using an iterative method like LSQR. The convergence of this alternating approach is guaranteed by the bi-convex nature of the functional  $\phi_{\mathbf{k}}$  [7].

Having solved either of the regularised problems for  $\mathbf{B}$  and in view of relation (2.16), we can compute the scattering potential from the reconstructed kernel by extracting the first column from  $\mathbf{B}$  and using a finite-difference approximation to compute the derivative.

### Choice of Regularisation Parameters

Both regularised formulations (LS and TLS) include regularisation parameter(s) that need to be estimated. In particular, for the TLS method, we need to estimate two parameters,  $\alpha, \beta$ . In practice, though we expect that  $\beta$  does not play a significant role, as the problem for  $\mathbf{e}$  is overdetermined,  $G(\mathbf{B}, \mathbf{k} + \mathbf{e}) = -S(\mathbf{k} + \mathbf{e})$  defines  $(m+1)^2$  equations in  $3m+1$  unknowns. Moreover, the corresponding system matrix consists of an identity matrix plus a small perturbation (cf. (2.68)), so the system is unlikely to be ill-posed. Thus, we pick a (small) reference value for  $\beta = \hat{\beta}$  and focus on estimating the remaining parameter,  $\alpha$ .

Ideally, we would pick  $\alpha$  to minimize the reconstruction error, i.e.,

$$\hat{\alpha} = \underset{\alpha}{\operatorname{argmin}} \|\hat{\mathbf{B}}_{\alpha} - \bar{\mathbf{B}}\|_2, \quad (2.73)$$

where  $\bar{\mathbf{B}}$  is the unregularised solution corresponding to noiseless data,  $\bar{\mathbf{k}}$ , (i.e.,  $G(\bar{\mathbf{B}}) = -S(\bar{\mathbf{k}})$ ), and  $\hat{\mathbf{B}}_{\alpha}$  denotes the optimal solution of either the LS or the TLS method corresponding to noisy data,  $\mathbf{k} = \bar{\mathbf{k}} + \varepsilon$ . For the sake of completeness, we mention below a number of commonly used

methods for choosing regularisation parameters and how these could potentially be applied in the problem of estimating  $\alpha$ .

A posteriori parameter selection methods aim to achieve this by using only knowledge of the data and the noise level. A well-known method in this class is the discrepancy principle. The particular nature of our problem (involving a product of  $\mathbf{B}$  and  $\mathbf{k}$ ) makes it difficult to apply such rules, however, as they would require an estimate of the residual at the optimal solution. To see why, note that the residual for (LS) is given by  $\|G(\overline{\mathbf{B}}, \boldsymbol{\varepsilon}) + S(\boldsymbol{\varepsilon})\|_2$ . The discrepancy principle then finds an  $\alpha$  such that

$$\|G(\widehat{\mathbf{B}}_\alpha, \mathbf{k}) + S(\mathbf{k})\|_2 \approx \|G(\overline{\mathbf{B}}, \boldsymbol{\varepsilon}) + S(\boldsymbol{\varepsilon})\|_2, \quad (2.74)$$

but this would require knowledge of the true kernel. For the total least squares approach, we could use the estimated error  $\widehat{\boldsymbol{\varepsilon}}_\alpha$  and find  $\alpha$  such that

$$\|\widehat{\boldsymbol{\varepsilon}}_\alpha\|_2 \approx \|\boldsymbol{\varepsilon}\|_2. \quad (2.75)$$

*Heuristic* methods such as the L-curve method could be applied. However, it is not clear how well they would perform on problems of this nature, as even for classical ill-posed linear inverse problems, such heuristic methods are not convergent [67]. Despite this theoretical shortcoming, such methods are often applied in practice with success [33].

## 2.5 Numerical Examples

In this subsection, we present a couple of numerical examples comparing the regularised approaches (LS and TLS) outlined above. The least-squares (sub-) problems are solved using LSQR. Unless stated otherwise, we use 10 iterations of the alternating method and 10 iterations of LSQR for the sub problems. The scattering potential is obtained by numerically differentiating the reconstructed kernel, as in (2.16).

We find that the TLS method is not sensitive to the choice of  $\beta$  (as argued in the previous section). We therefore use a fixed value of  $\beta = 1 \cdot 10^{-16}$  for all experiments. The remaining regularisation parameter  $\alpha$  for each method (LS and TLS) is obtained via (2.73). Although this requires knowledge of the noiseless data in order to compute  $\overline{\mathbf{B}}$ , it allows us to make a fair best-case comparison between the methods.

The reconstruction quality of the methods is measured by the relative  $L^2$ -error between the reconstructed kernel and the reference solution  $\overline{\mathbf{B}}$ .

The code used to produce the examples is available on:

<https://github.com/ucsi-consortium/1DInverseScatteringGLM/releases/tag/publication>.

### 2.5.1 Example 1: The Plasma Wave-Equation with a Smooth Potential

In this first numerical experiment, we consider the case where the scattering data are generated directly by the plasma wave equation. The measured scattering data and the scattering potential are shown in Figure 2.1.

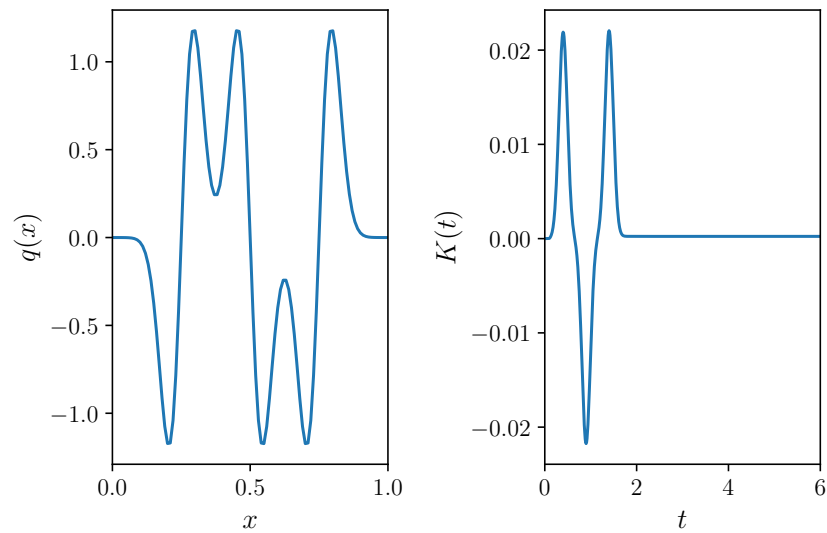


Figure 2.1: Scattering potential and scattering data. The scattering potential has a relatively smooth profile.

We apply the methods described in the previous subsections, and thus, we solve the GLM integral equation to find the GLM kernel and then the scattering potential. Figure 2.2 shows the solution of the GLM equation (matrix  $\mathbf{B}$ ) and the comparison between the true and the recovered potential. For such a smooth potential, the generated scattering data lead to a good reconstruction.

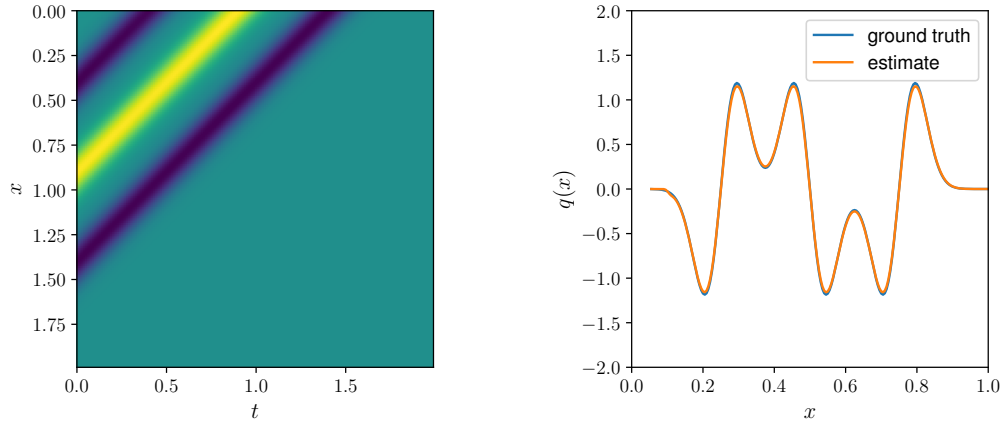


Figure 2.2: Reconstruction using the unregularised GLM approach from noiseless data. Shown are the kernel (**left**) and corresponding reconstructed scattering potential (**right**). The recovered scattering potential matches well with the ground truth.

As we studied previously, the presence of noise in the scattering data is expected to affect the reconstruction of both the GLM kernel and the potential. To test this, we add i.i.d. normally distributed random noise to the data with mean zero and variance  $\sigma^2$ . Reconstructions using the unregularised, LS and TLS approach for  $\sigma = 1 \cdot 10^{-3}$  are shown in Figure 2.3. The results for various noise levels are summarised in Table 2.1. In all cases, the TLS approach is superior and requires less regularisation (smaller value of  $\alpha$ ).

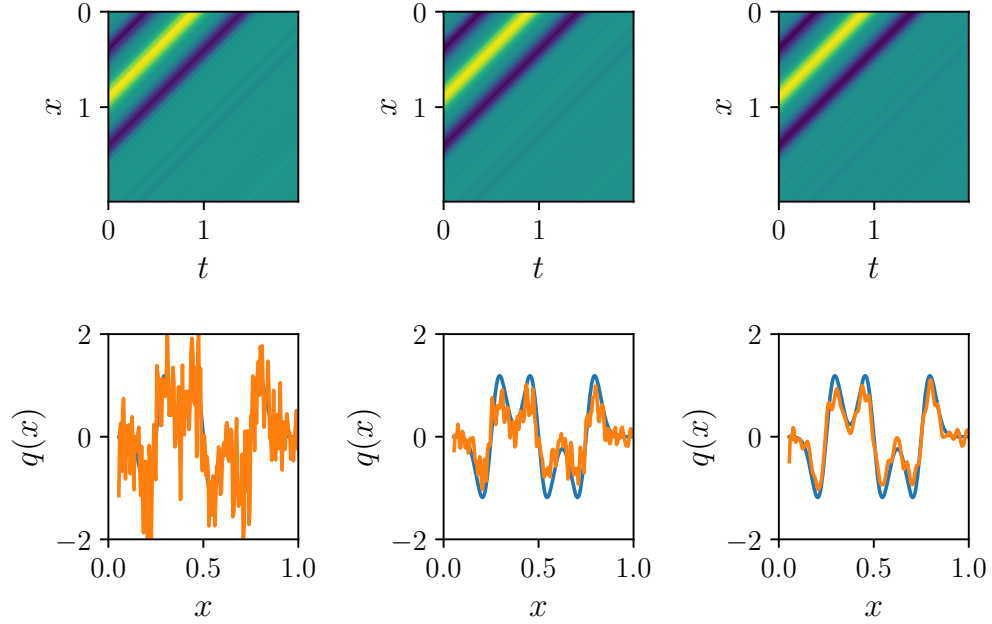


Figure 2.3: Comparison of the unregularised (**left**), LS (**middle**) and TLS (**right**) approaches on noisy data ( $\sigma = 1 \cdot 10^{-3}$ ). The true potential corresponds to the blue curve.

Table 2.1: Table for comparing the relative errors of the regularisation methods for various noise levels.

	Unregularised		LS		TLS	
$\sigma$	Rel. Error	$\alpha$	Rel. Error	$\alpha$	Rel. Error	
$1 \cdot 10^{-4}$	$9.30 \cdot 10^{-2}$	$1.99 \cdot 10^{-2}$	$9.30 \cdot 10^{-2}$	$1.68 \cdot 10^{-2}$	$6.48 \cdot 10^{-2}$	
$1 \cdot 10^{-3}$	$8.35 \cdot 10^{-1}$	1.34	$4.85 \cdot 10^{-1}$	$2.79 \cdot 10^{-1}$	$2.86 \cdot 10^{-1}$	
$1 \cdot 10^{-2}$	7.62	$6.27 \cdot 10^2$	$8.89 \cdot 10^{-1}$	$2.94 \cdot 10^1$	$7.52 \cdot 10^{-1}$	

## 2.5.2 Example 2: Data from the Wave Equation

In this second example, we consider scattering data generated from the wave equation with variable density,

$$\rho v_{tt} = \{\rho c^2 v_y\}_y.$$

The coefficients of the wave equation, the corresponding scattering potential and the measured data are shown in Figure 2.4. This example is more challenging than the previous one,

due to significant multiple scattering.

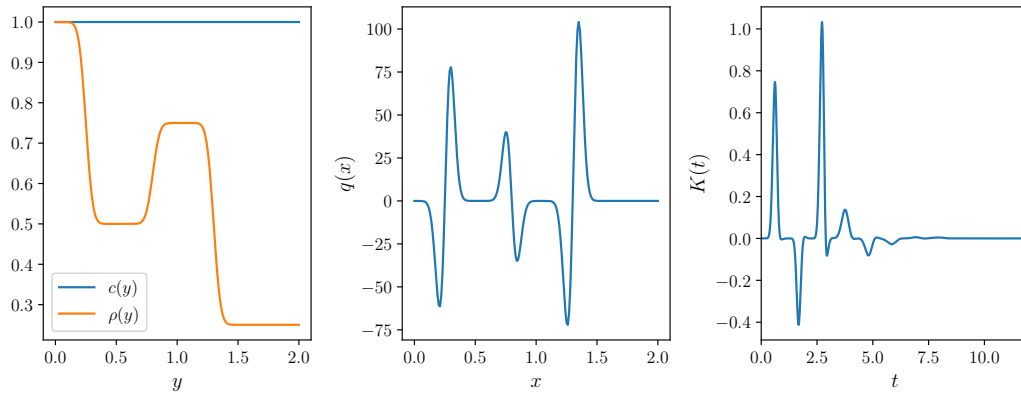


Figure 2.4: Shown are the the elastic parameters  $\rho, c$  (**left**), the corresponding scattering potential (**middle**) and the resulting scattering data (**right**). The chosen elastic parameters result in significant multiple scattering, seen on the right.

The results of the GLM method on noise-free data are shown in Figure 2.5. The band limitation of our source and the singular behaviour of the potential affects the reconstruction of  $q$ .

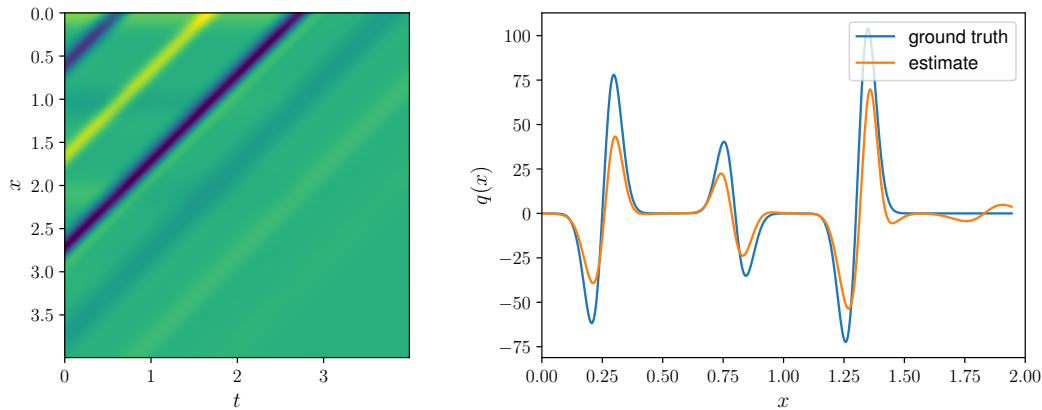


Figure 2.5: Results for noise-free data. Shown are the reconstructed kernel (**left**) and the reconstructed scattering potential (**right**). The band limitation of our source clearly affects the approximation.

Reconstructions using the unregularised, LS and TLS approach for  $\sigma = 1 \cdot 10^{-2}$  are shown in Figure 2.6. The results for various noise levels are summarised in Table 2.2. In all cases, the

TLS approach is superior.

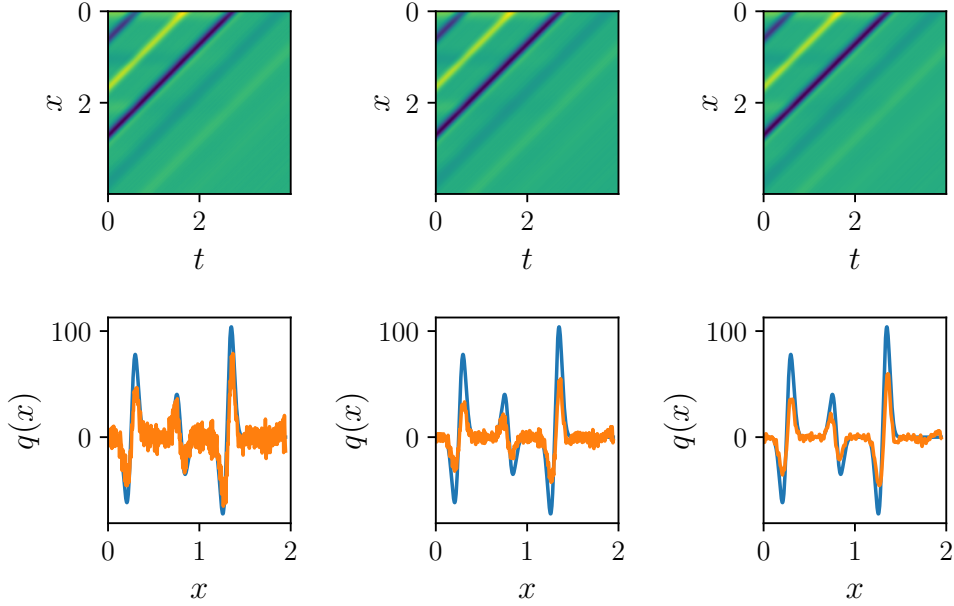


Figure 2.6: Comparison of the unregularised (**left**), LS (**middle**) and TLS (**right**) approaches on noisy data ( $\sigma = 1 \cdot 10^{-2}$ ). The true potential corresponds to the blue curve.

Table 2.2: Table for comparing the relative errors of the regularisation methods for various noise levels.

	Unregularised		LS		TLS	
$\sigma$	Rel. Error	$\alpha$	Rel. Error	$\alpha$	Rel. Error	
$1 \cdot 10^{-3}$	$3.81 \cdot 10^{-2}$	$6.56 \cdot 10^{-3}$	$3.91 \cdot 10^{-2}$	$9.52 \cdot 10^{-3}$	$3.26 \cdot 10^{-2}$	
$1 \cdot 10^{-2}$	$3.87 \cdot 10^{-1}$	$3.91 \cdot 10^{-1}$	$3.27 \cdot 10^{-1}$	$1.01 \cdot 10^{-1}$	$1.76 \cdot 10^{-1}$	
$1 \cdot 10^{-1}$	$3.59 \cdot 10^0$	$1.00 \cdot 10^2$	$8.05 \cdot 10^{-1}$	$1.68 \cdot 10^1$	$7.03 \cdot 10^{-1}$	

## 2.6 Discussion and Conclusions

We revisited some classical results from inverse scattering to solve the 1D inverse coefficient problem for the wave equation. In particular, we considered the GLM method with noisy data and proposed a regularised total least squares formulation in the infinite dimensional setting. We contributed an error bound for the unregularised GLM approach and have shown existence



of minimizers for the variational formulation of the TLS approach. Numerical results illustrate the approach, showing that the TLS approach gives superior results as compared to conventional Tikhonov regularisation.

The results from inverse scattering, in particular a GLM-like approach has recently received renewed attention in the geophysical literature. Noisy data is a significant source of error in these methods, and various discrete regularisation schemes have been proposed to address this issue. While these methods have been shown to work well in practice, careful analysis of the infinite dimensional problem has not been done. We believe that it is important to study this because it will yield new insight in the behaviour of practical approaches as they are pushed to include higher frequency data (and hence finer discretisation). Ultimately, these insights may lead to adaptive methods. Moreover, the 1D problem analysed here serves as a model problem for many practical problems in 2D and 3D, and the insights may inspire new approaches there as well.



## Chapter 3

# A Distributional Gelfand-Levitan-Marchenko Equation For The Helmholtz Scattering Problem On The Line

**Abstract:** We study an inverse scattering problem for the Helmholtz equation on the whole line. The goal of this chapter is to obtain a Gelfand-Levitan-Marchenko type equation for the Jost solution that corresponds to the 1D Helmholtz differential operator. We assume for simplicity that the refraction index is of compact support. Using the asymptotic behaviour of the Jost solutions with respect to the wave-number we derive a generalized Povzner-Levitan representation in the space of tempered distributions. Then, we apply the Fourier transform on the scattering relation that describes the solutions of the Helmholtz scattering problem and we derive a generalized Gelfand-Levitan-Marchenko equation. Finally, we discuss possible application of this new generalized GLM equation to the inverse medium problem. This chapter is based on our paper [59]

### 3.1 Introduction

The so-called inverse medium problem appears in many applications, where one aims to reconstruct unknown coefficients of a (partial) differential equation from traces of its solution. This way, one can study materials and internal structures of media that are not directly accessible. In geophysics for example, a well-known inverse problem is the estimation of the medium parameters of a subsurface domain from seismic measurements, see for example [5]. Similar inverse problems can be also found in ultrasound and ultrasonic non-destructive testing see for example [34]. The governing equation in these applications is a variable coefficient wave equation, and the measurements consist of boundary traces of the wavefield for a number of frequencies. A variety of methods for solving the resulting inverse medium problem have been developed over the previous decades. We roughly divide these methods into two classes. On the one end of the spectrum one can find "modern" variational formulations (that are often solved iteratively), such as full waveform inversion, see for example [3]. On the other end, one can find classical inverse scattering methods, see for example [5, 19]. Recently, classical results from inverse scattering have found renewed interest in the geophysical community and hybrid methods have been proposed [23].

In this chapter we revisit one such classical method based on the Gelfand-Levitan-Marchenko (GLM) equation. In particular we focus on the derivation of a GLM equation corresponding to the scattering problem for the Helmholtz equation with form

$$\left\{ -\frac{d^2}{dx^2} + k^2 n(x) \right\} y(k, x) = k^2 y(k, x), \quad x \in \mathbb{R}, \quad (3.1)$$

$$y(k, \cdot) = y^i(k, \cdot) + y^s(k, \cdot), \quad (3.2)$$

$y^i(k, x) = e^{-ikx}$ ,  $x \in \mathbb{R}$  and asymptotic boundary conditions

$$\lim_{x \rightarrow \pm\infty} \left\{ \frac{dy^s(k, x)}{dx} \mp ik y^s(k, x) \right\} = 0. \quad (3.3)$$

Originally, the GLM equation is a fundamental relation that can be used to solve the Schrödinger inverse scattering problem on the line [39]. It relates scattering data (reflection measurements) with the so-called Jost solutions of the Schrödinger operator (plane wave like, right or left propagating solutions). It is also well known that the Helmholtz equation can be transformed to the Schrödinger equation using the travel time coordinate transform. Therefore, by changing the setting, it is sufficient to just focus on the study of the transformed system governed by the Schrödinger equation see for example [60, 15, 66]. This equivalence allows us to use a wealth of mathematical tools available from the Schrödinger scattering theory, including of course the GLM equation.

One advantage of this approach is that the path leading from the measurements (scattering data) to the parameter of the differential operator involves linear steps (as opposed to full waveform inversion for example). Although this approach is known for a very long time, it is only limited to the 1D case. In higher dimensional media it is impossible to transform the Helmholtz equation to the Schrödinger equation. The only exception to this is when the medium is laterally stratified, see e.g. [18]. This creates the need of the development of a GLM framework that avoids the use of a transformation to the Schrödinger setting. The first step towards developing this new inversion method is given in the 1D case with this chapter.

The following basic observation is the starting point of our analysis. Let  $u^+$  be the Jost solution of the Helmholtz equation (3.1). Contrary to the Schrödinger case, the function of the wave number

$$k \mapsto |e^{-ikx}u^+(k, x) - 1|$$

might not have a growing behaviour that allows the use of the classical Paley-Wiener theory, but still grows in a controlled way as  $|k|$  grows. This allows us to use a distributional setting which also permits the definition of the Fourier transform.

Our main contribution are:

- The extension of the so-called Povzner-Levitan representation to the Jost solutions of the Helmholtz scattering problem
- The derivation of a generalised GLM equation for the Helmholtz problem in the space of the tempered distributions.

This chapter is organized as follows. In section 3.2 we formulate the direct scattering problem and we review basic properties of the solutions of the forward problem. Then follows section 3.3 that contains the main result of the chapter (and of our paper [59]) and breaks down its proof in multiple lemmas. We continue with section 3.4 where we propose a practical way for solving the inverse medium problem using the main result, and we conclude the chapter with a discussion section.

## 3.2 Preliminaries

In this section we present some well-known results regarding the forward scattering problem for the Helmholtz equation on the line. In subsection 3.2.1 we formulate the forward scattering problem and we give the definition of the Jost solutions of the Helmholtz equation. In subsection 3.2.2 we recall some fundamental properties of the solutions of the forward scattering problem and we define the reflection and the transmission coefficients.

### 3.2.1 Forward Scattering Problem

We consider the forward scattering problem for the 1D Helmholtz operator on the real line described by equations (3.1)-(3.3). We assume that the real valued coefficient,  $n$ , is sufficiently smooth, having a compact support with form

$$\text{supp}(n) = (0, b), \quad (3.4)$$

for some  $b > 0$  and that  $1 - n > 0$ . Also, the incident wave field is a plane wave (incoming from the right  $(+\infty)$ ),  $y^i(k, x) = e^{-ikx}$ ,  $x \in \mathbb{R}$ . Working the same way as in [39] we reduce the Helmholtz differential equation to the following Volterra integral equations.

**Proposition 3.2.1.** *The solutions of the following integral equations*

$$u(x) = e^{ikx} - \int_x^\infty k \sin(k(x-t))n(t)u(t)dt \quad (3.5)$$

$$u(x) = e^{-ikx} + \int_{-\infty}^x k \sin(k(x-t))n(t)u(t)dt. \quad (3.6)$$

*satisfy the Helmholtz differential equation (3.1). The solutions of these integral equations are the Jost solutions of the Helmholtz equation. Also, the following asymptotic behaviour holds true for the unique solution of (3.5), let  $u^+(k, \cdot)$ . For  $k \in \mathbb{R}$  we get*

$$|u^+(k, x) - e^{ikx}| \leq$$

$$c(k, n) \frac{k^2}{1+|k|} (1 + \max\{-x, 0\}) \int_x^\infty (1+|t|)|n(t)|dt \quad (3.7)$$

and

$$|\partial_x u^+(k, x) - ike^{ikx}| \leq$$

$$c(k, n) \frac{k^2}{1+|k|} \int_x^\infty (1+|t|)|n(t)|dt.$$

*We get similar asymptotic behaviour for the left-going Jost solution,  $u^-$ , which solves equation (3.6).*

We obtain the above result working the same way as in [39, Chapter 4] for the scattering potential  $Q := k^2 n$ . Also,  $c(k, n)$  grows faster than an exponential function as a function of  $k$ . Finally, we define the Fourier transform as

$$\widehat{f}(t) = (\mathcal{F}f)(t) = \frac{1}{\pi} \int_{\mathbb{R}} f(k) e^{2ikt} dk, t \in \mathbb{R},$$

$$f(k) = (\mathcal{F}^{-1}\widehat{f})(k) = \int_{\mathbb{R}} \widehat{f}(t) e^{-2ikt} dt, k \in \mathbb{R},$$

for  $f \in \mathcal{S}(\mathbb{R})$  (Schwartz functions).

### 3.2.2 Basic Properties of the Solutions of the Forward Problem

In this subsection we present essential properties of the Jost solutions and in turn of the solutions of the forward problem. Again, the next result is classic and we refer to [39] for its proof.

**Proposition 3.2.2.** *Let  $k \in \mathbb{R} \setminus \{0\}$  and  $f, g \in H_{loc}^2(\mathbb{R})$  solutions to the Helmholtz differential equation. Then the Wronskian of the two solutions  $W(f, g)$  is constant. In particular we get for the Jost solutions*

$$W(u^+(k, \cdot), u^+(-k, \cdot)) = -2ik$$

and

$$W(u^-(k, \cdot), u^-(-k, \cdot)) = 2ik.$$

**Remark 3.2.1.** *Since the solution space for the Helmholtz differential equation is 2-dimensional, we obtain that*

$$u^-(k, x) = a_k^+ u^+(k, x) + b_k^+ u^+(-k, x) \quad (3.8)$$

and

$$u^+(k, x) = a_k^- u^-(k, x) + b_k^- u^-(-k, x) \quad (3.9)$$

for  $x \in \mathbb{R}$ . This implies that

$$\begin{aligned} 2ik &= W(u^-(k, \cdot), u^-(-k, \cdot)) = \\ &W(a_k^+ u^+(k, \cdot) + b_k^+ u^+(-k, \cdot), a_{-k}^+ u^+(-k, \cdot) + b_{-k}^+ u^+(k, \cdot)) \Rightarrow \\ &1 = |b_k^+|^2 - |a_k^+|^2. \end{aligned} \quad (3.10)$$

**Remark 3.2.2.** For  $k \in \mathbb{R} \setminus \{0\}$  we define the reflection and the transmission coefficients as

$$T(k) = \frac{1}{b_k^+} \quad (3.11)$$

and

$$R^+(k) = \frac{a_k^+}{b_k^+}, \quad (3.12)$$

respectively. The  $+$  superscript in the reflection coefficient denotes reflection caused by an incoming plane wave from the right. Similarly we can define  $R^-$ , see figures 3.1 and 3.2 (assuming  $k > 0$  to make sense of "right" and "left").

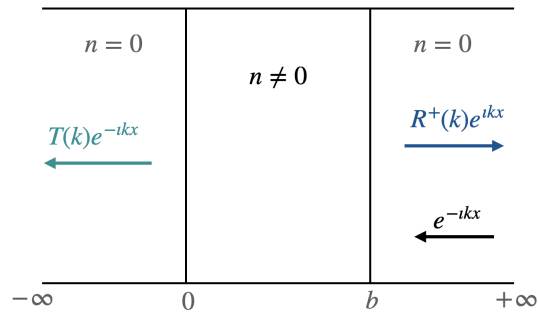


Figure 3.1:  $y^i = e^{-ik \cdot}$  enters from  $+\infty$  and creates reflection and transmission responses  $R^+$ ,  $T$  respectively.

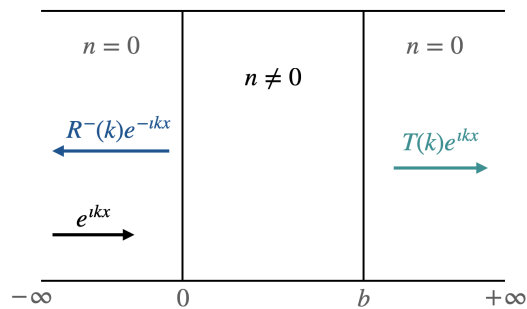


Figure 3.2:  $y^i = e^{ik \cdot}$  enters from  $-\infty$  and creates reflection and transmission responses  $R^-$ ,  $T$  respectively.



The transmission coefficient is the same regardless of right or left side of incidence. This is known as transmission reciprocity, see [49]. Therefore, using (3.10) we obtain the conservation of energy

$$|T(k)|^2 + |R^\pm(k)|^2 = 1, \quad k \in \mathbb{R} \setminus \{0\}. \quad (3.13)$$

Now, similarly to the Schrödinger equation case, the solution of the forward problem, (3.1)-(3.3), for  $k \in \mathbb{R} \setminus \{0\}$ , can be decomposed as

$$y(k, x) = T(k)u^-(k, x) = u^+(-k, x) + R^+(k)u^+(k, x), \quad (3.14)$$

for  $x \in \mathbb{R}$ . Finally, we get the following relations for  $k \in \mathbb{R} \setminus \{0\}$

$$R^+(k) = \frac{k}{2i} \int_{\mathbb{R}} n(x)y(k, x)e^{-ikx} dx \quad (3.15)$$

and

$$T(k) = 1 + \frac{k}{2i} \int_{\mathbb{R}} n(x)y(k, x)e^{ikx} dx. \quad (3.16)$$

### 3.3 Main Result

In this section we present our main finding, which is a generalized Gelfand-Levitan-Marchenko equation for the 1D Helmholtz scattering problem. The difference between our finding and the classical Gelfand-Levitan-Marchenko equation for the 1D Schrodinger scattering is the mathematical setting. In the latter case we are working in an  $L^2$ -setting due to the sufficiently regular asymptotic behaviour of the Schrödinger-Jost solution as a function of the wave-number. In our Helmholtz case we have a "less regular" asymptotic behaviour that requires the use of tempered distributions to do calculations. The following theorem is the main result of this chapter.

**Theorem 3.3.1.** *Let the Jost solution,  $u^+$ , of the Helmholtz problem, a fixed  $x \in \mathbb{R}$  and define*

$$v^+(k, x) := e^{-ikx}u^+(k, x).$$

*There exists a unique kernel  $B_x^+ \in \mathcal{S}'(\mathbb{R})$  such that*

$$v^+(k, x) = 1 + \pi \mathcal{F} B_x^+(k), \quad k \in \mathbb{R}. \quad (3.17)$$

*This kernel can be decomposed as*

$$B_x^+ = B_x^{+,L^p} + B_x^{+,\mathcal{G}'} \quad (3.18)$$

with  $B_x^{+,L^p} \in \cap_{p=1}^{\infty} L^p(\mathbb{R})$ , and  $B_x^{+,\mathcal{E}'} \in \mathcal{E}'(\mathbb{R})$ . Furthermore, the following GLM-like relation holds true in  $\mathcal{S}'(\mathbb{R})$

$$B_x^+ + K^+(x + \cdot) + K^+(x + \cdot) \star B_x^+ = \mathcal{F} \{k \mapsto T(k)v^-(k, x) - 1\} \quad (3.19)$$

with  $\star$  denoting correlation, and

$$K^+ = \mathcal{F}R^+ \in L^2(\mathbb{R}). \quad (3.20)$$

**Remark 3.3.1.** *It is clear that relation (3.19) has exactly the same form as in the Schrödinger case. In section 3.4 we will discuss the use of this GLM-type relation. We can derive a similar GLM expression for  $B^-$  using  $K^- = \mathcal{F}R^-$ .*

We will break down the proof of theorem 3.3.1 in multiple lemmas. At the end of section (3.3) we will combine the results to the proof of the main theorem.

### 3.3.1 Generalised Povzner-Levitan Representation

Similarly to the Schrödinger equation case, in this section we obtain a generalized Povzner-Levitan representation for the right-going Jost solution of the Helmholtz equation. The major difference between the Schrödinger and the Helmholtz case is that in the latter equation case we must work in a distributional setting. We show that the Jost solutions  $u^\pm(\cdot, x)$  behave "nicely" at infinity as a functions of  $k$ . But before elaborating more on our theory, for the sake of completeness we show how one can transform the Helmholtz equation to the Schrodinger equation using the travel-time transform. We only use the equivalence between the Helmholtz and the Schrödinger problems to show the Povzner-Levitan representation and to show regularity properties of the kernel and of the scattering data. It is important to notice that the travel time transformation is the mean to show the generalized Povzner-Levitan representation. Obviously this particular writing for the Jost solutions holds true independently of how one shows it. But possibly the simplest way to prove it is the one we follow.

We define the new travel-time variable as

$$z(x) = \int_0^x \sqrt{m(y)} dy, \quad x \in \mathbb{R}, \quad (3.21)$$

with  $m = 1 - n > 0$ . The scattering potential,  $q$ , depends only on  $m$  and it is defined similarly as in the acoustic case, see [66, 15] Also  $q$  is compactly supported on  $(0, z(b))$ , see e.g. [2]. The new equation now is

$$\left\{ -\frac{d^2}{dz^2} + q(z) \right\} f(k, z) = k^2 f(k, z), \quad z \in \mathbb{R}. \quad (3.22)$$

Assuming that  $u$  solves the Helmholtz differential equation,  $f$  is connected with  $u$  via the formula

$$f(k, z(x)) = \theta(x)u(k, x) \quad (3.23)$$

with  $\theta(x) = (m(x))^{1/4}$ . The following result follows.

**Proposition 3.3.1.** *Let the Jost solutions,  $u^\pm(k, \cdot)$  of (3.1) and  $f^\pm(k, \cdot)$  of (3.22). We get that*

$$f^+(k, z(x)) = \theta(x)e^{ik(I_b - b)}u^+(k, x), \quad x \in \mathbb{R}, \quad (3.24)$$

and

$$f^-(k, z(x)) = \theta(x)u^-(k, x), \quad x \in \mathbb{R}, \quad (3.25)$$

with  $I_b = \int_0^b \sqrt{m(y)}dy$ .

*Proof.* Let the Jost solution of the Helmholtz equation,  $u^+(k, \cdot)$  with

$$u^+(k, x) = e^{ikx}, \quad x > b.$$

We want to show that the Jost solutions of equations (3.22) and (3.1) respectively are related. By relation (3.23) we get that  $u^+(k, \cdot)$  is related to a solution  $f(k, \cdot)$  of the Schrödinger equation with  $f(k, z(x)) = \theta(x)u^+(k, x)$ ,  $x \in \mathbb{R}$ . This gives

$$f(k, z(x)) = e^{ikx}, \quad x > b \quad (z(x) > z(b)). \quad (3.26)$$

Keep in mind that  $\theta(x) = 1$  if  $x > b$ . Now for  $x > b$  we also get

$$z(x) = \int_0^b \sqrt{m(y)}dy + \int_b^x dy = I_b + (x - b).$$

Combining the above, (3.26) gives

$$f(k, z(x))e^{ik(I_b - b)} = e^{ikx}e^{ik(I_b - b)} = e^{ikz(x)}, \quad x > b.$$

Therefore  $e^{ik(I_b - b)}f(k, \cdot)$  solves the Schrödinger equation and behaves as a plane wave when  $z > z(b)$ . Now, since the solution space of the Schrödinger equation is spanned by the Jost solutions  $f^+(k, \cdot), f^+(-k, \cdot)$  we get

$$e^{ik(I_b - b)}f(k, z) = a_1f^+(k, z) + b_1f^+(-k, z), \quad z \in \mathbb{R} \Rightarrow$$

$$e^{ik(I_b-b)} f(k, z) = a_1 e^{ikz} + b_1 e^{-ikz}, \quad z > z(b). \quad (3.27)$$

Therefore,  $a_1 = 1$  and  $b_1 = 0$ , thus

$$e^{ik(I_b-b)} f(k, z) = f^+(k, z), \quad z \in \mathbb{R}. \quad (3.28)$$

Similarly, for the left propagating Jost solution we get

$$u^-(k, x) = e^{-ikx}, \quad x < 0. \quad (3.29)$$

Since  $z = x$ ,  $\theta(x) = 1$  for  $x < 0$  we obtain that  $g = \theta u^-$  solves the Schrödinger equation and for  $x < 0$

$$e^{-ikx} = e^{-ikz} = g(k, z) \Rightarrow \quad (3.30)$$

$$g(k, z) = f^-(k, z(x)) = \theta(x) u^-(k, x), \quad x \in \mathbb{R}. \quad (3.31)$$

□

**Remark 3.3.2.** *In view of relations (3.24) and (3.25) the Jost solutions  $u^\pm(\cdot, x)$  are continuous as functions of  $k$  see [39, Corollary 4.1.4, Theorem 4.1.8]. We can also define complex analytic extensions of the Jost solutions.*

Using the above results we show the following distributional Povnzer-Levitan representation for the right-going Jost solution,  $u^+$  of the Helmholtz equation. Before proceeding to the result we remind the reader a basic result from the theory of distributions.

**Lemma 3.3.1.** *Let a function  $f \in L^1_{loc}(\mathbb{R}; \mathbb{C})$ , such that  $|f(x)| = O(1 + |x|)$ ,  $|x| \rightarrow \infty$ . Then the map  $\mathcal{S}'(\mathbb{R}) \ni \phi \mapsto \int_{\mathbb{R}} f(x)\phi(x)dx$  defines an element of  $\mathcal{S}'(\mathbb{R})$ .*

*Proof.* See [32, page 105]. □

**Lemma 3.3.2.** *Let  $x \in \mathbb{R}$  fixed. Then there exists a tempered distribution  $V_x^+ = V^+(x, \cdot)$  such that*

$$\mathbb{R} \ni k \mapsto v^+(k, x) = 1 + \mathcal{F}^{-1} V_x^+(k), \quad \text{is in } \mathcal{S}'(\mathbb{R}) \quad (3.32)$$

*as an  $L^1_{loc}(\mathbb{R})$  function that defines distribution through integration.*

*Proof.* Let  $x$  fixed and  $k \in \mathbb{R}$ . We can change the spatial variable using relation (3.21). Since

$$f^+(k, z) = \theta(x)e^{ik(I_b-b)}u^+(k, x), \quad x \in \mathbb{R}, \quad (3.33)$$

we set  $\tilde{\theta} = \theta e^{ik(I_b-b)}$  and we obtain

$$|u^+(k, x) - e^{ikx}| = \left| \frac{f^+(k, z)}{\tilde{\theta}(x)} - e^{ikx} \right| \leq \quad (3.34)$$

$$\left| \frac{f^+(k, z)}{\tilde{\theta}(x)} - \frac{e^{ikz}}{\tilde{\theta}(x)} \right| + \left| \frac{e^{ikz}}{\tilde{\theta}(x)} - e^{ikx} \right| \leq \quad (3.35)$$

$$\frac{1}{|\theta(x)|} |f^+(k, z) - e^{ikz}| + 1 + \frac{1}{|\theta(x)|}. \quad (3.36)$$

Now, we know that for  $k \in \mathbb{R}$ , the Jost solution of the Schrödinger problem has the following behaviour,

$$|f^+(k, z) - e^{ikz}| \leq \frac{C(q)(1 + \max\{-z, 0\})}{1 + |k|} \int_z^\infty (1 + |z|)q(z)dz, \quad (3.37)$$

see [39, chapter 4]. Therefore, for fixed  $x$  the map

$$\mathbb{R} \ni k \mapsto |u^+(k, x) - e^{ikx}| \quad (3.38)$$

behaves asymptotically at most as a constant  $A \in \mathbb{R}$ . Similarly,

$$\mathbb{R} \ni k \mapsto |u^+(k, x)e^{-ikx} - 1| \quad (3.39)$$

behaves at most as a constant, therefore it defines a tempered distribution as a locally integrable function. Now, since the Fourier transform is a homeomorphism

$$\mathcal{F} : \mathcal{S}'(\mathbb{R}) \rightarrow \mathcal{S}'(\mathbb{R})$$

and similarly

$$\mathcal{F}^{-1} : \mathcal{S}'(\mathbb{R}) \rightarrow \mathcal{S}'(\mathbb{R})$$

is also a homeomorphism (onto), there exist a tempered distribution  $V^+(x, \cdot) \in \mathcal{S}'(\mathbb{R})$  such that

$$\mathbb{R} \ni k \mapsto u^+(k, x)e^{-ikx} = 1 + \mathcal{F}^{-1}V_x^+(k), \quad \text{in } \mathcal{S}'(\mathbb{R}). \quad (3.40)$$

□

**Corollary 3.3.1.** *Let  $x \in \mathbb{R}$  fixed. The function*

$$\mathbb{R} \ni k \mapsto u^\pm(k, x) e^{\mp ikx} \quad (3.41)$$

*defines a tempered distribution as a locally integrable function.*

**Remark 3.3.3.** *In the Schrödinger equation case, it is well known that the Fourier kernel of the Povzner-Levitan representation is supported in  $\mathbb{R}_{>0}$ . In the next section we will clarify what the support of  $V^+(x, \cdot)$  is.*

**Remark 3.3.4.** *We can also write*

$$\mathbb{R} \ni k \mapsto v^+(k, x) = 1 + \pi \mathcal{F} B_x^+ \quad (3.42)$$

with  $B_x^+ = \mathcal{R}V_x^+$ ,

$$\mathcal{R}\phi(x) = \phi(-x), \quad x \in \mathbb{R},$$

for  $\phi \in \mathcal{S}(\mathbb{R})$ . Obviously, we have a similar writing for  $v^-$ .

### 3.3.2 Properties of the GLM Kernel and of the Scattering Data

Essentially, we can consider the quantities involved in the GLM equation only as distributions. But the equivalence between the Schrödinger and the Helmholtz equation in 1D naturally lets us to "gain more regularity" for the scattering data and the kernel  $B_x^+$ . Our GLM equation would still hold but it would be given in a more abstract form than its current compact writing (3.19). Following the classical method of associating the Helmholtz equation with the Schrödinger equation, we obtain that the associated Schrödinger scattering problem is

$$\left\{ -\frac{d^2}{dz^2} + q(z) \right\} f(k, z) = k^2 f(k, z) \quad (3.43)$$

$$f(k, z) = e^{-ikz} + f^s(k, z) \quad (3.44)$$

$$\lim_{z \rightarrow \pm\infty} \left\{ \frac{d}{dz} f^s(k, z) \mp ik f^s(k, z) \right\} = 0 \quad (3.45)$$

**Remark 3.3.5.** *Take a solution, let  $u$ , of the Helmholtz scattering problem. Define*

$$\tilde{f} = \theta u. \quad (3.46)$$

$\tilde{f}$  now solves the Schrödinger equation as we have discussed, and we would like to see how  $\tilde{f}$  compares with the solution of the Schrödinger scattering problem. First, observe that

$$\tilde{f}(k, z) = \theta(x)u(k, x) = \theta(x)\{u^+(-k, x) + R^+(k)u^+(k, x)\} = \quad (3.47)$$

$$\theta(x)\left\{\frac{e^{ik(I_b-b)}}{\theta(x)}f^+(-k, z) + R^+(k)\frac{e^{-ik(I_b-b)}}{\theta(x)}f^+(k, z)\right\}, \quad (3.48)$$

$x \in \mathbb{R}$ . This gives

$$\tilde{f}(k, z)e^{-ik(I_b-b)} = f^+(-k, z) + R^+(k)e^{-2ik(I_b-b)}f^+(k, z). \quad (3.49)$$

Similarly,

$$\tilde{f}(k, z) = T(k)u^-(k, x)\theta(x) = T(k)f^-(k, z). \quad (3.50)$$

Therefore

$$\tilde{f}(k, z)e^{-ik(I_b-b)} \sim e^{-ikz} + R^+(k)e^{-2ik(I_b-b)}e^{ikz}, \quad z \rightarrow \infty,$$

and

$$\tilde{f}(k, z)e^{-ik(I_b-b)} \sim e^{-ik(I_b-b)}T(k)e^{-ikz}, \quad z \rightarrow -\infty.$$

Since  $\tilde{f}(k, z)e^{-ik(I_b-b)} - e^{-ikz}$ ,  $z \in \mathbb{R}$ , is radiating (i.e. satisfies (3.45)), and since solutions of the scattering problem are unique, we obtain that

$$\tilde{R}^+(k) = R^+(k)e^{-2ik(I_b-b)} \quad \text{and} \quad \tilde{T}(k) = T(k)e^{-ik(I_b-b)},$$

where  $\tilde{R}^+$  and  $\tilde{T}$  are the reflection and transmission coefficients of the Schrödinger scattering problem respectively.

The previous remark leads to the following proposition.

**Proposition 3.3.2.** *The following relations hold true,*

$$|R^+(k)| = |\tilde{R}^+(k)|, \quad \forall k \in \mathbb{R} \setminus \{0\}, \quad (3.51)$$

$$|T(k)| = |\tilde{T}(k)|, \quad \forall k \in \mathbb{R} \setminus \{0\}. \quad (3.52)$$

We also get the following.

**Corollary 3.3.2.**  $K^+ = \mathcal{F}R^+$  is a well defined  $L^2(\mathbb{R})$ -element.

*Proof.* For the Schrödinger equation case the reflection coefficient is an element of  $L^2(\mathbb{R})$ , see [39]. Since the absolute values of the  $R^+$  and  $\tilde{R}^+$  coincide we get the result.  $\square$

**Lemma 3.3.3.** Let  $x \in \mathbb{R}$ . Then  $V_x^+ \in \mathcal{S}'(\mathbb{R})$  is a distribution that consists of a singular part and an  $L^p$ -part. The same holds for  $B_x^+$ .

*Proof.* Let  $x \in \mathbb{R}$ . We get for  $k \in \mathbb{R}$

$$e^{-ikx}u^+(k, x) = 1 + \mathcal{F}^{-1}V_x^+(k) \quad (3.53)$$

and

$$e^{-ikz(x)}f^+(k, z(x)) = 1 + \mathcal{F}^{-1}\tilde{V}_{z(x)}^+(k), \quad (3.54)$$

using the classical Paley-Wiener theory to the solution of the Jost solution  $f^+$ , see [39]. Now, we use relation (3.24) and we get

$$e^{-ikz(x)}\theta(x)e^{ik(I_b-b)}u^+(k, x) = 1 + \mathcal{F}^{-1}\tilde{V}_{z(x)}^+(k) \Rightarrow$$

$$e^{-ikz(x)}\theta(x)e^{ik(I_b-b)}e^{ikx}\left(1 + \mathcal{F}^{-1}V_x^+(k)\right) =$$

$$1 + \mathcal{F}^{-1}\tilde{V}_{z(x)}^+(k).$$

We define  $\lambda = (\lambda(x) = )z(x) - x - I_b + b$ , thus

$$\theta(x)e^{-ik\lambda} + \theta(x)e^{-ik\lambda}\mathcal{F}^{-1}V_x^+(k) = 1 + \mathcal{F}^{-1}\tilde{V}_{z(x)}^+(k) \Rightarrow \quad (3.55)$$

$$\theta(x)e^{-ik\lambda}\mathcal{F}^{-1}V_x^+(k) = -\theta(x)e^{-ik\lambda} + 1 + \mathcal{F}^{-1}\tilde{V}_{z(x)}^+(k) \Rightarrow \quad (3.56)$$

$$\mathcal{F}^{-1}V_x^+(k) = -1 + \frac{e^{ik\lambda}}{\theta(x)} + \frac{e^{ik\lambda}}{\theta(x)}\mathcal{F}^{-1}\tilde{V}_{z(x)}^+(k). \quad (3.57)$$

Now since  $\tilde{V}_{z(x)}^+ \in L^p(\mathbb{R})$  for every  $p \in [1, \infty]$  and since the Fourier transform of complex exponential functions are Dirac-delta distributions we obtain the result.  $\square$

**Remark 3.3.6.** We can identify the support of  $V_x^+$  in view of relation (3.57). Moreover, (3.57) gives a full description of the singularities of the kernel  $V_x^+$ .



### 3.3.3 Proof of Theorem 3.3.1

In this subsection we combine our findings and give the proof of our main result.

*Theorem 3.3.1.* Let  $x \in \mathbb{R}$ . The scattering identity that describes the solutions of the forward problem reads

$$y(k, x) = T(k)u^-(k, x) = u^+(-k, x) + R^+(k)u^+(k, x),$$

$k \in \mathbb{R} \setminus \{0\}$ . As before, we set  $v^\pm(k, x) = e^{\mp ikx}u^\pm(k, x)$  and we take

$$T(k)v^-(k, x) = v^+(-k, x) + R^+(k)e^{2ikx}v^+(k, x), \quad k \in \mathbb{R} \setminus \{0\}. \quad (3.58)$$

We can view relation (3.58) in  $\mathcal{S}'(\mathbb{R})$  since  $v^\pm(\cdot, x) \in \mathcal{S}'(\mathbb{R})$  (corollary 3.3.1) and  $|T|, |R^+| < 1$ . We get  $\forall \psi \in \mathcal{S}(\mathbb{R})$

$$\begin{aligned} \langle \mathcal{F}\{k \mapsto T(k)v^-(k, x)\}, \psi \rangle &= \langle \mathcal{F}\{k \mapsto v^+(-k, x)\}, \psi \rangle + \\ &\langle \mathcal{F}\{k \mapsto R^+(k)e^{2ikx}v^+(k, x)\}, \psi \rangle, \end{aligned} \quad (3.59)$$

(with the sense that we transform the distributions that are defined through integration). Using relation (3.32) we get

$$\begin{aligned} \mathbb{R} \ni k \mapsto v^+(-k, x) &= 1 + (\mathcal{F}^{-1}V_x^+)(-k) = \\ &1 + (\mathcal{R}\mathcal{F}^{-1}V_x^+)(k), \end{aligned} \quad (3.60)$$

therefore we obtain

$$\begin{aligned} \langle \mathcal{F}\{k \mapsto T(k)v^-(k, x) - 1\}, \psi \rangle &= \langle \mathcal{F}\mathcal{R}\mathcal{F}^{-1}V_x^+, \psi \rangle + \\ &\langle \mathcal{F}\{k \mapsto R^+(k)e^{2ikx}, \psi \rangle + \\ &\langle \mathcal{F}\{k \mapsto R^+(k)e^{2ikx}(\mathcal{F}^{-1}V_x^+)(k)\}, \psi \rangle. \end{aligned} \quad (3.61)$$

Now, for  $\phi \in \mathcal{S}(\mathbb{R})$

$$\langle \mathcal{F}\mathcal{R}\mathcal{F}^{-1}V_x^+, \phi \rangle = \langle \mathcal{R}\mathcal{F}^{-1}V_x^+, \mathcal{F}\phi \rangle = \quad (3.62)$$

$$\begin{aligned}
\langle \mathcal{F}^{-1}V_x^+, \mathcal{R}\mathcal{F}\phi \rangle &= \langle \mathcal{F}^{-1}V_x^+, \mathcal{F}\mathcal{R}\phi \rangle = \langle \mathcal{F}\mathcal{F}^{-1}V_x^+, \mathcal{R}\phi \rangle \\
&= \langle \mathcal{R}V_x^+, \phi \rangle.
\end{aligned} \tag{3.63}$$

Therefore we have for the first term of (3.61) that

$$\mathcal{F}\mathcal{R}\mathcal{F}^{-1}V_x^+ = \mathcal{R}V_x^+, \text{ in } \mathcal{S}'(\mathbb{R}). \tag{3.64}$$

Now, observe that  $R^+ = \mathcal{F}^{-1}(K^+)$  and  $\mathcal{F}^{-1}\delta_{-x} = k \mapsto e^{2ikx}$ . We take for  $\psi \in \mathcal{S}(\mathbb{R})$

$$\langle \mathcal{F}\{k \mapsto R^+(k)e^{2ikx}\}, \psi \rangle = \langle \mathcal{F}\{\mathcal{F}^{-1}K^+\mathcal{F}^{-1}\delta_{-x}\}, \psi \rangle = \tag{3.65}$$

$$\langle \mathcal{F}\mathcal{F}^{-1}(K^+ * \delta_{-x}), \psi \rangle = \langle K^+(x+\cdot), \psi \rangle. \tag{3.66}$$

Now, since  $V_x^+ = V_x^{+, \mathcal{E}'} + V_x^{+, L^p}$  the convolution of  $V_x^+$  and the shifted scattering data  $K^+(x+\cdot) \in L^2(\mathbb{R})$  makes sense and we obtain

$$\begin{aligned}
k \mapsto R^+(k)e^{2ikx}(\mathcal{F}^{-1}V_x^+)(k) &= \mathcal{F}^{-1}(K^+(x+\cdot))\mathcal{F}^{-1}(V_x^+) = \\
&\mathcal{F}^{-1}(K^+(x+\cdot) * V_x^+).
\end{aligned}$$

Combining the above we get

$$\begin{aligned}
\mathcal{F}\{k \mapsto R^+(k)e^{2ikx}(\mathcal{F}^{-1}V_x^+)(k)\} &= K^+(x+\cdot) * V_x^+ = \\
&K^+(x+\cdot) \star \mathcal{R}V_x^+,
\end{aligned} \tag{3.67}$$

where for tempered distributions we define  $f \star g = f * \mathcal{R}g$ . Now putting all of our findings together we get that

$$\begin{aligned}
\mathcal{R}V_x^+ + K^+(x+\cdot) + K^+(x+\cdot) \star \mathcal{R}V_x^+ &= \\
\mathcal{F}\{k \mapsto T(k)v^-(k, x) - 1\}
\end{aligned} \tag{3.68}$$

or equivalently

$$B_x^+ + K^+(x+\cdot) + K^+(x+\cdot) \star B_x^+ = \mathcal{F}\{k \mapsto T(k)v^-(k, x) - 1\} \tag{3.69}$$

□

### 3.4 Inversion

In this section we use some of our theoretical findings to propose a practical method for solving the inverse medium problem. The right hand side of the GLM equation (3.19) depends on unknown quantities assuming that we only consider one-sided reflection measurements. To get around this obstacle we will need to consider two sided data, namely,  $R^+, R^-, T$ , for all frequencies. Using them, we can form a coupled system for the GLM kernels  $B^+, B^-$  of the right and left-going Jost solutions respectively. After obtaining the Jost solutions, then either using equations (3.5)-(3.6) or the equation error method [8], we can obtain the coefficient of the Helmholtz operator.

First, observe that we can write  $T(k) = 1 + \tau(k)$   $k \in \mathbb{R} \setminus \{0\}$  with  $\tau(k) = \frac{k}{2i} \int_{\mathbb{R}} n(x)y(k,x)e^{ikx}dx$ .  $\tau$  is also well defined. Now, for fixed  $x \in \mathbb{R}$  we have that

$$u^-(k,x)e^{ikx} = 1 + \mathcal{F}^{-1}V_x^-(k), \quad k \in \mathbb{R}. \quad (3.70)$$

Considering this, we can compute the right hand side of the GLM equation as

$$\text{r.h.s.} = \mathcal{F}\{(1 + \tau)(1 + \mathcal{F}^{-1}V_x^-) - 1\}. \quad (3.71)$$

The argument of the Fourier transform is  $(1 + \tau)(1 + \mathcal{F}^{-1}V_x^-) - 1 = 1 + \tau + \mathcal{F}^{-1}V_x^- + \tau\mathcal{F}^{-1}V_x^- - 1 = \tau + \mathcal{F}^{-1}V_x^- + \tau\mathcal{F}^{-1}V_x^-$ . Therefore

$$\begin{aligned} \mathcal{F}\{\tau + \tau\mathcal{F}^{-1}V_x^- + \mathcal{F}^{-1}V_x^-\} &= L + L * V_x^- + V_x^- = \\ &L + L * B_x^- + \mathcal{R}B_x^- \end{aligned} \quad (3.72)$$

with  $B_x^- = \mathcal{R}V_x^-$  and  $L = \mathcal{F}\tau$ . We can set up an auxiliary scattering problem of the following form. We consider an incident wave travelling from  $-\infty$  to  $+\infty$  of the form  $u^i(k,x) = e^{ikx}$ ,  $x \in \mathbb{R}$ . The scattering identity of this problem is

$$u^-(-k,x) + R^-(k)u^-(k,x) = T(k)u^+(k,x). \quad (3.73)$$

As before, we compute

$$\begin{aligned} u^-(-k,x)e^{-ikx} + R^-(k)u^-(k,x)e^{-ikx}e^{ikx}e^{-ikx} = \\ T(k)u^+(k,x)e^{-ikx} \iff \end{aligned} \quad (3.74)$$

$$v^-(-k,x) + R^-(k)v^-(k,x)e^{-2ikx} = T(k)v^+(k,x) \iff \quad (3.75)$$

$$\begin{aligned} \mathcal{F}^{-1}V_x^-(k) + R^-(k)e^{-2ikx} + R^-(k)e^{-2ikx} \mathcal{F}^{-1}V_x^-(k) = \\ T(k)v^+(k, x) - 1. \end{aligned} \quad (3.76)$$

Now, we compute the Fourier transform to obtain

$$\begin{aligned} \mathcal{R}V_x^- + K^-(-x + \cdot) + K^-(-x + \cdot) * V_x^- = \\ \mathcal{F}\{T(k)v^+(k, x) - 1\}. \end{aligned} \quad (3.77)$$

Therefore, we get the GLM equation

$$\begin{aligned} B_x^- + K^-(-x + \cdot) + K^-(-x + \cdot) * B_x^- =, \\ \mathcal{F}\{k \mapsto T(k)v^+(k, x) - 1\} \end{aligned} \quad (3.78)$$

with  $\mathcal{R}V_x^- = B_x^-$ . Similarly as before, we obtain

$$\mathcal{F}\{k \mapsto T(k)v^+(k, x) - 1\} = L + L * B_x^- + \mathcal{R}B_x^- \quad (3.79)$$

Combining our findings we are left with a system of two equations and two unknowns,  $B_x^-, B_x^+$

$$B_x^+ + K^+(x + \cdot) + K^+(x + \cdot) * B_x^+ = L + L * B_x^- + \mathcal{R}B_x^- \quad (3.80)$$

$$B_x^- + K^-(-x + \cdot) + K^-(-x + \cdot) * B_x^- = L + L * B_x^+ + \mathcal{R}B_x^+ \quad (3.81)$$

Assuming the knowledge of discrete  $K^+, K^-$  and  $L$  we can solve for the GLM kernels  $B_x^+$  and  $B_x^-$ . The solution of the system can be found using a conventional least squares solver, see [60]. Once we know  $B_x^+$ , we also know  $u^+$  (relation (3.17)). Thus we can solve for  $n$  in (3.5). Alternatively, we can use the equation error method, see [8], to obtain  $n$ , since  $u^+$  also obeys the Helmholtz equation.

**Remark 3.4.1.** *The coupled system of equations (3.80) and (3.81) yields the exact solutions  $B_x^\pm$  assuming  $K^\pm$  and  $L$ . Though one could consider only one sided reflection data and solve only (3.80) (or (3.81)) by approximating its right hand side with zero for example. For a discussion and comparison of the use of one sided versus two sided data for the computational solution of an inverse problem of estimating a diffusion potential from boundary measurements we refer to [25].*

### 3.5 Discussion and Conclusions

We have revisited the classical 1D Helmholtz scattering problem and we have derived a generalised Gelfand-Levitan-Marchenko equation in the space of tempered distributions. In particular, we showed that the Jost solution of the Helmholtz equation minus a plane wave grows in a controlled way as the wave number grows. This allows us to consider a distributional framework where we derived a generalized version of the Gelfand-Levitan-Marchenko equation. We finally discussed a way to solve the inverse medium-problem using 2-sided data, whereas one-sided should theoretically suffice. In the future we will seek an explanation on why this is the case.

Recently, GLM-like methods have received renewed attention, especially in the area of seismic imaging. Though, the most significant limitation of GLM-like approaches for the Helmholtz equation is the difficulty of extending them in higher dimensional media. Without assuming symmetry to the medium (e.g. laterally stratified) we cannot transform the Helmholtz equation to the Schrödinger equation. With our new point of view, we believe that we have made a first step towards a possible extension of this particular GLM method to 2 and 3D Helmholtz scattering problems using the least amount of a-priori assumptions.

### 3.6 Appendix: Calculations with Distributions and Schwartz Functions

In this last part of the chapter we recall certain properties of distributions that we used above.

$$\begin{aligned} \frac{1}{2\pi} \int_{\mathbb{R}} e^{i\omega t} d\omega = \delta(t) &\iff \frac{1}{2\pi} \int_{\mathbb{R}} e^{2ikt} 2dk = \\ &\frac{1}{\pi} \int_{\mathbb{R}} e^{2ikt} dk = \delta(t) \end{aligned} \quad (3.82)$$

According to our notation

$$\mathcal{F}(1)(t) = \delta(t). \quad (3.83)$$

Similarly

$$\frac{1}{\pi} \int_{\mathbb{R}} e^{2ikt} e^{2ikg} dk = \frac{1}{\pi} \int_{\mathbb{R}} e^{2ik(t+g)} dk = \delta(t+g) \quad (3.84)$$

therefore

$$\mathcal{F}(e^{2ikg}) = \delta(t+g). \quad (3.85)$$

Similarly

$$\begin{aligned} \frac{1}{\pi} \int_{\mathbb{R}} e^{2ikt} e^{ikg} dk &= \frac{1}{\pi} \int_{\mathbb{R}} e^{2ik(t+\frac{g}{2})} dk = \frac{1}{\pi} \int_{\mathbb{R}} e^{ik(2t+g)} dk = \\ &= \frac{2}{2\pi} \int_{\mathbb{R}} e^{ik(2t+g)} dk = 2\delta(2t+g) \end{aligned} \quad (3.86)$$

therefore

$$\mathcal{F}(e^{ikg}) = 2\delta(2t+g) = \delta\left(t + \frac{g}{2}\right). \quad (3.87)$$

Another important property is the following

$$(\delta_a * f)(t) = f(t-a) \quad (3.88)$$

for  $f \in L^2(\mathbb{R})$  with  $\delta_a(t) = \delta(t-a)$ . Also previously, using the  $\mathcal{R}$  (reflection) operator we exchanged between the convolution and the correlation of distributions. Assuming a function  $b \in \mathcal{S}(\mathbb{R})$  we get

$$(K(x+\cdot) * b)(t) = \int_{\mathbb{R}} K(x+z)b(t-z)dz. \quad (3.89)$$

Now we set  $\zeta = -t+z$  and obtain  $z = t+\zeta$ . We get

$$\begin{aligned} (K(x+\cdot) * b)(t) &= \int_{\mathbb{R}} K(x+t+\zeta)b(-\zeta)d\zeta = \\ &= (K(x+\cdot) \star \mathcal{R}b)(t) \end{aligned} \quad (3.90)$$

For tempered distributions we define

$$\langle \mathcal{R}f, \phi \rangle = \langle f, \mathcal{R}\phi \rangle$$

see [31, page 334]. Also  $\mathcal{R}^2 = I$  since

$$\langle f, \phi \rangle = \langle f, \mathcal{R}^2\phi \rangle = \langle \mathcal{R}f, \mathcal{R}\phi \rangle = \langle \mathcal{R}^2f, \phi \rangle. \quad (3.91)$$

Finally,  $\mathcal{F}$  and  $\mathcal{R}$  commute since

$$\begin{aligned} \mathcal{R}\mathcal{F}\phi(t) &= \frac{1}{\pi} \int_{\mathbb{R}} \phi(k)e^{-ikt} dk = \frac{1}{\pi} \int_{\mathbb{R}} \phi(-k)e^{ikt} dk = \\ &= \mathcal{F}(\mathcal{R}\phi)(t) \end{aligned} \quad (3.92)$$

and this gives

$$\begin{aligned} \langle \mathcal{F}\mathcal{R}f, \phi \rangle &= \langle \mathcal{R}f, \mathcal{F}\phi \rangle = \\ \langle f, \mathcal{R}\mathcal{F}\phi \rangle &= \langle f, \mathcal{F}\mathcal{R}\phi \rangle = \langle \mathcal{F}f, \mathcal{R}\phi \rangle = \langle \mathcal{R}\mathcal{F}f, \phi \rangle \end{aligned} \quad (3.93)$$

## Chapter 4

# A Data-Driven Approach to Solving a 1D Inverse Scattering Problem

**Abstract:** In this chapter, we extend the ROM-based approach for inverse scattering with Neumann boundary conditions, introduced by Druskin et al. (Inverse Problems 37, 2021), to the 1D Schrödinger equation with impedance (Robin) boundary conditions. We also propose a novel data-assimilation (DA) inversion method based on the ROM approach, thereby avoiding the need for a Lanczos-orthogonalization (LO) step. Furthermore, we present a detailed numerical study and comparison of the accuracy and stability of the DA and LO methods. This chapter is based on our paper [43]

## 4.1 Introduction

Inverse scattering appears in many applications, including medical imaging, non-destructive testing, and geophysical exploration [51]. While acquisition setups differ, at their core all these inverse problems involve a wave-equation and require estimation of its variable coefficients from boundary data. Approaches to solving the resulting non-linear inverse problem can be classified as either *direct* or *indirect* methods. The direct methods originate in classical inverse scattering theory and rely on formulating a linear relation between scattering data and the medium parameters, see e.g. [66]. The indirect methods formulate a non-linear data-fitting problem that can be solved iteratively [58].

The direct methods have recently attracted renewed attention, in particular in the geophysical community [13]. A recent development is the use of data-driven reduced-order models for solving the inverse problem [26]. We summarize this procedure below.

### 4.1.1 Approach

The state equation is denoted as

$$(A_q + k^2 I) u(k) = s,$$

with  $u$  denoting the state for wavenumber  $k$ ,  $s$  the source term, and  $q$  the variable coefficient included in the differential operator  $A_q$ . The measurements are given by  $f_i = \langle s, u_i \rangle = \langle s, (A_q + k_i^2 I)^{-1} s \rangle$  for  $i = 0, 1, \dots, m-1$ . The approach is to first estimate the states  $u_i$  from the measurements, and subsequently estimate  $q$  from these using the state equation.

The first step of estimating the states is approached via a reduced-order model which looks for a solution of the state equation in  $\mathcal{U} = \text{span}(\{u_i\}_{i=0}^{m-1})$  by projecting the state equation on this subspace. This requires computing  $\langle u_i, u_j \rangle$  and  $\langle u_i, A_q u_j \rangle$ . Remarkably, this can be done directly in terms of the measurements, without explicit reference to the states  $u_i$ . To approximate the states, then, we solve the projected state equation and represent the solution in a basis  $\mathcal{U}^{(0)}$  of solutions  $u_i^{(0)}$  for a given  $q_0$ . This last step is intricate and requires a Lanczos orthogonalization, see [26] for more details.

The next step of retrieving  $q$  from the approximated states,  $\tilde{u}_i$ , can be approached in different ways. We can follow an equation error approach (see e.g. [38]) and solve  $q$  from

$$(A_q + k_i^2 I) \tilde{u}_i = s.$$

Alternatively, we can solve it from a Lipmann-Schwinger integral equation (see, e.g. [40])

$$f_i - f_i^{(0)} = - \langle u_i^{(0)}, (A_q - A_0) \tilde{u}_i \rangle.$$



### 4.1.2 Contributions and Outline

The ROM-based approach has been applied in various settings, including time domain wave propagation, see e.g. [10] and frequency-domain diffusion processes, see [26]. As a first step towards extending this procedure to frequency-domain wave-problems, we extend the approach to a 1D Schrödinger equation with impedance boundary conditions. It turns out that both reflection and transmission measurements are needed to compute the ROM matrices from the data. Furthermore, we propose an alternative approach to the Lanczos-based state estimation approach described by [26]. To study the accuracy and stability properties of the resulting methods, we present numerical experiments.

The chapter is organized as follows. First, we review the forward problem and present the relations between the boundary data and required ROM matrices. Then, we discuss the two-step approach to solve the inverse problem; state estimation and subsequent estimation of the scattering potential from the state. We then present numerical experiments to illustrate the accuracy and stability of both methods on noisy data. We conclude the chapter with a brief summary of the main findings and discussion on further work.

## 4.2 The Forward Problem

Consider a Schrödinger equation

$$-u''(x;k) + q(x)u(x;k) - k^2u(x;k) = 0, \quad x \in (0,1) \quad (4.1)$$

with boundary conditions

$$u'(0;k) + iku(0;k) = 2ik, u'(1;k) - iku(1;k) = 0, \quad (4.2)$$

which corresponds to an incoming plane wave from  $-\infty$ . The scattering potential is assumed to have compact support in  $(0,1)$ . The measurements are given by

$$f(k) = u(0;k), \quad g(k) = u(1;k). \quad (4.3)$$

Well-posedness of this forward problem has been well-established (at least when  $q$  is continuous), since the boundary value problem can be transformed to the Lippmann-Schwinger integral. Then it is sufficient to study just the integral equation see e.g. [41].

### 4.2.1 A Reduced-Order Model

The point of departure for the ROM-based approach is the weak formulation of (4.1)

$$\langle u', \phi' \rangle + \langle qu, \phi \rangle - k^2 \langle u, \phi \rangle - ik \left( f(k) \overline{\phi(0)} + g(k) \overline{\phi(1)} \right) = -2ik \overline{\phi(0)}, \quad (4.4)$$

where  $\langle \cdot, \cdot \rangle$  denotes the standard inner product in  $L^2(0, 1)$  and  $\bar{\cdot}$  denotes complex conjugation.

Using a basis of solutions  $\{u_i\}_{i=0}^{m-1}$  with  $u_i \equiv u(\cdot; k_i)$ , the resulting system matrices are defined correspondingly

$$S_{ij} = \langle u'_j, u'_i \rangle + \langle qu_j, u_i \rangle, \quad (4.5)$$

$$M_{ij} = \langle u_j, u_i \rangle, \quad (4.6)$$

$$B_{ij} = f_j \bar{f}_i + g_j \bar{g}_i, \quad (4.7)$$

and right-hand-side

$$b_i = -2ik \bar{f}_i. \quad (4.8)$$

The main feature making this approach useful for solving the inverse problem is that the system matrices can be computed from the data directly, as per the following Lemma.

**Lemma 4.2.1.** *The ROM system matrices  $S, M$  (equations (4.5) and (4.6)) are given in terms of the boundary data  $\{f_i\}_{i=0}^{m-1}$  and  $\{g_i\}_{i=0}^{m-1}$  (equation (4.3)) as*

$$S_{ij} = \iota \left( \frac{k_i k_j B_{ij}}{k_i - k_j} - 2 \frac{k_j^2 k_i f_j + k_i^2 k_j \bar{f}_i}{k_i^2 - k_j^2} \right), \quad i \neq j$$

$$S_{ii} = k_i^2 (\Re(f_i) \Im(f'_i) - \Im(f_i) \Re(f'_i) + \Re(g_i) \Im(g'_i) - \Im(g_i) \Re(g'_i) - \Im(f'_i) - \Im(f_i)/k_i).$$

$$M_{ij} = \iota \left( \frac{B_{ij}}{k_i - k_j} - 2 \frac{k_i f_j + k_j \bar{f}_i}{k_i^2 - k_j^2} \right), \quad i \neq j$$

$$M_{ii} = \Re(f_i) \Im(f'_i) - \Im(f_i) \Re(f'_i) + \Re(g_i) \Im(g'_i) - \Im(g_i) \Re(g'_i) - \Im(f'_i) + \Im(f_i)/k_i.$$

The proof of this lemma can be found in paragraph 4.6.1.

Correspondingly, the approximate solution is then given by

$$\tilde{u}(x; k) = \sum_{i=0}^{m-1} c_i(k) u_i(x), \quad (4.9)$$

with

$$(S - k^2 M - ikB) \mathbf{c}(k) = \mathbf{b}(k).$$

**Remark 4.2.1.** *From the proof of lemma 4.2.1 we see that  $c_i(k_j) = \delta_{ij}$ . Thus  $\tilde{u}$  will match the boundary data.*

We refer the reader to [30, 46, 63, 54] for the discussion regarding the approximation error of such ROM-approximations.

### 4.3 The Inverse Problem

The inverse problem is now to retrieve  $q$  from boundary measurements at wave numbers  $\{k_i\}_{i=0}^{m-1}$ . As outlined in the introduction of this chapter, this is achieved in a 2-step procedure. First the states  $\{u_i\}_{i=0}^{m-1}$  are estimated from the data, and subsequently the scattering potential is estimated from these approximated states.

#### 4.3.1 Estimating the State

As outlined in the previous section, we can compute the *coefficients* in (4.9) directly from the data following the ROM-based approach. Since the basis  $\{u_i\}_{i=0}^{m-1}$  needed to evaluate (4.9) is unknown, however, we need to use a different basis. The basic idea is to use states  $\{u_i^{(0)}\}_{i=0}^{m-1}$  corresponding to a given  $q^{(0)}$  instead. It is tempting to directly replace (4.9) by

$$\tilde{u}(x; k) = \sum_{i=0}^{m-1} c_i(k) u_i^{(0)}(x),$$

however, this will not work as it would yield  $\tilde{u}(x; k_i) = u_i^{(0)}(x)$ , see Remark 4.2.1. Below, we discuss two alternatives.

#### Lanczos Orthogonalization

The authors of [26] propose to use an orthogonalization procedure as follows. They first apply the  $M$ -orthogonal Lanczos procedure to  $M^{-1}S$ , which yields matrices  $Q \in \mathbb{C}^{m \times r}$  and  $T \in \mathbb{C}^{r \times r}$ , where  $r \leq m$ , satisfying

$$Q^* S Q = T, \quad Q^* M Q = I.$$

The ROM-approximation of the state is then given by

$$\tilde{u}(x; k) = \sum_{i=0}^{m-1} c_i(k) v_i(x), \tag{4.10}$$

with  $\mathbf{c}$  satisfying

$$(T - k^2 I - ik Q^* B Q) \mathbf{c}(k) = Q^* \mathbf{b}(k),$$

and  $\{v_i\}_{i=0}^{r-1}$  an *orthogonal* basis w.r.t. the regular  $L^2$ -inner product defined as

$$v_j = \sum_{i=0}^{m-1} Q_{ij} u_i.$$

The expression in (4.10) is equivalent to (4.9) (although the coefficients differ). Because we do not have access to the states  $\{u_i\}_{i=0}^{m-1}$ , and cannot form the orthogonal basis  $\{v_i\}_{i=0}^{r-1}$ , we replace it by  $\{v_i^{(0)}\}_{i=0}^{r-1}$ , obtained as

$$v_j^{(0)} = \sum_{i=0}^{m-1} Q_{ij}^{(0)} u_i^{(0)},$$

where the states  $u_i^{(0)}$  are the solutions for a reference scattering potential  $q^{(0)}$  and  $Q^{(0)}$  is obtained by applying the Lanczos procedure to the corresponding system matrices.

**Remark 4.3.1.** *In practice, we replace  $M$  by  $M + \varepsilon I$  for some  $\varepsilon > 0$  to ensure it is invertible and to stabilize the Lanczos procedure.*

### Data-Assimilation

An alternative approach is inspired by [42] and sets up an overdetermined system of equations which ensures that the resulting estimate of the internal solution closely matches the data. We directly define the approximated state in terms of the reference solutions

$$\tilde{u}(x; k) = \sum_{i=0}^{m-1} c_i(k) u_i^{(0)}(x),$$

where the coefficients  $\mathbf{c}(k)$  are obtained by solving the following least-squares problem

$$\min_{\mathbf{c}} \left\| \begin{pmatrix} S - k^2 M - ikB \\ \rho \mathbf{f}^{(0)T} \\ \rho \mathbf{g}^{(0)T} \end{pmatrix} \mathbf{c} - \begin{pmatrix} \mathbf{b}(k) \\ \rho f(k) \\ \rho g(k) \end{pmatrix} \right\|_2, \quad (4.11)$$

where  $\rho > 0$  is a penalty parameter controlling the trade-off between data-fit and model-fit. The required data  $f(k)$  and  $g(k)$  can be obtained by solving (4.9) and using the coefficients to interpolate them.

### 4.3.2 Estimating the Scattering Potential

Using the weak formulation of the differential equation we obtain a Lippmann-Schwinger-type equation,

$$f(k) - f^{(0)}(k) = -\frac{1}{2ik} \int_0^1 u^{(0)}(x; k) u(x; k) (q(x) - q_0(x)) dx. \quad (4.12)$$

Representing  $q$  in terms of a suitable basis and enforcing the equation for wavenumbers  $\{k_i\}_{i=0}^{m-1}$  yields a system of equations. In practice, we replace  $u$  by its approximation  $\tilde{u}$  and solve it in a least-squares sense to obtain an estimate of  $q$ :

$$\min_{\mathbf{q}} \|K\mathbf{q} - (\mathbf{f} - \mathbf{f}^{(0)})\|_2^2 + \alpha \|\mathbf{q}\|_2^2. \quad (4.13)$$

**Remark 4.3.2.** Note that replacing  $u$  by  $\tilde{u}$  in (4.12) induces an error in  $K$ . To explicitly account for this, a Total Least-Squares (TLS) formulation (see e.g. [60] for its use in inverse scattering) might be beneficial.

## 4.4 Numerical Results

The inversion procedure consists of two steps; state estimation and estimation of the scattering potential from the states. For the first step, we use either the Lanczos orthogonalization approach (LO) with parameter  $\varepsilon$ , or the data-assimilation approach (DA) with parameter  $\rho$ . With the approximated states, the scattering potential is then estimated by solving the regularized Lippmann-Schwinger equation, with parameter  $\alpha$ . This two-step algorithm is outlined in Algorithm 1. Implementation of the described method is fairly straightforward. The code used to produce these results is available at:

<https://github.com/ucsi-consortium/1DInverseScatteringROM>.

---

**Algorithm 1** Overview of the two-step inversion procedure to estimate the states and scattering potential from boundary data.

---

**Require:** reference  $q^{(0)}$ , data  $f, g$  at wavenumbers  $\{k_i\}_{i=0}^{m-1}$ , regularisation parameters  $((\varepsilon, \alpha)$  or  $(\rho, \alpha)$ )

**Ensure:** reconstructed states  $\{\tilde{u}_i\}_{i=0}^{m-1}$  and scattering potential  $\tilde{q}$ .

*Step 1: state estimation*

    Compute ROM-matrices  $M, S, B$  according to Lemma 4.2.1

    Compute reference states  $\{u_i^{(0)}\}_{i=0}^{m-1}$  corresponding to  $q^{(0)}$ .

    Compute approximate states  $\{\tilde{u}_i\}_{i=0}^{m-1}$  at wavenumbers  $\{k_i\}_{i=0}^{m-1}$  according to the LO or DA procedures (outlined in sections 3.1.1, 3.1.2 resp.)

*Step 2: estimating the scattering potential*

    Reconstruct the scattering potential  $\tilde{q}$  according to the procedure outlined in the above section

---

### 4.4.1 Experimental Settings

To illustrate the methods, we use the scattering potential depicted in figure 4.1. The data are obtained by numerically solving the Schrödinger equation for  $m = 10$  equispaced wave numbers in the interval  $(0, 10)$ .

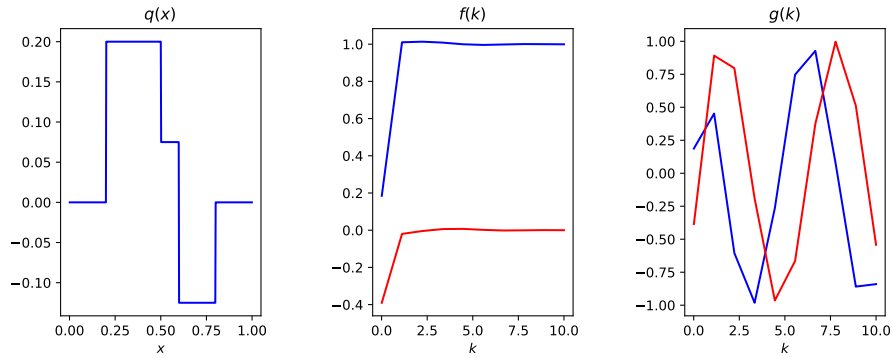


Figure 4.1: From left to right, the scattering potential  $q$ , the real (blue) and imaginary (red) part of the reflection data,  $f$ , and the real and imaginary part of the transmission data,  $g$ .

### 4.4.2 Benchmark Results

As a benchmark, we reconstruct the scattering potential using the approach described in section 4.3.2 using the true states (as the ideal setting) and the reference states for  $q^{(0)} = 0$  (which corresponds to the Born approximation). The results are shown in figures 4.2 and 4.3. Even using the true states we do not get a perfect reconstruction of the scattering potential due to the band-limited nature of the data. Furthermore, the inferior result obtained using the Born approximation underlines the need for non-linear inversion.

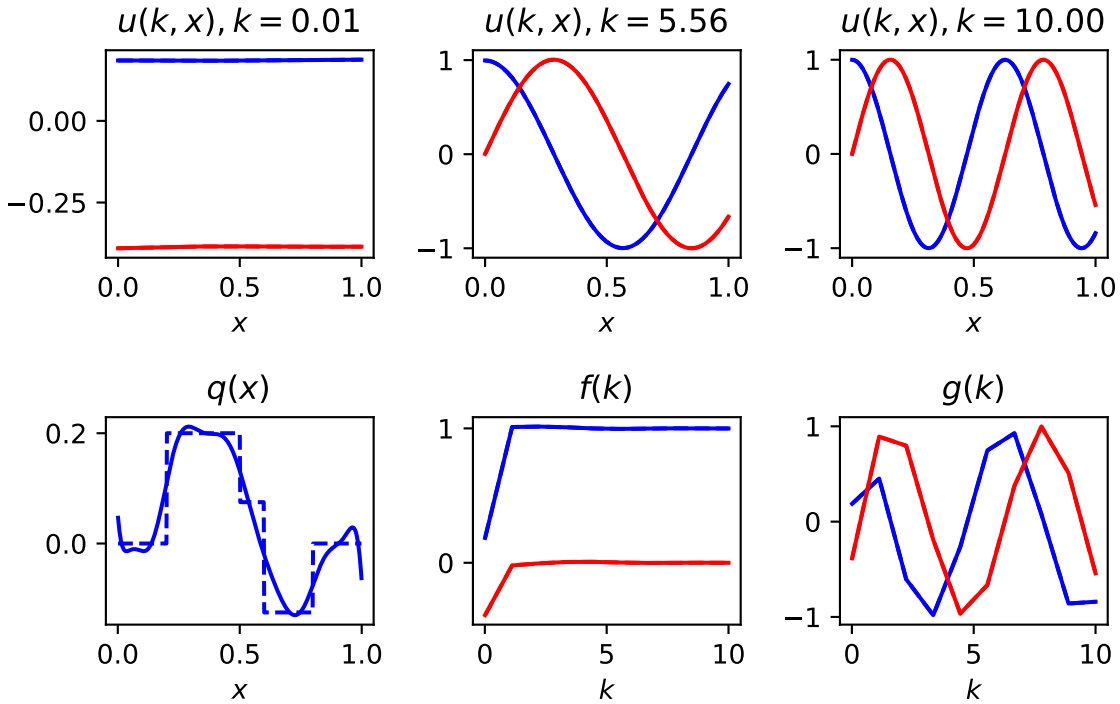


Figure 4.2: Results using the true state to reconstruct the scattering potential. The top row shows the (reconstructed) states (solid) used in the subsequent step to estimate the scattering potential as well as the true states (dashed). In the second row we see the reconstructed scattering potential (solid) and the corresponding data. The real part of the quantities is shown in blue, while the imaginary part is shown in red.

### 4.4.3 Noiseless Data

Next, we present the results yielded by the (LO) and (DA) methods for noise-free data in figures 4.4, 4.5 respectively. We observe that the DA method gives slightly more accurate reconstructions of the states. The corresponding reconstructed scattering potentials are slightly different, but there seems to be little difference in the accuracy of the reconstructions.

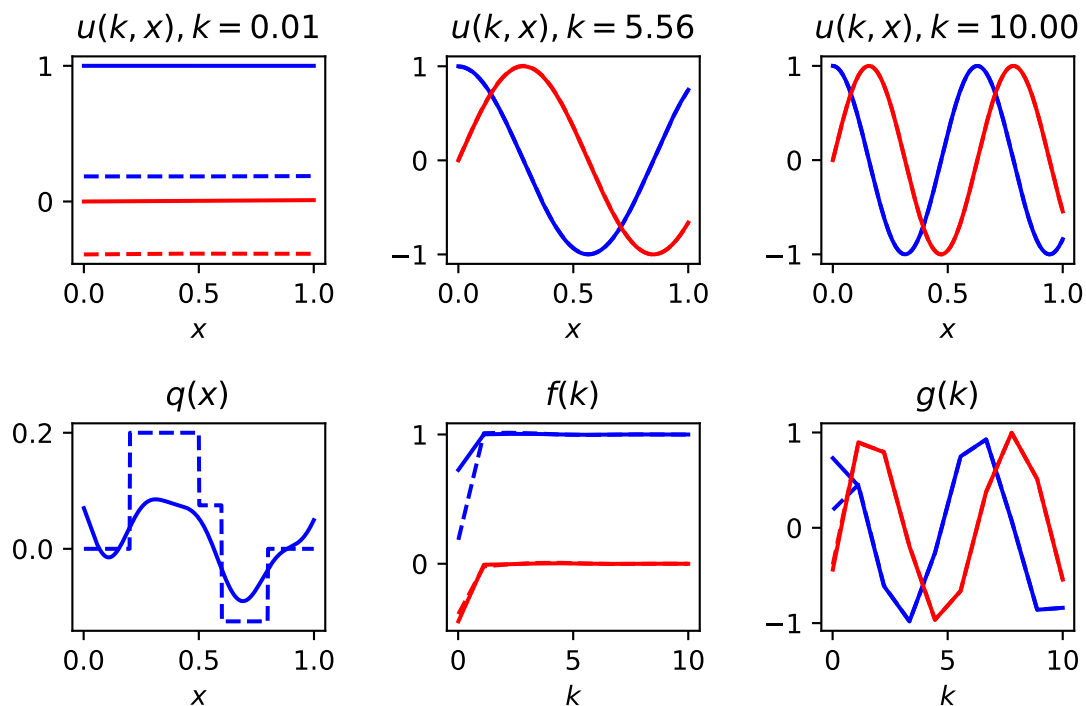


Figure 4.3: Results using the reference state to reconstruct the scattering potential (i.e., the Born approximation). The top row shows the (reconstructed) states (solid) used in the subsequent step to estimate the scattering potential as well as the true states (dashed). In the second row we see the reconstructed scattering potential (solid) and the corresponding data. The real part of the quantities is shown in blue, while the imaginary part is shown in red.



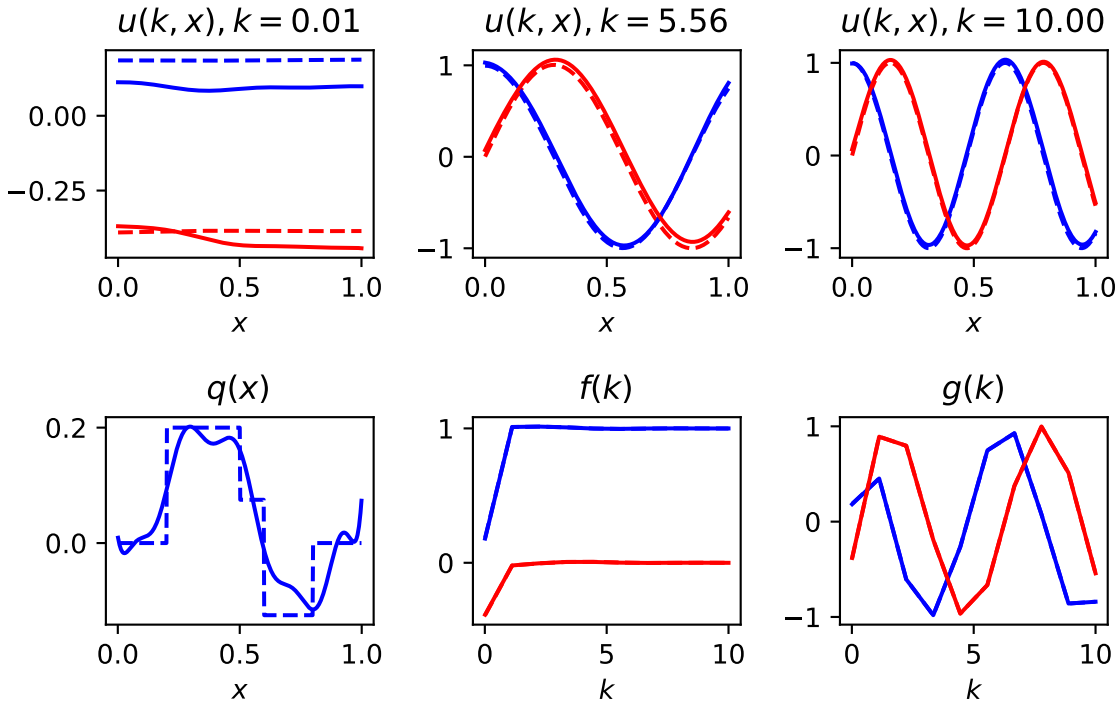


Figure 4.4: Results using LO-approach on noiseless data. The top row shows the (reconstructed) states (solid) used in the subsequent step to estimate the scattering potential as well as the true states (dashed). In the second row we see the reconstructed scattering potential (solid) and the corresponding data. The real part of the quantities is shown in blue, while the imaginary part is shown in red.

#### 4.4.4 Noisy Data

In this subsection we compare the methods on noisy data. In particular, we add i.i.d. normally distributed noise to the data with mean zero and variance  $\sigma^2$ . The parameters  $\varepsilon, \rho, \alpha$  are chosen to yield the best approximation (as measured by the  $L^2$  error between the reconstructions and the ground-truth, averaged over 100 realizations of the noise). The corresponding plots showing the dependence of the error on the parameters are included in section 4.6. In table 4.1 we summarize the results for varying  $\sigma$ . The corresponding plots are shown in figure 4.6. As expected, the noise influences the reconstruction of the state and consequently the reconstruction of the scattering potential. Overall, we see that the DA method gives superior estimates of the state. In terms of the scattering potential there is no significant difference between both methods, how-

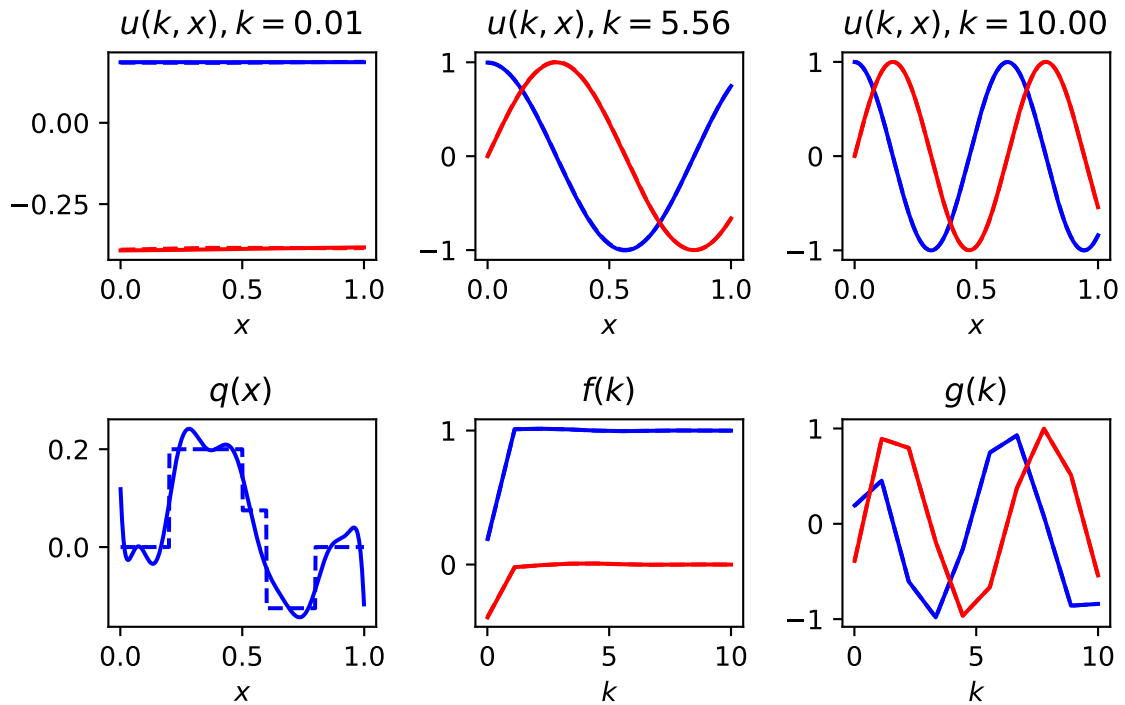


Figure 4.5: Results using DA-approach on noiseless data. The top row shows the (reconstructed) states (solid) used in the subsequent step to estimate the scattering potential as well as the true states (dashed). In the second row we see the reconstructed scattering potential (solid) and the corresponding data. The real part of the quantities is shown in blue, while the imaginary part is shown in red.

ever, for moderate noise levels the DA method gives more stable results with a much smaller variance in the error.

$\sigma$	method	parameters	error in $u$	error in $q$
$10^{-6}$	LO( $\varepsilon, \alpha$ )	$(10^{-3}, 10^{-3})$	$1.5 \cdot 10^{-1} (1.6 \cdot 10^{-3})$	$4.7 \cdot 10^{-1} (3.2 \cdot 10^{-3})$
	DA( $\rho, \alpha$ )	$(10^{-2}, 10^{-4})$	$6.1 \cdot 10^{-3} (1.4 \cdot 10^{-5})$	$3.9 \cdot 10^{-1} (2.3 \cdot 10^{-3})$
$10^{-5}$	LO( $\varepsilon, \alpha$ )	$(10^{-2}, 10^{-3})$	$1.5 \cdot 10^{-1} (5.3 \cdot 10^{-4})$	$4.6 \cdot 10^{-1} (2.3 \cdot 10^{-3})$
	DA( $\rho, \alpha$ )	$(10^{-1}, 10^{-3})$	$6.1 \cdot 10^{-3} (3.0 \cdot 10^{-5})$	$4.5 \cdot 10^{-1} (2.8 \cdot 10^{-3})$
$10^{-4}$	LO( $\varepsilon, \alpha$ )	$(10^{-2}, 10^{-2})$	$1.8 \cdot 10^{-1} (1.5 \cdot 10^{-1})$	$5.7 \cdot 10^{-1} (1.4 \cdot 10^{-1})$
	DA( $\rho, \alpha$ )	$(10^{-1}, 10^{-2})$	$6.2 \cdot 10^{-3} (3.4 \cdot 10^{-4})$	$5.3 \cdot 10^{-1} (3.2 \cdot 10^{-3})$
$10^{-3}$	LO( $\varepsilon, \alpha$ )	$(10^{-1}, 10^{-2})$	$2.1 \cdot 10^{-1} (1.2 \cdot 10^{-1})$	$6.2 \cdot 10^{-1} (1.3 \cdot 10^{-1})$
	DA( $\rho, \alpha$ )	$(10^0, 10^{-2})$	$6.4 \cdot 10^{-3} (7.0 \cdot 10^{-4})$	$6.0 \cdot 10^{-1} (5.9 \cdot 10^{-2})$
$10^{-2}$	LO( $\varepsilon, \alpha$ )	$(10^{-1}, 10^{-1})$	$2.6 \cdot 10^{-1} (7.1 \cdot 10^{-1})$	$9.2 \cdot 10^{-1} (9.4 \cdot 10^{-2})$
	DA( $\rho, \alpha$ )	$(10^1, 10^{-1})$	$1.4 \cdot 10^{-2} (4.4 \cdot 10^{-3})$	$9.2 \cdot 10^{-1} (9.0 \cdot 10^{-2})$

Table 4.1: Comparison between the relative errors in reconstructed states and scattering potential for both methods. We report the average and standard deviation over 100 realizations of the noise.

## 4.5 Discussion and Conclusions

We treat the inverse problem of retrieving the scattering potential in a 1D Schrödinger equation from boundary data. To do this, we propose a two-step approach inspired by a previously-published ROM-based method. We extend this method, previously applied to 1D diffusion problems with Neumann boundary conditions, to the 1D Schrödinger equation with impedance boundary conditions. In particular, we presented explicit expressions for retrieving the ROM-matrices from boundary data and proposed a novel approach for approximating the state from these matrices. This approach, based on ideas from data-assimilation, is an alternative to the previously proposed method based on Lanczos-orthogonalization. Given the estimates of the states, the scattering potential is obtained by solving an integral equation.

We compared the two approaches numerically on a simulated example with varying noise levels. These experiments suggest that the data-assimilation approach for estimating the state is more accurate and stable and leads to a more stable estimate of the scattering potential for moderate noise levels.

This work is the first step towards extending the ROM-based approach to frequency-domain wave-like problems (e.g., the Helmholtz equation) and 2D/3D. Other open questions for further research include the approximation error, stability estimates, and more practical aspects such an iterative approach where the reference potential is iteratively updated.

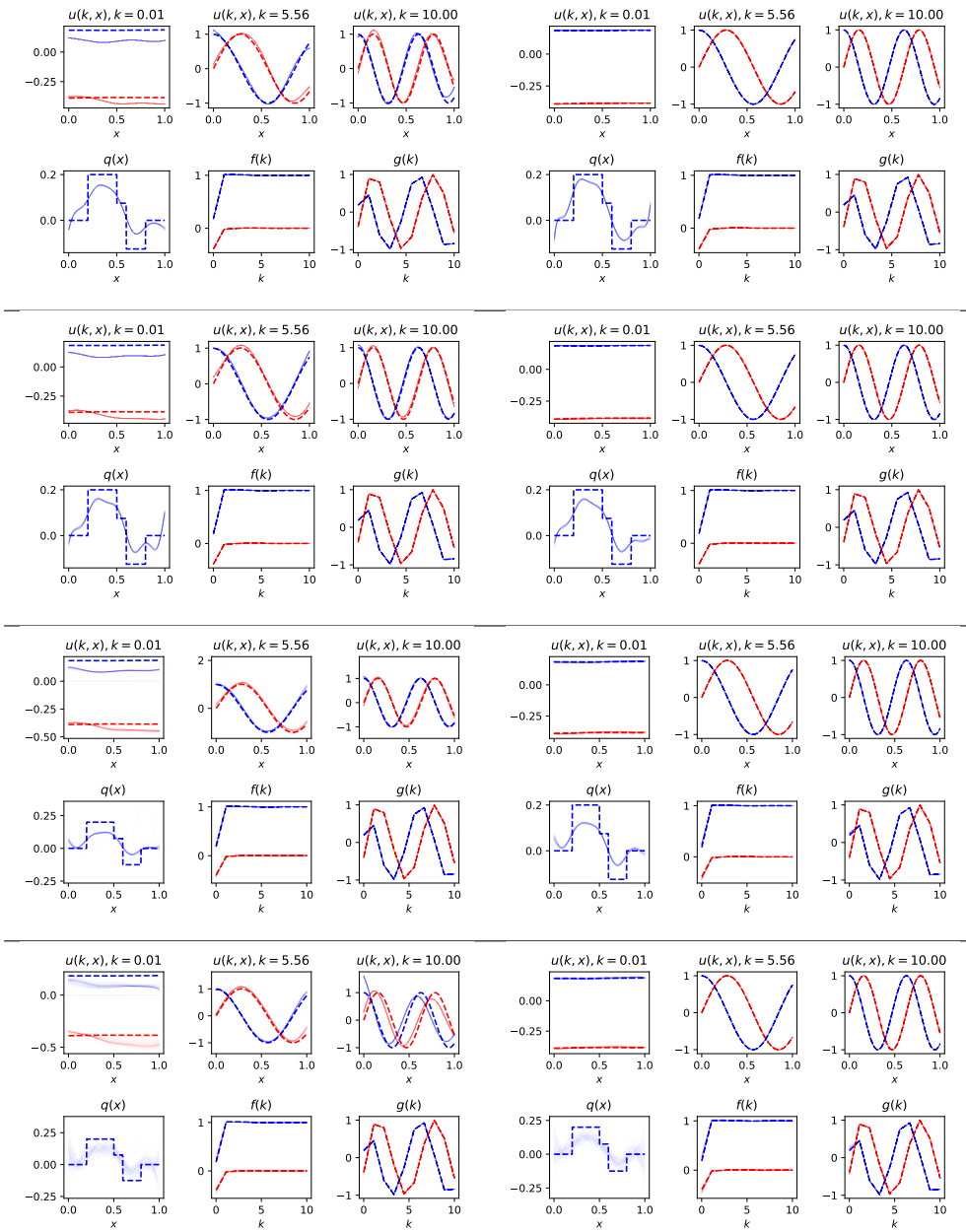


Figure 4.6: Results for the LO (left) and DA (right) methods for varying noise levels ( $\sigma = 10^{-6}, 10^{-5}, 10^{-4}, 10^{-3}$  respectively from top to bottom). The subplots follow the same layout as the previous figures. Individual results for different realizations of the noise are superimposed to clearly show the variation.

## 4.6 Appendix: Proofs and Regularization Parameter Selection

### 4.6.1 Proofs

*Proof of lemma 4.2.1.* From the weak form we find

$$S_{ij} - k_j^2 M_{ij} - \iota k_j B_{ij} = -2\iota k_j \bar{f}_i,$$

and

$$S_{ji} - k_i^2 M_{ji} - \iota k_i B_{ji} = -2\iota k_i \bar{f}_j,$$

from which (by taking the conjugate transpose and using the fact that the matrices involved are Hermitian)

$$S_{ij} - k_i^2 M_{ij} + \iota k_i B_{ij} = 2\iota k_i f_j.$$

Combining these yields

$$(k_i^2 - k_j^2) M_{ij} - \iota(k_i + k_j) B_{ij} = -2\iota(k_i f_j + k_j \bar{f}_i),$$

and

$$(k_i^2 - k_j^2) S_{ij} - \iota(k_j^2 k_i + k_i^2 k_j) B_{ij} = -2\iota(k_j^2 k_i f_j + k_i^2 k_j \bar{f}_i),$$

from which we can compute  $M_{ij}$  and  $S_{ij}$ :

$$M_{ij} = \iota \left( \frac{B_{ij}}{k_i - k_j} - 2 \frac{k_i f_j + k_j \bar{f}_i}{k_i^2 - k_j^2} \right).$$

$$S_{ij} = \iota \left( \frac{k_i k_j B_{ij}}{k_i - k_j} - 2 \frac{k_j^2 k_i f_j + k_i^2 k_j \bar{f}_i}{k_i^2 - k_j^2} \right).$$

For the diagonal elements we need to take a limit of the above two relations. We first compute the diagonal elements of  $M$ . We set  $\lambda = k_j^2$ , and  $k_i^2 = \lambda + h$ . We also define  $f(k_j) = \phi(\lambda) = \phi_1 + \iota\phi_2$  and  $\phi(\lambda + h) = \phi_1^h + \iota\phi_2^h$  and similarly  $\gamma(\lambda) = g(k_j)$ . Since  $\Im(M_{jj}) = 0$ , we obtain

$$\begin{aligned} M_{jj} &= \lim_{h \rightarrow 0} \left\{ -2 \frac{\sqrt{\lambda} \phi_2^h - \sqrt{\lambda + h} \phi_2}{h} - \frac{\gamma_2 \gamma_1^h - \gamma_1 \gamma_2^h + \phi_2 \phi_1^h - \phi_1 \phi_2^h}{\sqrt{\lambda + h} - \sqrt{\lambda}} \right\} = \\ &= -2 \left( \sqrt{\lambda} \frac{d\phi_2}{d\lambda}(\lambda) - \frac{1}{2} \lambda^{-1/2} \phi_2(\lambda) \right) - \gamma_2(\lambda) 2\sqrt{\lambda} \frac{d\gamma_1}{d\lambda}(\lambda) + \gamma_1(\lambda) 2\sqrt{\lambda} \frac{d\gamma_2}{d\lambda}(\lambda) - \end{aligned}$$

$$\phi_2(\lambda)2\sqrt{\lambda}\frac{d\phi_1}{d\lambda}(\lambda) + \phi_1(\lambda)2\sqrt{\lambda}\frac{d\phi_2(\lambda)}{d\lambda}. \quad (4.14)$$

The product rule gives that  $\frac{d\phi}{d\lambda} = \frac{df}{dk} \frac{dk}{d\lambda} = f'(k)(2k)^{-1}$ . Combining gives,

$$M_{jj} = \left\{ -2 \left( k \frac{1}{2k} \mathfrak{I}(f') - \frac{1}{2k} \mathfrak{I}(f) \right) - \mathfrak{I}(g)2k \frac{1}{2k} \Re(g) + \Re(g)2k \frac{1}{2k} \mathfrak{I}(g) - \mathfrak{I}(f)2k \frac{1}{2k} \Re(f) + \Re(f)2k \frac{1}{2k} \mathfrak{I}(f) \right\} \Big|_{k=k_j},$$

which gives

$$M_{jj} = \Re(f_j)\mathfrak{I}(f'_j) - \mathfrak{I}(f_j)\Re(f'_j) + \Re(g_j)\mathfrak{I}(g'_j) - \mathfrak{I}(g_j)\Re(g'_j) - \mathfrak{I}(f'_j) + \mathfrak{I}(f_j)/k_j.$$

We obtain similarly the relation for the diagonal of  $S$ . □

## 4.6.2 Regularization Parameter Selection

The LO and DA methods both have two regularization parameters that regularize the problem. These parameters are chosen to minimize the expected reconstruction error for the given noise level. We approximate the expected error by averaging the error over 100 realization of the noise. The plots corresponding to the results presented in table 4.1 and figures 4.4, 4.5, and 4.6 are shown in figure 4.7.

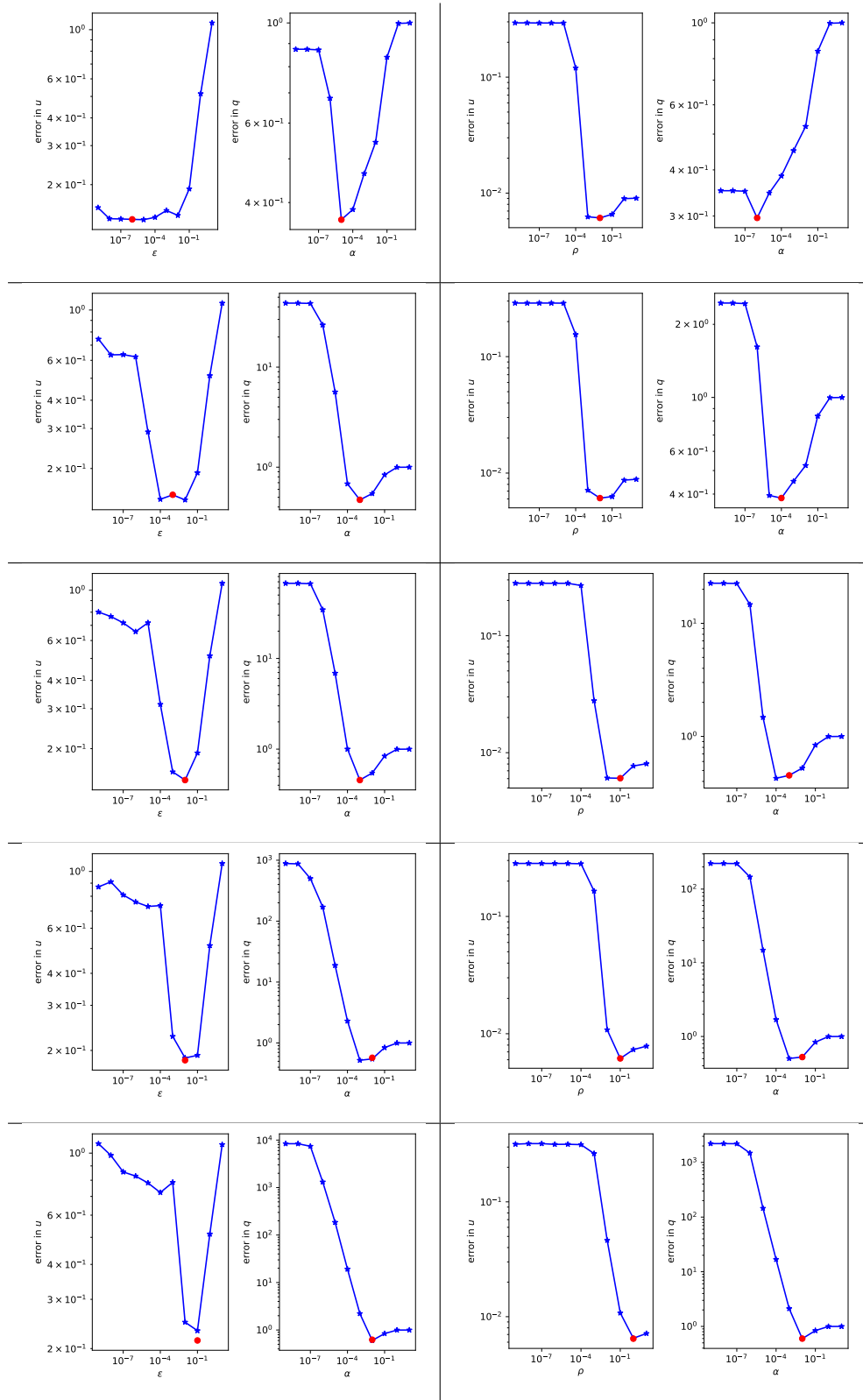


Figure 4.7: Average error for both methods (LO, left and DA, right) for various noise levels ( $0, 10^{-6}, 10^{-5}, 10^{-4}, 10^{-3}$  respectively from top to bottom).



## Chapter 5

# Reduced Order Model Based Nonlinear Waveform Inversion for the 1D Helmholtz Equation

**Abstract:** In this chapter we study a reduced order model (ROM) based waveform inversion method applied to a Helmholtz problem with impedance boundary conditions and variable refractive index. Our first goal is to obtain relations that allow the reconstruction of the Galerkin projection of the continuous problem to the space spanned by solutions of the Helmholtz equation. Our second goal is to study the newly introduced nonlinear optimization method based on the ROM aimed to estimate the refractive index from reflection and transmission data. Finally we compare numerically our method to the conventional full waveform inversion method.

## 5.1 Introduction

Reduced order model techniques have been studied for a long time in the context of solving boundary value problems numerically. The main difference between conventional finite element methods and the ROM approach is that in the latter, one approximates the solution of the problem in a finite-dimensional subspace spanned by solutions of the PDE itself (i.e. solutions for different wavenumbers in case of the Helmholtz equation). The advantage of using the ROM method for solving forward boundary value problems is the rapid convergence of the approximates to the true solution of the problem. We refer the interested reader to [30, 46, 63, 54] and the references therein for more information on the subject.

Recently, reduced order model techniques have received attention and have been applied to Neumann inverse boundary value problems for estimating coefficients of diffusion type elliptic partial differential equations, see [26] [9]. In short, in the cited papers, the authors consider boundary traces of solutions of the diffusion equation that correspond to a discrete set of spectral parameters. Using these measurements they reconstruct the so-called ROM matrices, which describe the projection of the continuous forward problem onto the finite dimensional space spanned by solutions of the forward problem. Using the Lanczos algorithm (see [50]) and the ROM projections as input, it is possible to linearise the inverse problem by obtaining an estimate of the state using some knowledge of the background coefficient, which refers to a known approximation of the unknown coefficient. Subsequently, the unknown coefficient can be estimated by solving an integral equation. Roughly speaking, the use of the ROM method to obtain a linearised solution of the inverse problem can be thought as a discrete analog of the classical Gelfand-Levitan-Marchenko approach, see [59, 60, 66, 15, 39].

The approach that we take in this chapter was initially developed for time-domain wave propagation with Dirichlet boundary conditions, see [11], [47] and [10]. For practical applications, however, impedance boundary conditions are of great interest since they are equivalent to the Sommerfeld radiation condition in 1D (and an approximation of the radiation condition in two and three dimensions). In this chapter therefore, we extend the ROM based FWI method introduced in [10, 11] and [47] to the 1D Helmholtz equation with impedance boundary conditions.

The motivation behind studying the ROM method within an optimization framework is the promising results that have been observed in the time-domain setting. Also, as we shall see in detail, in the case where we consider impedance boundary conditions, the stiffness and mass (ROM) matrices do not depend linearly on the data. Thus we expect different convexity properties for misfit functionals based on the ROM approach compared with functionals based on the conventional FWI approach.

Our contributions include the extension of the ROM based FWI in the frequency domain, and the study of the nonlinear inverse problem in an infinite dimensional framework. We also

compare our method to the conventional full waveform inversion method in terms of the convexity of the misfit functionals, and how accurately each method reconstructs a coefficient (refractive index of Helmholtz operator) using both noiseless and noisy measurements.

The chapter is organized as follows. We start with section 5.2 where we present a couple of well-posedness results regarding the forward problem. In section 5.3 we present the main results. In particular we explain how to recover the ROM matrices using double sided data. We also study the well-posedness of the associated nonlinear variational inverse problem and we present the optimality condition. We continue with section 5.4 where we present several numerical experiments of our ROM based FWI method and we conclude the chapter with a discussion section.

## 5.2 Preliminaries

Our forward problem is to find a weak solution  $u \in H^1(0, 1)$  such that

$$\left(-\frac{d^2}{dx^2} - k^2 m\right)u(k) = 0, \quad x \in (0, 1) \quad (5.1)$$

$$u'(k) + ik u(k) = 1, \quad x = 0 \quad (5.2)$$

$$u'(k) - ik u(k) = 0, \quad x = 1. \quad (5.3)$$

We assume for simplicity that the coefficient  $m$ , is an element of  $H^1((0, 1); [1, \infty))$ , with  $m(0) = m(1) = 1$ , and  $k > 0$ . We also note that for  $m > 0$  bounded we can prove existence and uniqueness of solutions. In a variational framework, the above differential equation becomes,

$$(u'(k), \psi') - k^2(mu(k), \psi) - ik\{u(k)|_{x=1}\overline{\psi(1)} + u(k)|_{x=0}\overline{\psi(0)}\}) = -\overline{\psi(0)}, \quad (5.4)$$

$$\forall \psi \in H^1(0, 1).$$

Here,  $(\cdot, \cdot)$  denotes the  $L^2$ -inner product. We also assume to have measurements of the solutions for a discrete set of wavenumbers,

$$\mathbb{W} = \{k_i : i = 1, \dots, N\},$$

of the form

$$f(k^2) = u(k)|_{x=0}, \quad g(k^2) = u(k)|_{x=1}. \quad (5.5)$$

The feature that sets apart our setting from what has been implemented in the past [26, 9], is that we consider double sided data (reflection and transmission). From the data we reconstruct the ROM projection of the forward scattering problem onto the finite dimensional space

$$\mathbb{X}_N = \text{span}\{u_i : i = 1, \dots, N\}, \quad (5.6)$$

with  $u_i = u(k_i)$ . As we shall see in detail, this projection yields three matrices, the stiffness, the mass and the boundary matrix,  $S, M, B$  respectively.

We now present some known results about the forward problem. Well-posedness of the forward problem can be shown either using the Lax-Milgram theory, see for example [65] or [4], or using the equivalent Lippmann-Schwinger equation of the direct scattering problem. We denote the anti-dual of  $H^1$  as  $\overline{H^1}$  and the brackets  $\langle \cdot, \cdot \rangle$  denote duality.

**Proposition 5.2.1.** *Given  $k > 0$ , there exist a unique solution  $u(k, m) \in H^1(0, 1)$  that satisfies the state equation (5.1)-(5.3).*

*Proof.* A more detailed sketch of the proof can be found in the appendix of this chapter, and for full details we refer to [66, 4]. In short, the forward problem can be reduced to the following linear problem, of finding  $u \in H^1(0, 1)$  :

$$\Phi \mathcal{T}(\mathcal{I} + k^2 \mathcal{A})u = -\delta_0, \overline{H^1(0, 1)}' \quad (5.7)$$

where  $\Phi$  is the linear Riesz isomorphism,  $\mathcal{T}$  is defined through the form

$$a_1(u, v) = \int_0^1 u' \overline{v'} dx - ik \{(u\overline{v})|_{x=0} + (u\overline{v})|_{x=1}\}, \quad u, v \in H^1 \quad (5.8)$$

such that

$$a_1(u, v) = (\mathcal{T}u, v)_{H^1}, \quad u, v \in H^1. \quad (5.9)$$

We define  $\mathcal{V}$  such that

$$\langle \mathcal{V}u, v \rangle = a_2(u, v) = \int_0^1 mu\overline{v} dx, \quad u, v \in H^1, \quad (5.10)$$

and  $\mathcal{A} = \mathcal{T}^{-1}\Phi^{-1}\mathcal{V}i_{H^1 \rightarrow L^2}$ , where  $i_{H^1 \rightarrow L^2}$  is the compact embedding operator of  $H^1(0, 1)$  to  $L^2(0, 1)$ .  $\square$

**Corollary 5.2.1.** *The traces*

$$f(\lambda) = u(\sqrt{\lambda})|_{x=0}, \quad g(\lambda) = u(\sqrt{\lambda})|_{x=1}, \quad \lambda > 0 \quad (5.11)$$

*are well defined.*

## 5.3 Main Results

In this section we present our main results. We start with describing how to recover the so-called ROM matrices from double-sided data. We then continue with the study of our ROM based nonlinear inversion method.

### 5.3.1 ROM Matrices Construction Using Two-Sided Data

In this paragraph we describe the passage from boundary measurements to the ROM projections of the forward problem. We can express (5.4) equivalently as

$$(\mathcal{S} - k^2 \mathcal{M}(m) - ik\mathcal{B})u = -\delta_0, \quad (5.12)$$

as an  $\overline{H^1(0,1)}$ ' relation. For example

$$\mathcal{S} : H^1(0,1) \rightarrow \overline{H^1(0,1)}' \quad (5.13)$$

acts as follows

$$\langle \mathcal{S}y, \phi \rangle = (y', \phi'). \quad (5.14)$$

Similarly, we define  $\mathcal{M}, \mathcal{B}$ .

**Remark 5.3.1.** *For the shake of completeness, it is useful to connect  $\mathcal{S}, \mathcal{M}, \mathcal{B}$  with the operators used in the proof of proposition 5.2.1. We get*

$$\langle (\mathcal{S} - k^2 \mathcal{M}(m) - ik\mathcal{B})u, v \rangle = -\langle \delta_0, v \rangle, \quad \forall v \in H^1, \quad (5.15)$$

or

$$\langle (\mathcal{S} - k^2 \mathcal{M}(m) - ik\mathcal{B})u, v \rangle = a_1(u, v) - k^2 a_2(u, v) = (\mathcal{T}(I + k^2 \mathcal{A})u, v)_{H^1} = \quad (5.16)$$

$$\langle \Phi \mathcal{T}(I + k^2 \mathcal{A})u, v \rangle, \quad \forall v \in H^1, \quad (5.17)$$

Therefore

$$\mathcal{S} - k^2 \mathcal{M}(m) - ik\mathcal{B} = \Phi \mathcal{T}(\mathcal{S} + k^2 \mathcal{A}) \quad (5.18)$$

We now consider relation (5.12) on  $\mathbb{X}_N$  which is spanned by exact solutions that correspond to different wavenumbers, as explained before. We first observe that we can restrict  $\mathcal{S}$  on  $\mathbb{X}_N$  such that

$$\langle \mathcal{S}|_{\mathbb{X}_N} u, \phi \rangle = \langle \mathcal{S}u, \phi \rangle, u \in \mathbb{X}_N, \phi \in H^1(0, 1). \quad (5.19)$$

and subsequently the elements

$$\langle \mathcal{S}|_{\mathbb{X}_N} u, \phi \rangle = \langle \mathcal{S}u, \phi \rangle, u \in \mathbb{X}_N, \phi \in \mathbb{X}_N. \quad (5.20)$$

This way, we define the stiffness matrix,  $S \in \mathbb{C}^{N \times N}$  with entries

$$S_{ij} = \langle \mathcal{S}u_i, u_j \rangle = (u'_i, u'_j), i, j \in \{1, \dots, N\}. \quad (5.21)$$

Similarly, we define the mass matrix

$$M_{ij} = (mu_i, u_j), i, j \in \{1, \dots, N\}. \quad (5.22)$$

The main characteristic making this approach useful for solving the inverse problem, is that the ROM matrices can be computed directly from the data. From now on we denote

$$f_i = f(k_i^2), i = 1, \dots, N,$$

and

$$g_i = g(k_i^2), i = 1, \dots, N.$$

**Lemma 5.3.1.** *The ROM system matrices  $S, M$  are given in terms of the boundary data*

$$M_{ij} = -\frac{\bar{f}_j - f_i}{k_j^2 - k_i^2} + i \frac{g_i \bar{g}_j + f_i \bar{f}_j}{k_j - k_i}, i \neq j, \quad (5.23)$$

$$M_{ii} = \left\{ -\frac{d\text{Re}(f)}{d\lambda}(\lambda) - \text{Im}(g)(\lambda) 2\sqrt{\lambda} \frac{d\text{Re}(g)}{d\lambda}(\lambda) + \text{Re}(g)(\lambda) 2\sqrt{\lambda} \frac{d\text{Im}(g)}{d\lambda}(\lambda) - \right. \\ \left. \text{Im}(f)(\lambda) 2\sqrt{\lambda} \frac{d\text{Re}(f)}{d\lambda}(\lambda) + \text{Re}(f)(\lambda) 2\sqrt{\lambda} \frac{d\text{Im}(f)}{d\lambda}(\lambda) \right\} \Big|_{\lambda=k_i^2} \quad (5.24)$$

$$S_{ij} = -\frac{k_j^2 \bar{f}_j - k_i^2 f_i}{k_j^2 - k_i^2} + i(k_j^2 k_i + k_i^2 k_j) \frac{g_i \bar{g}_j + f_i \bar{f}_j}{k_j^2 - k_i^2}, i \neq j, \quad (5.25)$$

$$S_{ii} = \left\{ \begin{aligned} &(-\lambda \frac{dRe(f)}{d\lambda}(\lambda) - Re(f)(\lambda)) - Im(g)(\lambda) 2\lambda^{3/2} \frac{dRe(g)}{d\lambda}(\lambda) + \\ &Re(g)(\lambda) 2\lambda^{3/2} \frac{dIm(g)}{d\lambda}(\lambda) + Re(f)(\lambda) 2\lambda^{3/2} \frac{dIm(f)}{d\lambda}(\lambda) - \\ &Im(f)(\lambda) 2\lambda^{3/2} \frac{dRe(f)}{d\lambda}(\lambda) \end{aligned} \right\} \Big|_{\lambda=k_i^2}, \quad (5.26)$$

$i, j = 1, \dots, N$ .

*Proof.* The proof can be found in the appendix 5.6.2.  $\square$

### 5.3.2 Solving the Inverse Problem with Nonlinear Optimization

In this paragraph we study a nonlinear inversion method based on the ROM approach. In particular, after acquiring the ROM matrix,  $S = S^{obs.}$ , we set up the following nonlinear optimization problem of estimating the refractive index  $m$ , using the stiffness matrix  $S^{obs.}$  as input:

$$\min\{\phi(m) : m \in H^1((0, 1); [1, \infty)), m(0) = m(1) = 1\} \quad (5.27)$$

with

$$\phi(m) = \frac{1}{2} \|S^{obs.} - S(m)\|_F^2 + \frac{\varepsilon}{2} \|m\|_{H^1(0,1)}^2, \text{ for some } \varepsilon > 0. \quad (5.28)$$

$S(m)$  is given according to relation (5.21) for a given  $m$ , and  $\|\cdot\|_F$  is the Frobenius norm (i.e. we try to estimate  $m$  by matching modelled  $S(m)$  with true  $S^{obs.}$ ). The special form of the functional that implicitly defines  $\phi$ , let  $J$ , (product of wavefields in the computation of the modelled stiffness) makes showing existence of minimizers interesting. In particular since  $J$  is a sum of both weakly lower semicontinuous and not weakly lower semicontinuous functionals there is no guarantee on the behaviour of  $\phi$  in terms of weak lower semicontinuity.

#### Existence of Minimizers

There are many ways of showing existence of minimizers in optimal control problems, see e.g. [36]. Here, the form that the elements of our modeled data have (elements of  $S$  are  $L^2$  inner-products of the derivatives of the states) are not standard and create challenges in proving existence of solutions for the inverse problem. To be specific, the functional that implicitly defines  $\phi$  through the reduced formulation includes non-weakly lower semicontinuous terms. In this framework, it is convenient to analyse the coefficient to state map  $m \mapsto u(m)$  for showing

well-posedness for the optimization problem. Showing "smoothness" of the coefficient to state map has been shown formally in the  $\mathbb{R}^{2,3}$  scattering problem, see [20]. We work similarly here. We define the admissible set

$$\mathbb{K}_{ad} = \{m \in H^1((0, 1); [1, \infty)), m(0) = m(1) = 1\}. \quad (5.29)$$

Also, with  $\partial_1, \partial_2$  we denote the partial Fréchet derivatives with respect to the first and second variables of a function respectively.

We consider the function  $F : C([0, 1]; (0, \infty)) \times H^1(0, 1) \rightarrow \overline{H^1(0, 1)'}$  given by

$$F(m, u) = (\mathcal{S} - k^2 \mathcal{M}(m) - ik\mathcal{B})u + \delta_0, \quad (m, u) \in C([0, 1]; (0, \infty)) \times H^1(0, 1). \quad (5.30)$$

Using the implicit function theorem applied on  $F$ , we obtain that a wavefield  $u$  is a smooth function of the coefficient  $m$  as stated below.

**Lemma 5.3.2.** *Given  $k > 0$ , the map  $C([0, 1]; (0, \infty)) \ni m \rightarrow u(k, m) \in H^1(0, 1)$  is continuous and Fréchet differentiable.*

All details on the above lemma are given in the appendix 5.6.3. Now, we are ready to show existence of minimizers for the variational inverse problem of our study.

**Remark 5.3.2.** *As will shall see in the proof of the following theorem, it is convenient to study the smoothness of  $u$  as a function of  $m \in C[0, 1]$  since we will make a passage from  $H^1$ –weakly convergent sequence of coefficients to  $C[0, 1]$ –strongly convergent sequences.*

**Theorem 5.3.1.** *The misfit functional  $\phi$  obtains minimizers on  $\mathbb{K}_{ad}$ .*

*Proof.* We denote

$$\begin{aligned} \phi(m) &= \frac{1}{2} \sum_{i,j=1}^N \left\{ |S_{ij}(m) - S_{ij}^{obs.}|^2 \right\} + \frac{\varepsilon}{2} \|m\|_{H^1(0,1)}^2 = \\ &= \frac{1}{2} \sum_{i,j=1}^N \phi_{ij}(m) + \frac{\varepsilon}{2} \|m\|_{H^1(0,1)}^2, m \in \mathbb{K}_{ad}. \end{aligned} \quad (5.31)$$

Let  $(i, j) \in \{1, \dots, N\}^2$ . Since  $\phi \geq 0$  for all  $m \in \mathbb{K}_{ad}$ , there exists  $\mu > 0$  such that

$$\mu = \inf_{m \in \mathbb{K}_{ad}} \phi_{ij}(m). \quad (5.32)$$

Therefore there is a sequence

$$(\phi(m_\nu))_{\nu \in \mathbb{N}} \subset \{\phi(m) : m \in \mathbb{K}_{ad}\} \quad (5.33)$$



such that

$$\phi(m_\nu) \rightarrow \mu, \nu \rightarrow \infty. \quad (5.34)$$

Since we use a regularization parameter, and since  $\{\phi(m_\nu)\}_\nu$  is included in a ball, it follows that the sequence  $(m_\nu)_{\nu \in \mathbb{N}} \subset \mathbb{K}_{ad}$  is bounded. Therefore, there is a subsequence  $(m_\nu)_{\nu \in N_1} \subset (m_\nu)_{\nu \in \mathbb{N}}$  that has a weak limit, let  $\widehat{m}$ , in  $\sigma(H^1, H^1')$ . Symbolically

$$m_\nu \rightharpoonup \widehat{m} \text{ in } \sigma(H^1((0,1), \mathbb{R}), H^1((0,1), \mathbb{R})'). \quad (5.35)$$

$\widehat{m}$  is included in  $\mathbb{K}_{ad}$  since the set is closed and convex. Due to the Sobolev's compact embedding we also obtain that

$$m_\nu \rightarrow \widehat{m} \text{ in } C([0,1]; \mathbb{R}). \quad (5.36)$$

Since  $u(k, \cdot)$  is continuous as a function of  $m$ , we obtain for every  $i, j = 1, \dots, N$  that

$$u(k_i, m_\nu) \rightarrow u(k_i, \widehat{m}), \text{ in } H^1(0,1) \quad (5.37)$$

and

$$u(k_j, m_\nu) \rightarrow u(k_j, \widehat{m}), \text{ in } H^1(0,1), \quad (5.38)$$

as  $\nu \rightarrow \infty$ . Since  $\frac{d}{dx} : H^1(0,1) \rightarrow L^2(0,1)$  is bounded, we obtain that

$$\frac{du(k_i, m_\nu)}{dx} \rightarrow \frac{du(k_i, \widehat{m})}{dx}, \text{ in } L^2(0,1) \quad (5.39)$$

and

$$\frac{du(k_j, m_\nu)}{dx} \rightarrow \frac{du(k_j, \widehat{m})}{dx}, \text{ in } L^2(0,1), \quad (5.40)$$

as  $\nu \rightarrow \infty$ , for all  $i, j = 1, \dots, N$ . Finally, for all  $i, j = 1, \dots, N$  we obtain that

$$\begin{aligned} \lim_\nu \phi_{ij}(m_\nu) &= \lim_\nu \left| \int u_i(m_\nu)' \overline{u_j(m_\nu)'} dx - S_{ij}^{obs.} \right|^2 = \\ &= \left| \int u_i(\widehat{m})' \overline{u_j(\widehat{m})'} dx - S_{ij}^{obs.} \right|^2 = \phi_{ij}(\widehat{m}), \end{aligned}$$

since the absolute value function is continuous and the following limit exists,

$$\lim_\nu \int_0^1 u_i(m_\nu)' \overline{u_j(m_\nu)'} dx \in \mathbb{C}. \quad (5.41)$$

Therefore by the strong convergence of the sequences  $(\phi_{ij}(m_\nu))_\nu$ ,  $i, j = 1, \dots, N$  and the weak lower semicontinuity of the norm, we obtain

$$\mu = \lim_\nu \phi(m_\nu) \geq \liminf_\nu \phi(m_\nu) = \sum_{ij=1}^N \phi_{ij}(\widehat{m}) + \frac{\varepsilon}{2} \liminf_\nu \|m_\nu\|_{H^1}^2 \geq \phi(\widehat{m}) \geq \mu \quad (5.42)$$

□

### Derivative of Misfit and Optimality Condition

Here we derive the first order optimality condition of the problem in the continuous setting. We first define the form

$$b(u, v) = \int_0^1 u'v' dx, \quad u, v \in H^1(0, 1). \quad (5.43)$$

We obtain the following result.

**Proposition 5.3.1.** *Let  $(i, j) \in \{1, \dots, N\}^2$ . Then the function  $\phi_{ij} : H^1((0, 1); (0, \infty)) \rightarrow [0, \infty]$  is  $C^1$ , with derivative at an  $m_0$*

$$\begin{aligned} \langle D_m \phi_{ij}(m_0), h \rangle = & \operatorname{Re}(\{b(u_i(m_0), \overline{u_j(m_0)}) - S_{ij}^{obs.}\} \{ \langle b(\cdot, \overline{u_j(m_0)}), Du_i(m_0)h \rangle + \\ & \langle b(u_i(m_0), \cdot), D_m \overline{u_j(m_0)h} \rangle \}) + \frac{\mathcal{E}}{N}(m_0, h)_{H^1(0,1)}, \end{aligned}$$

for a direction  $h \in H^1((0, 1); \mathbb{R})$ .

*Proof.* We know that if

$$q : H^1((0, 1); \mathbb{R}) \rightarrow \mathbb{C} \quad (5.44)$$

is differentiable, then

$$\frac{1}{2} \langle D_m |q(m_0)|^2, h \rangle = \operatorname{Re}(q(m_0) \langle D_m q(m_0), h \rangle) \quad (5.45)$$

In our case,  $q(m_0) = b(u_i(m_0), \overline{u_j(m_0)}) - S_{ij}$ , with

$$\langle Db(u, v), (h, z) \rangle = b(u, z) + b(h, v) \quad (5.46)$$

at  $(u, v) \in \{H^1(0, 1)\}^2$ , at direction  $(h, z)$ . Therefore

$$\begin{aligned} \langle D_m q(m_0), h \rangle = & \langle Db(u_i(m_0), \overline{u_j(m_0)}) \circ D_m(u_i(m_0), \overline{u_j(m_0)}), h \rangle = \\ & \langle Db(u_i(m_0), \overline{u_j(m_0)}), D_m(u_i(m_0), \overline{u_j(m_0)})h \rangle = \\ & b(\overline{D_m u_j(m_0)h}, u_i(m_0)) + b(D_m u_i(m_0)h, \overline{u_j(m_0)}) = \\ & \langle b(u_i(m_0), \cdot), \overline{D_m u_j(m_0)h} \rangle \rangle + \langle b(\cdot, \overline{u_j(m_0)}), Du_i(m_0)h \rangle. \end{aligned} \quad (5.47)$$

□

We define  $\mathcal{G} : H^1(0, 1) \rightarrow H^1(0, 1)'$  such that

$$\langle \mathcal{G}\phi, u \rangle = \int_0^1 u' \overline{\phi'} dx = b(u, \overline{\phi}). \quad (5.48)$$

This gives for a direction  $h \in H^1((0, 1); \mathbb{R})$

$$\begin{aligned} b(\overline{D_m u_j(m_0) h}, u_i(m_0)) &= \overline{b(D_m u_j(m_0) h, u_i(m_0))} = \\ &= \overline{\langle \mathcal{G} u_i, D_m u_j h \rangle} = \overline{\langle (D_m u_j)^* \mathcal{G} u_i, h \rangle}. \end{aligned}$$

Since  $h = \overline{h}$  ( $h$  is real), we obtain the following (see [48, page 37])

$$\begin{aligned} \overline{\langle (D_m u_j)^* \mathcal{G} u_i, h \rangle} &= \overline{\langle (D_m u_j)^* \mathcal{G} u_i, \overline{h} \rangle} = \\ &= \overline{\langle (D_m u_j)^* \mathcal{G} u_i, h \rangle}. \end{aligned} \quad (5.49)$$

We obtain similarly,

$$b(D_m u_i(m_0) h, \overline{u_j(m_0)}) = \langle (D_m u_i)^* \mathcal{G} u_j, h \rangle$$

Combining the above we obtain the following theorem.

**Theorem 5.3.2.** *The function  $\phi : H^1((0, 1); (0, \infty)) \rightarrow [0, \infty]$  is  $C^1$ , with derivative at an  $m_0$*

$$\begin{aligned} D_m \phi(m_0) &= \sum_{i,j=1}^N \operatorname{Re} \left( \left\{ \overline{(D_m u_j)^* \mathcal{G} u_i} + (D_m u_i)^* \mathcal{G} u_j \right\} (b(u_i(m_0), \overline{u_j(m_0)}) - S_{ij}^{obs.}) \right) + \\ &= \mathcal{E}(m_0, \cdot)_{H^1(0,1)}. \end{aligned}$$

**Remark 5.3.3.** *Since we have derived the analytical expression of the  $F$ -derivative of  $\phi$ , then the optimality condition is a variational inequality of the form,*

$$\langle D_m \phi(\widehat{m}), m - \widehat{m} \rangle \geq 0, \quad \forall m \in \mathbb{K}_{ad}, \quad (5.50)$$

with  $D_m \phi(\widehat{m})$  given above at a local minimizer,  $\widehat{m}$ .

## 5.4 Numerical Results

In this section we include a number of numerical experiments/comparisons between the ROM based FWI method and the conventional FWI method. Before doing so, we include a paragraph regarding the discrete optimality condition of the ROM based misfit functional.

### 5.4.1 Numerical Implementation: Discrete Optimality Condition

In this paragraph we derive the discrete optimality condition that we use for the numerical computation of the gradient of the ROM based misfit functional. In the discrete case, given  $L$ , a first order finite-difference matrix and  $\eta = 1/N_x$  being the length of the spatial discretisation ( $N_x$  spatial points) we have that

$$S_{ij} = \eta(Lu_i, Lu_j)_{\mathbb{C}^{N_x}}, \quad (5.51)$$

assuming that we realize  $(u_i)_{i=1}^N$  in the discrete sense. Now, in order to follow similar steps as in the continuous case, we take a direction  $h \in \mathbb{R}^n$  and we consider as before,  $\phi = \sum_{i,j=1}^N \phi_{ij}$  (for simplicity we take  $\varepsilon = 0$ ).

$$\begin{aligned} (D_m \phi_{ij}(m_0), h)_{\mathbb{R}^n} &= \text{Re}\{(D_m(S_{ij}(m_0) - S_{ij}^{obs.}), D_m S_{ij}(m)h)_{\mathbb{C}^{N_x}}\} = \\ & \text{Re}\{((D_m S_{ij}(m))^* \{S_{ij}(m_0) - S_{ij}^{obs.}\}, h)_{\mathbb{C}^{N_x}})\}. \end{aligned} \quad (5.52)$$

We obtain that

$$D_m S_{ij} = \eta(D_m u_j)^* L^* Lu_i + \eta u_j^* L^* L(D_m u_i) \Rightarrow \quad (5.53)$$

$$(D_m S_{ij})^* = \eta u_i^* L^* L(D_m u_j) + \eta(D_m u_i)^* L^* Lu_j. \quad (5.54)$$

Also,

$$D_m \phi_{ij} = \text{Re}\{\eta(u_i^* L^* L(D_m u_j) + \eta(D_m u_i)^* L^* Lu_j)[S_{ij} - S_{ij}^{obs.}]\}. \quad (5.55)$$

Now,

$$\eta u_i^* L^* L(D_m u_j) = \eta(L(D_m u_j), Lu_i)_{\mathbb{C}^{N_x}} = \eta \overline{(Lu_i, LD_m u_j)_{\mathbb{C}^{N_x}}} = \eta \overline{D_m u_j^* L^* Lu_i}, \quad (5.56)$$

therefore we get

$$D_m \phi_{ij} = \eta \text{Re}\{[S_{ij} - S_{ij}^{obs.}](\overline{D_m u_j^* L^* Lu_i} + D_m u_i^* L^* Lu_j)\}$$

**Remark 5.4.1.** *Instead of using a variational inequality as our optimality conditions, we can seek for simplicity solutions such that  $D_m \phi(\hat{m}) = 0$ .*

**Remark 5.4.2.** *In the continuous case we defined an operator  $\mathcal{G}$  such that*

$$\langle \mathcal{G} \phi, u \rangle = \int_0^1 \overline{\partial_x \phi} \partial_x u dx. \quad (5.57)$$

*In the discrete sense this means that*

$$\langle \mathcal{G} \phi, u \rangle \approx \eta(L\bar{\phi}, Lu)_{\mathbb{R}^{N_x}} = \eta(L^* L\bar{\phi}, u)_{\mathbb{R}^{N_x}} = \eta \phi^* L^* Lu,$$

*where  $L^*$  is the adjoint of  $L$  defined by the inner product,  $(\bar{\cdot}, \cdot)$ .*

### 5.4.2 Comparison with Conventional FWI: Convexity

In this section we compare our ROM based FWI approach with the conventional FWI. We use double sided data for both methods. We can now consider  $u$  as a function of discrete values of  $x$  (assuming as before  $N_x$  amount of spatial nodes). We also recall that we use  $N$ -samples of the wavenumber. We formulate the FWI problem as follows; given observations  $z_i \in \mathbb{C}^2$  with

$$z_i = (f(k_i), g(k_i)),$$

and sampling matrix

$$P = \begin{pmatrix} 1 & 0 & \cdots & 0 \\ 0 & 0 & \cdots & 1 \end{pmatrix} \in \mathbb{R}^{2 \times N_x},$$

find  $m$  such that the following functional

$$\phi_{fwi}(m) = \frac{1}{2} \sum_{i=1}^N \|Pu(k_i, m) - z_i\|_2^2$$

is minimized. As we shall see in the chosen examples, the ROM based method has a convex profile that avoids local minimizers of the conventional FWI functional. We showcase that by performing three experiments. In the first two we use measurements corresponding to relatively high wavenumbers compared to the maximum value of the respective  $m$ . In the last one we use both high wavenumber measurements and strong contrast.

We show that the ROM based FWI misfit avoids the local minimizers of the FWI functional by plotting the values of the two misfits as functions of  $m$ , when  $m = m_0 + adm$ , with  $m_0 = 1$ , and with  $a$  having range in an interval  $I_a$  such that there exists  $a' \in I_a$  with  $m_{\text{true}} = m_0 + a'dm$ , ( $dm = m_{\text{true}} - m_0$ ). We observe that in the first two examples the ROM misfit functional is convex. In the third example the functional is not convex, but the local minimizers of the conventional FWI are avoided.

### 5.4.3 Comparison with conventional FWI: reconstruction of a smooth coefficient

We split this section in two parts. In the first part we compare the two methods assuming that we have access to noiseless measurements. In the second part we add noise to the measurements.

#### Reconstruction Using Noiseless Data.

Following the standard adjoint state method, we present the numerical reconstruction of a refractive index using the ROM based FWI. For the numerical reconstruction we use a standard

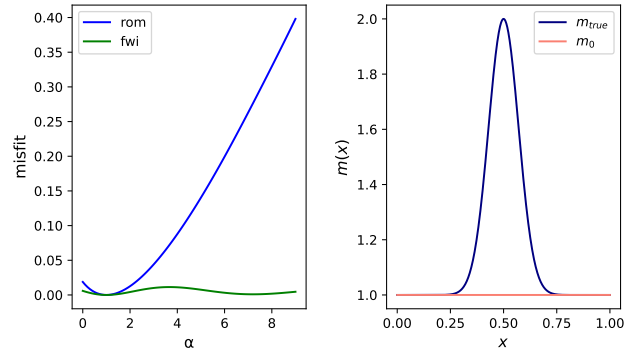


Figure 5.1: Comparison between the ROM based FWI and the conventional FWI when we use 10 wavenumbers with  $k_{min} = 18$  and  $k_{max} = 24$ . On the right we show  $m_0$  and  $m_{true}$ .

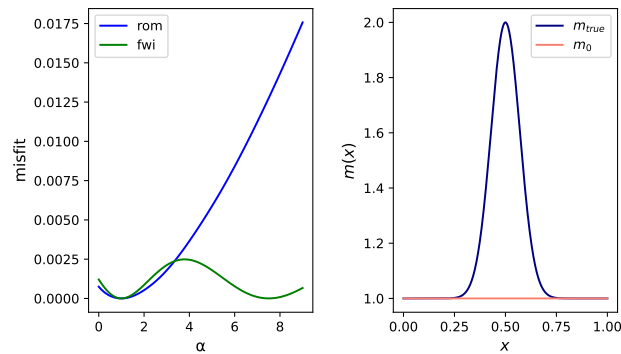


Figure 5.2: Comparison between the ROM based FWI and the conventional FWI when we use 2 wavenumbers  $k = 20, 20.1$ . On the right we show  $m_0$  and  $m_{true}$ .

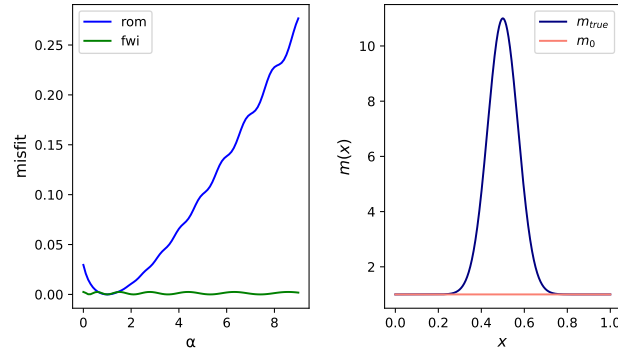


Figure 5.3: Comparison between the ROM based FWI and the conventional FWI when we use 2 wavenumbers with  $k = 20, 20.1$ . On the right we show  $m_0$  and  $m_{true}$ .

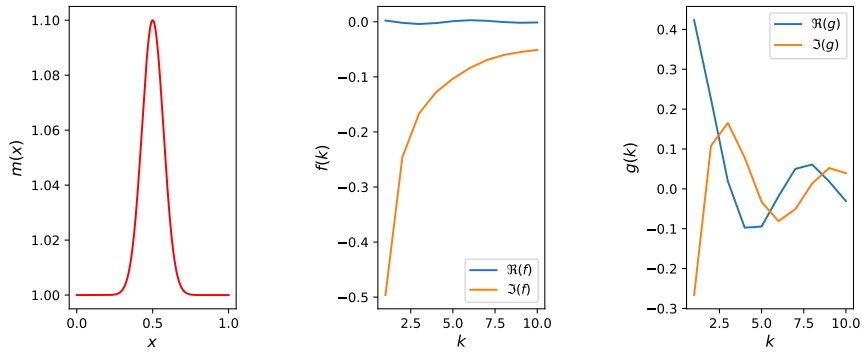


Figure 5.4: From left to right. The coefficient, the reflection data  $f$ , the transmission data  $g$ .

fixed point iteration of the form

$$m^{(\kappa+1)} = m^{(\kappa)} - \omega D_m \phi(m^{(\kappa)}), \quad \kappa = 1, 2, \dots, \quad (5.58)$$

with step  $\omega$ . In figure 5.4 we show the refractive index of our experiment, the reflection and the transmission data. We compare the results of our method with the results of the conventional FWI method using the same step  $\omega$  for both methods, and when we run the fixed point iteration for 15, 30 and 45 steps. Results can be seen in figures 5.5-5.7. Finally, figure 5.8 shows that after a sufficiently large number of iterations, the ROM based method recovers a coefficient that is closer to the true one. Also, the data fit of the reflection data is slightly better when we follow the ROM based method. The data fit of the transmission data does not seem to improve when following the ROM based method.

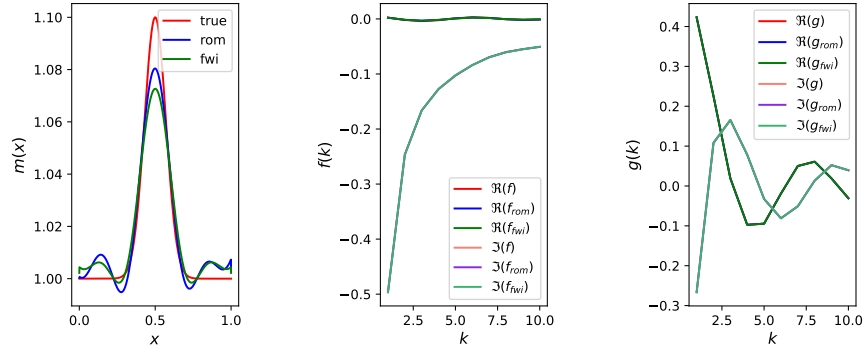


Figure 5.5: Comparison between the results produced by the ROM based and conventional FWI methods after 15 steps of the fixed point iteration. On the left, comparison between reconstructed coefficients. The errors are  $\|m_{rom} - m\|_2 = 0.214$  and  $\|m_{fwi} - m\|_2 = 0.271$ . In the middle and on the right we compare data-fit (transmission and reflection).

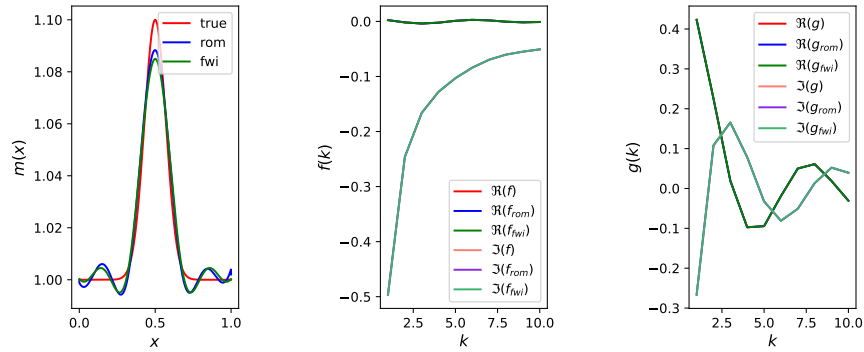


Figure 5.6: Comparison between the results produced by the ROM based and conventional FWI methods after 30 steps of the fixed point iteration. On the left, comparison between reconstructed coefficients. The errors are  $\|m_{rom} - m\|_2 = 0.152$  and  $\|m_{fwi} - m\|_2 = 0.169$ . In the middle and on the right we compare data-fit (transmission and reflection).



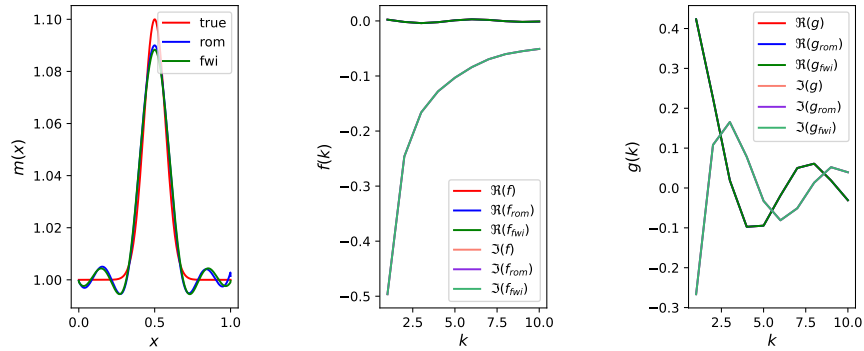


Figure 5.7: Comparison between the results produced by the ROM based and conventional FWI methods after 45 steps of the fixed point iteration. On the left, comparison between reconstructed coefficients. The errors are  $\|m_{rom} - m\|_2 = 0.145$  and  $\|m_{fwi} - m\|_2 = 0.156$ . In the middle and on the right we compare data-fit (transmission and reflection).

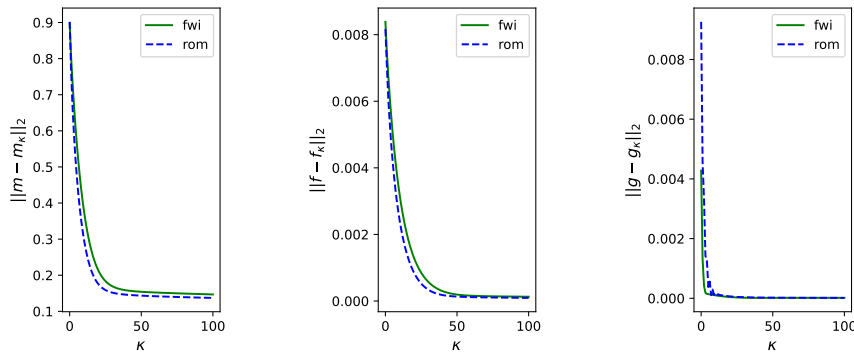


Figure 5.8: From left to right. On the left, comparison of the misfit  $\|m - m_\kappa\|_2$  when  $m_\kappa$  is recovered doing  $\kappa$ - steps of the fixed point iterations either of the conventional or the ROM based FWI method. We compare similarly the misfits of the reflection and the transmission data yielded by the respective  $m_\kappa$ . We used the same step  $\omega$  in both fixed point iterations.

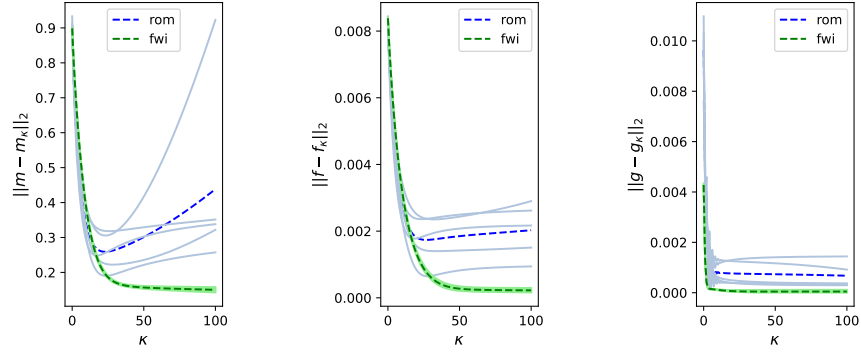


Figure 5.9: Comparison of the two methods when there is noise in the measurements ( $\sigma = 1 \times 10^{-4}$ ). On the left, comparison of the misfit  $\|m - m_\kappa\|_2$  when  $m_\kappa$  is recovered doing  $\kappa$ -steps of the fixed point iterations either of the conventional or the ROM based FWI method (dotted lines show average of 5 experiments). We compare similarly the average of the misfits of the reflection and the transmission data yielded by the respective  $m_\kappa$ . We used the same step in both fixed point iterations.

#### Reconstruction with Noise in the Data.

In this subsection we compare the methods on noisy data. We add i.i.d. normally distributed noise to the data with mean zero and variance  $\sigma^2$ . We study the case when  $\sigma = 1 \times 10^{-4}$ . We do not add any additional regularization. The results are shown in figure 5.9. We observe that the ROM based approach is affected by the noise and it yields inferior results compared with the conventional FWI method.

## 5.5 Discussion and Conclusions

In this chapter we studied a nonlinear optimization problem which can be viewed as a modified FWI problem using the stiffness ROM matrix as input. Due to the unconventional form of the misfit functional that includes not weakly lower semicontinuous terms, we studied well-posedness of the problem and we compared numerically our proposed method with the conventional FWI method. As we observed through our numerical experiments, the ROM based FWI misfit functional seems to have a convex profile, something that the conventional FWI lacks when we use relatively high frequency data. This observed convex behaviour of the ROM based functional makes the extension of the method to 2 and 3 dimensional inverse problems for the Helmholtz equation interesting. With this chapter we believe that we have made the first steps towards this extension. Of course, different variations of the ROM based FWI methods

can be proposed, in the sense of using  $M$  (or even  $B$ ) as input. The study of these cases are interesting and in the future we plan on analysing these variations. Finally, it is worth noting that our method might have some desired properties, such as improved convexity of the misfit for example, but it is sensitive in the presence of noise. We also plan to investigate various ways of improving the performance of the ROM based FWI method when the measurements are not exact.

## 5.6 Appendix: Proofs

### 5.6.1 Proof of Proposition 5.2.1

*Proof of proposition 5.2.1.* For the sake of completeness we include a sketch of the proof. We refer to [65] and [4] for more details. We define the forms  $a_1, a_2 : H^1(0, 1)^2 \rightarrow \mathbb{C}$  with

$$a_1(u, v) = \int_0^1 u' \bar{v}' dx - ik \{ (u\bar{v})|_{x=0} + (u\bar{v})|_{x=1} \}, \quad (5.59)$$

$$a_2(u, v) = - \int_0^1 mu\bar{v} dx, \quad u, v \in H^1(0, 1). \quad (5.60)$$

We note that  $a_1$  is coercive and that  $a_1, a_2$  are bounded forms. For  $a_1$ , we denote with  $L, U$  the low bound in the coercivity estimate, and the upper bound for the continuity estimate respectively. We define the linear Riesz isomorphism,

$$\Phi : H^1(0, 1) \rightarrow \overline{H^1(0, 1)}', \quad (5.61)$$

with  $\Phi u = (u, \cdot)_{H^1}, u \in H^1(0, 1)$ . Since  $a_1(u, \cdot)$  is an antilinear functional on  $H^1(0, 1)$ , and using the Riesz representation theorem we define  $\mathcal{T} : H^1(0, 1) \rightarrow H^1(0, 1)$  with

$$a_1(u, v) = (\mathcal{T}u, v)_{H^1}. \quad (5.62)$$

$\mathcal{T}$  is one-to-one onto and we have the estimates  $\|\mathcal{T}\|_\infty \leq U, \|\mathcal{T}^{-1}\|_\infty \leq L$ . Also, we define the linear operator  $\mathcal{V} : L^2(0, 1) \rightarrow \overline{H^1(0, 1)}', s \mapsto a_2(s, \cdot)$ . We also define the linear map

$$\mathcal{A}_1 = \mathcal{T}^{-1} \Phi^{-1} \mathcal{V} : L^2(0, 1) \rightarrow H^1(0, 1) \quad (5.63)$$

and

$$\mathcal{A} = \mathcal{A}_1 \circ i_{H^1 \rightarrow L^2} : H^1(0, 1) \xrightarrow{c} L^2(0, 1) \rightarrow H^1(0, 1), s \mapsto \mathcal{A}_1 s. \quad (5.64)$$

$\mathcal{A}$  is bounded as composition of bounded operators. Also, for  $s \in H^1(0,1), w \in H^1(0,1)$ , we have  $a_1(\mathcal{A}s, w) = a_2(s, w)$ . We claim that  $\mathcal{T} + k^2\mathcal{A}$  is one-to-one. Let now  $u \in H^1(0,1)$ . Finding a solution of the differential equation, is equivalent to finding  $u \in H^1(0,1)$  that satisfies

$$\begin{aligned} a_1(u, v) + k^2 a_2(u, v) &= -\langle \delta_0, v \rangle, \forall v \in H^1(0,1) \iff \\ a_1(u, v) + k^2 a_1(\mathcal{A}u, v) &= -\langle \delta_0, v \rangle, \forall v \in H^1 \iff \\ a_1(u + k^2 \mathcal{A}u, v) &= -\langle \delta_0, v \rangle, \forall v \in H^1 \iff \end{aligned} \quad (5.65)$$

$$(\mathcal{T}(u + k^2 \mathcal{A}u), v)_{H^1(0,1)} = -\langle \delta_0, v \rangle, \forall v \in H^1 \Rightarrow \quad (5.66)$$

$$\Phi \mathcal{T}(\mathcal{T} + k^2 \mathcal{A})u \stackrel{H^1(0,1)'}{=} -\delta_0 \iff (\mathcal{T} + k^2 \mathcal{A})u = \mathcal{T}^{-1} \Phi^{-1}(-\delta_0) \in H^1(0,1). \quad (5.67)$$

Since  $\mathcal{A} \in \mathcal{L}(H^1(\Omega), H^1(\Omega))$  is compact and  $\mathcal{T} + k^2\mathcal{A}$  is injective, using the Fredholm alternative we obtain that there exists a unique element  $u \in H^1(\Omega)$  that satisfies the last equation. Finally, we obtain the forward stability estimate

$$\|u\|_{H^1(0,1)} \leq \|(\mathcal{T} + k^2\mathcal{A})^{-1}\|_{\mathcal{L}(H^1, H^1)} \|\mathcal{T}^{-1}\|_{\mathcal{L}(H^1, H^1)} \|\Phi^{-1}\|_{\mathcal{L}(H^1, \overline{H^1})'} \|\delta_0\|_{\overline{H^1}'}. \quad \square$$

## 5.6.2 Proof of Lemma 5.3.1

*Proof of lemma 5.3.1.* We take  $k = k_i$  and we write  $u_i = u(k_i, \cdot)$ . Take  $\phi = u_j$ ,

$$(u'_i, u'_j) - k_i^2 (mu_i, u_j) - ik_i u_i(1) \overline{u_j(1)} - ik_i u_i(0) \overline{u_j(0)} = -\overline{u_j(0)} \quad (5.68)$$

Now we denote

$$M_{ij} = (mu_i, u_j) \quad (5.69)$$

$$S_{ij} = (u'_i, u'_j) \quad (5.70)$$

and we obtain

$$S_{ij} - k_i^2 M_{ij} = -\overline{f_j} + ik_i \{g_i \overline{g_j} + f_i \overline{f_j}\} \quad (5.71)$$

Similarly for  $k = k_j$

$$(u'_j, u'_i) - k_j^2(mu_j, u_i) - ik_j u_j(1)\overline{u_i(1)} - ik_j u_j(0)\overline{u_i(0)} = -\overline{u_i(0)}, \quad (5.72)$$

which gives

$$S_{ji} - k_j^2 M_{ji} = -\overline{f_i} + ik_j \{g_j \overline{g_i} + f_j \overline{f_i}\}. \quad (5.73)$$

Taking the complex conjugate of the above relation we obtain

$$\overline{S_{ji} - k_j^2 M_{ji}} =$$

$$S_{ij} - k_j^2 M_{ij} = -f_i - ik_j \{g_i \overline{g_j} + f_i \overline{f_j}\}. \quad (5.74)$$

Subtracting (5.71) - (5.74) we arrive at

$$S_{ij} - k_i^2 M_{ij} - S_{ij} + k_j^2 M_{ij} = -\overline{f_j} + ik_i \{g_i \overline{g_j} + f_i \overline{f_j}\} + f_i + ik_j \{g_i \overline{g_j} + f_i \overline{f_j}\} \Rightarrow$$

$$(-k_i^2 + k_j^2)M_{ij} = -\overline{f_j} + f_i + ik_i \{g_i \overline{g_j} + f_i \overline{f_j} + f_i\} + ik_j \{g_i \overline{g_j} + f_i \overline{f_j}\} \Rightarrow \quad (5.75)$$

$$M_{ij} = \frac{-\overline{f_j} + f_i + ik_i \{g_i \overline{g_j} + f_i \overline{f_j}\} + ik_j \{g_i \overline{g_j} + f_i \overline{f_j}\}}{k_j^2 - k_i^2} \Rightarrow \quad (5.76)$$

$$M_{ij} = -\frac{\overline{f_j} - f_i}{k_j^2 - k_i^2} + i \frac{(k_i + k_j)(g_i \overline{g_j} + f_i \overline{f_j})}{k_j^2 - k_i^2} \Rightarrow \quad (5.77)$$

$$M_{ij} = -\frac{\overline{f_j} - f_i}{k_j^2 - k_i^2} + i \frac{g_i \overline{g_j} + f_i \overline{f_j}}{k_j - k_i}. \quad (5.78)$$

Similarly we multiply (5.71) by  $k_j^2$  and (5.74) by  $k_i^2$  and we obtain

$$k_j^2 S_{ij} - k_j^2 k_i^2 M_{ij} = -k_j^2 \overline{f_j} + ik_j^2 k_i \{g_i \overline{g_j} + f_i \overline{f_j}\} \quad (5.79)$$

$$k_i^2 S_{ij} - k_j^2 k_i^2 M_{ij} = -k_i^2 f_i - ik_i^2 k_j \{g_i \overline{g_j} + f_i \overline{f_j}\} \quad (5.80)$$

Subtracting the above two relations,

$$(k_j^2 - k_i^2)S_{ij} = -k_j^2 \overline{f_j} + ik_j^2 k_i \{g_i \overline{g_j} + f_i \overline{f_j}\} + k_i^2 f_i + ik_i^2 k_j \{g_i \overline{g_j} + f_i \overline{f_j}\} \Rightarrow \quad (5.81)$$

$$S_{ij} = \frac{-k_j^2 \overline{f_j} + k_i^2 f_i}{k_j^2 - k_i^2} + i(k_j^2 k_i + k_i^2 k_j) \frac{g_i \overline{g_j} + f_i \overline{f_j}}{k_j^2 - k_i^2} \Rightarrow \quad (5.82)$$

$$S_{ij} = -\frac{k_j^2 \overline{f_j} - k_i^2 f_i}{k_j^2 - k_i^2} + i(k_j^2 k_i + k_i^2 k_j) \frac{g_i \overline{g_j} + f_i \overline{f_j}}{k_j^2 - k_i^2}. \quad (5.83)$$

Now, we derive the formula for the diagonal elements of  $M$ . First of all, consider

$$\int_0^1 mu(\lambda) \overline{u(\mu)} dx := \mathcal{M}(\lambda, \mu) : [\lambda_{\min}, \lambda_{\max}] \times [\mu_{\min}, \mu_{\max}] \rightarrow \mathbb{C}. \quad (5.84)$$

$\mathcal{M}$  is a continuous function, thus, if we fix  $\mu = \mu_0$ , then the following limit exists

$$\lim_{\lambda \rightarrow \mu_0} M(\lambda, \mu_0) = \|u(\mu_0)\|_{L^2(0,1,mdx)} > 0 \quad (5.85)$$

The elements of the mass matrix  $\mathcal{M}$  are given by relation (5.78) above. Let  $k_i^2 = \lambda$  and  $k_j^2 = \lambda + h$ , with  $h \in \mathbb{R}$ . Take

$$M_{ij} = M(\lambda, \lambda + h) = -\frac{\overline{f(\lambda + h)} - f(\lambda)}{h} + i \frac{g(\lambda) \overline{g(\lambda + h)} + f(\lambda) \overline{f(\lambda + h)}}{\sqrt{\lambda + h} - \sqrt{\lambda}} \quad (5.86)$$

We write  $f = Re(f) + iIm(f)$  and  $g = Re(g) + iIm(g)$ . The first term of (5.86) can be written as

$$\begin{aligned} -\frac{\overline{f(\lambda + h)} - f(\lambda)}{h} &= -\frac{Re(f)(\lambda + h) - iIm(f)(\lambda + h) - Re(f)(\lambda) - iIm(f)(\lambda)}{h} = \\ &= -\frac{Re(f)(\lambda + h) - Re(f)(\lambda)}{h} + i \frac{Im(f)(\lambda + h) + Im(f)(\lambda)}{h}. \end{aligned} \quad (5.87)$$

The second term of (5.86) is

$$\begin{aligned} i \frac{g(\lambda) \overline{g(\lambda + h)} + f(\lambda) \overline{f(\lambda + h)}}{\sqrt{\lambda + h} - \sqrt{\lambda}} &= \\ i \frac{Re(g)Re(g^h) + Im(g)Im(g^h) + Re(f)Re(f^h) + Im(f)Im(f^h)}{\sqrt{\lambda + h} - \sqrt{\lambda}} &+ \end{aligned}$$

$$\left( -\frac{\operatorname{Im}(g)\operatorname{Re}(g^h) - \operatorname{Re}(g)\operatorname{Im}(g^h) + \operatorname{Im}(f)\operatorname{Re}(f^h) - \operatorname{Re}(f)\operatorname{Im}(f^h)}{\sqrt{\lambda+h} - \sqrt{\lambda}} \right), \quad (5.88)$$

since

$$g\bar{g}_h = (\operatorname{Re}(g) + i\operatorname{Im}(g))(\operatorname{Re}(g^h) - i\operatorname{Im}(g^h)) = \\ \operatorname{Re}(g)\operatorname{Re}(g^h) + \operatorname{Im}(g)\operatorname{Im}(g^h) + i\operatorname{Im}(g)\operatorname{Re}(g^h) - i\operatorname{Im}(g^h)\operatorname{Re}(g),$$

where we used the shorthand notation  $f^h = f(\lambda+h)$  (also for  $g$ ). Now, since this limit exists,

$$\lim_{h \rightarrow 0} M(\lambda, \lambda+h) = \|u(\lambda)\|_{L^2(0,1,mdx)} \in \mathbb{R},$$

we obtain that

$$\lim_{h \rightarrow 0} \Im(M(\lambda, \lambda+h)) = 0, \quad (5.89)$$

thus

$$\lim_{h \rightarrow 0} \left\{ \frac{\operatorname{Im}(f)^h + \operatorname{Im}(f)}{h} + \frac{\operatorname{Re}(g)\operatorname{Re}(g^h) + \operatorname{Im}(g)\operatorname{Im}(g^h) + \operatorname{Re}(f)\operatorname{Re}(f^h) + \operatorname{Im}(f)\operatorname{Im}(f^h)}{\sqrt{\lambda+h} - \sqrt{\lambda}} \right\} = 0.$$

Therefore

$$M_{ii} = \lim_{h \rightarrow 0} \left\{ -\frac{\operatorname{Re}(f)(\lambda+h) - \operatorname{Re}(f)(\lambda)}{h} - \frac{\operatorname{Im}(g)\operatorname{Re}(g^h) - \operatorname{Re}(g)\operatorname{Im}(g^h) + \operatorname{Im}(f)\operatorname{Re}(f^h) - \operatorname{Re}(f)\operatorname{Im}(f^h)}{\sqrt{\lambda+h} - \sqrt{\lambda}} \right\} = \\ \lim_{h \rightarrow 0} \left\{ -\frac{\operatorname{Re}(f)(\lambda+h) - \operatorname{Re}(f)(\lambda)}{h} - \frac{\operatorname{Im}(g)\operatorname{Re}(g^h) - \operatorname{Re}(g)\operatorname{Im}(g) + \operatorname{Re}(g)\operatorname{Im}(g) - \operatorname{Re}(g)\operatorname{Im}(g)^h}{\sqrt{\lambda+h} - \sqrt{\lambda}} - \frac{\operatorname{Re}(f)\operatorname{Im}(f)^h - \operatorname{Im}(f)\operatorname{Re}(f)^h}{\sqrt{\lambda+h} - \sqrt{\lambda}} \right\} \Rightarrow \\ M_{ii} = -\frac{d\operatorname{Re}(f)}{d\lambda}(\lambda) - \operatorname{Im}(g)(\lambda)2\sqrt{\lambda}\frac{d\operatorname{Re}(g)}{d\lambda}(\lambda) + \operatorname{Re}(g)(\lambda)2\sqrt{\lambda}\frac{d\operatorname{Im}(g)}{d\lambda}(\lambda) - \\ \operatorname{Im}(f)(\lambda)2\sqrt{\lambda}\frac{d\operatorname{Re}(f)}{d\lambda}(\lambda) + \operatorname{Re}(f)(\lambda)2\sqrt{\lambda}\frac{d\operatorname{Im}(f)}{d\lambda}(\lambda) \quad (5.90)$$

We compute the diagonal of  $S$  similarly.  $\square$

### 5.6.3 Proof of Lemma 5.3.2

We start by stating the implicit function theorem.

**Theorem 5.6.1.** *Let a function  $F : C \times P \rightarrow W$ ,  $C, P, W$  being Banach spaces. We assume that there exists an open set  $C_0 \subset C$  such that for every  $m \in C_0$  there exists a unique  $u = u(m) \in P$  such that*

$$F(m, u) = 0. \quad (5.91)$$

Then if

$$F : C \times P \rightarrow W \quad (5.92)$$

is continuous, if

$$\partial_2 F : C \times P \rightarrow W \quad (5.93)$$

is continuous and if

$$(\partial_2 F(m, u))^{-1} : W \rightarrow P, \forall m \in C_0, \quad (5.94)$$

exists and is bounded, then there exists a continuous map such that

$$C_0 \ni m \mapsto u(m) \in P. \quad (5.95)$$

Also, if  $\partial_1 F$  is continuous, we obtain that  $u$  is Fréchet differentiable.

**Lemma 5.6.1.** *The requirements of theorem 5.6.3 hold for  $F$ .*

*Proof.* Let  $P = H^1(0, 1)$ . For all  $m \in C_0 = C([0, 1]; (0, \infty)) \subset C = C([0, 1]; \mathbb{R})$  there exists  $u$  such that  $F(m, u) = 0$ . Second, we want to show continuity of  $F$ . We get for  $(\delta m, \delta u) \in C \times H^1$

$$\begin{aligned} F(m + \delta m, u + \delta u) - F(m, u) &= \\ \mathcal{S}(u + \delta u) - k^2 \mathcal{M}(m + \delta m)(u + \delta u) - ik\mathcal{B}(u + \delta u) + \delta_0 - \\ &\quad (\mathcal{S}(u) - k^2 \mathcal{M}(m)(u) - ik\mathcal{B}(u) + \delta_0) = \\ \mathcal{S}(\delta u) - k^2 \mathcal{M}(\delta m)(u) - k^2 \mathcal{M}(m)(\delta u) - k^2 \mathcal{M}(\delta m)(\delta u) - ik\mathcal{B}(\delta u). \end{aligned} \quad (5.96)$$



Now, for  $\phi \in H^1(0, 1)$

$$\begin{aligned} |\langle \mathcal{M}(\delta m)(u), \phi \rangle| &= \left| \int_0^1 (\delta m)u\bar{\phi} dx \right| \leq \|\delta m\|_\infty \int_0^1 |u\bar{\phi}| dx \leq \\ &\|\delta m\|_\infty \|u\|_\infty \int_0^1 |\bar{\phi}| dx \leq \|\delta m\|_\infty \|u\|_\infty \|\phi\|_\infty \leq \gamma^2 \|\delta m\|_\infty \|u\|_{H^1} \|\phi\|_{H^1}, \end{aligned}$$

where  $\gamma$  is the bound of the Sobolev imbedding from  $H^1$  to  $C[0, 1]$ . Similarly,

$$|\langle \mathcal{M}(m)(\delta u), \phi \rangle| \leq \gamma^2 \|\delta u\|_{H^1} \|m\|_\infty \|\phi\|_{H^1}, \quad (5.97)$$

$$|\langle \mathcal{M}(\delta m)(\delta u), \phi \rangle| \leq \gamma^2 \|\delta u\|_{H^1} \|\delta m\|_\infty \|\phi\|_{H^1}. \quad (5.98)$$

Also,

$$|\langle \mathcal{S}\delta u, \phi \rangle| = |(\delta u', \phi')| \leq \|\delta u'\|_{L^2} \|\phi'\|_{L^2} \leq \|\delta u\|_{H^1} \|\phi\|_{H^1}, \quad (5.99)$$

$$\begin{aligned} |\langle \mathcal{B}(\delta u), \phi \rangle| &= |(\delta u\phi)|_{x=0} + |(\delta u\phi)|_{x=1} \leq \|\delta u\|_\infty \|\phi\|_\infty + \|\delta u\|_\infty \|\phi\|_\infty \leq \\ &2\gamma \|\delta u\|_{H^1} \|\phi\|_{H^1}. \end{aligned}$$

All the above relations yield that

$$\|F(m + \delta m, u + \delta u) - F(m, u)\|_{\overline{H^1}'} \rightarrow 0 \text{ as } \delta m, \delta u \rightarrow 0. \quad (5.100)$$

Also, since for fixed  $m$ ,  $F(m, \cdot)$  is affine on  $u$ , we get that

$$\partial_2 F(m, u) \in \mathcal{L}(H^1, \overline{H^1}'), \quad u \in H^1, \quad (5.101)$$

and at a point  $(m, u)$  at a direction  $s$  we get

$$\partial_2 F(m, u)s = \langle (\mathcal{S} - k^2 \mathcal{M}(m) - tk\mathcal{B})s, \cdot \rangle, \quad s \in H^1. \quad (5.102)$$

As before,  $\partial_2 F$  is continuous as a function of  $(m, u)$ . Similarly, for fixed  $u$ , we obtain at  $(m, u)$  in a direction  $h$

$$\partial_1 F(m, u)h = -k^2 \langle \mathcal{M}(u)h, \cdot \rangle \Rightarrow \quad (5.103)$$

$$\partial_1 F(m, u)h = -k^2 \langle \mathcal{M}(u)h, \cdot \rangle, \quad \forall (m, u) \in C \times H^1(0, 1), \quad (5.104)$$

and  $\partial_1 F$  is continuous on  $C \times H^1$ . Since the partial derivatives of  $F$  are continuous we conclude that the gradient of  $F$  exists and is continuous. Finally, since at any point of evaluation,

$$\partial_2 F(m, u) = \mathcal{I} - k^2 \mathcal{M}(m) - ik\mathcal{B} = \Phi \mathcal{T}(\mathcal{I} + k^2 \mathcal{A}) \quad (5.105)$$

is invertible, we obtain that the following map

$$C([0, 1]; (0, \infty)) \ni m \mapsto u(k, m) \in H^1(0, 1) \quad (5.106)$$

is well-defined, continuous and is F-differentiable. □

*Proof of lemma 5.3.2.* The proof of the lemma is a corollary of the above result □

# Chapter 6

## Outlook and Conclusions

In this thesis we studied the GLM and ROM based inversion methods for solving inverse scattering problems. In particular, our contributions are the following:

1. **Variational TLS regularization for classical GLM inversion:** We revisited some classical results from inverse scattering to solve the 1D inverse coefficient problem for the frequency domain wave equation. We considered the GLM method with noisy data and proposed a regularised total least squares formulation in the infinite dimensional setting. We contributed an error bound for the unregularised GLM approach and have shown existence of minimizers for the variational formulation of the TLS approach. Finally, we illustrated numerically that the TLS approach gives superior results as compared to conventional Tikhonov regularisation.
2. **A generalized GLM equation for the 1D Helmholtz scattering:** We revisited the classical 1D Helmholtz scattering problem and we derived a generalised Gelfand-Levitan-Marchenko equation in the space of tempered distributions. We showed that the Jost solution of the Helmholtz equation minus a plane wave grows in a controlled way as the wave number grows. This allowed us to consider a distributional framework where we derived a distributional version of the Gelfand-Levitan-Marchenko equation.
3. **Data driven 1D inverse Schrödinger scattering:** We treated the inverse problem of retrieving the scattering potential in a 1D Schrödinger equation from boundary data. To do this, we proposed a two-step approach inspired by a previously-published ROM-based method. We extended this method, previously applied to 1D diffusion problems with Neumann boundary conditions, to the 1D Schrödinger equation with impedance boundary conditions. In particular, we presented explicit expressions for retrieving the ROM-matrices from boundary data and proposed a novel approach for approximating the state

from these matrices. This approach, based on ideas from data-assimilation, is an alternative to the previously proposed method based on Lanczos-orthogonalization. Given the estimates of the states, the scattering potential is obtained by solving an integral equation.

4. **ROM based nonlinear waveform inversion** We studied a reduced order model (ROM) based waveform inversion method applied to a Helmholtz problem with impedance boundary conditions and variable refractive index. We obtained relations that allow the reconstruction of the Galerkin projection of the continuous problem onto the space spanned by solutions of the Helmholtz equation. We also studied the nonlinear optimization method based on the ROM aimed to estimate the refractive index from reflection and transmission data.

In the next two paragraphs we elaborate on future research directions both in the GLM and the ROM based inversion.

## 6.1 Future Work on the Gelfand-Levitan-Marchenko Inversion

In this paragraph we discuss interesting future work directions on the GLM based inversion. First of all, it is interesting to study the numerical solution of the coupled system (3.80) (3.81). The most interesting research direction however, is the extension of the distributional GLM method to the Helmholtz problem in 2,3D. Since there is no transformation from the Helmholtz equation to the Schrödinger equation, the distributional point of view that we introduced can be useful. We can even give some more details. For example, take the following scattering problem,

$$(-\Delta - k^2 m(x))u(k, x) = 0, \quad x \in \mathbb{R}^\delta, \quad \delta = 2, 3, \quad (6.1)$$

$$u(k, x) = u^s(k, x) + e^{ikx \cdot d}, \quad x \in \mathbb{R}^\delta \quad (6.2)$$

$$\lim_{r \rightarrow \infty} r^{\frac{\delta-1}{2}} \left( \frac{\partial u^s(k, r)}{\partial r} - ik u^s(k, r) \right) = 0, \quad (6.3)$$

where  $d \in \{x \in \mathbb{R}^\delta : |x| = 1\}$  and  $r = |x|$ . It is interesting to study  $u$  as a function of  $k$ , and particularly to examine the growth properties of the solution in terms of the wave-number. That would be a first step towards a possible extension of our point of view to 2,3D.

## 6.2 Future Work on Reduced Order Model Inversion

In this paragraph we discuss interesting future work directions on the ROM based inversion. We start by discussing possible research directions based on chapter 4. Worth noting is understanding why when orthogonalizing the snapshot space using the Lanczos algorithm, we obtain a basis that depends weakly on the medium. Working towards this direction is interesting regardless of the framework (scattering or diffusion). Also, it is interesting to extend the ROM based techniques that we introduced in chapter 4 to the Helmholtz case and to 2,3D. Some other open questions based on the techniques of chapter 4 include the approximation error, stability estimates, and more practical aspects such an iterative approach where the reference potential is iteratively updated.

Now, there are many different research routes we can follow by taking inspiration from our work on the ROM based FWI of chapter 5. First of all, different variations of the ROM based FWI methods can be proposed, in the sense of using the mass matrix (or even  $B$ ) as input. It would be interesting to investigate how a method in the spirit of the ROM based FWI method would compare in 2 and 3D with the conventional FWI. It would be also interesting to combine the Lanczos algorithm with a ROM based FWI method applied to inverse Schrödinger scattering. This could be set up as follows. Define  $A = M^{-1}S$  and let  $T$  be the tridiagonal matrix that the Lanczos algorithm returns after giving as input  $A$  and  $M^{-1}f$ . It would be interesting to study the problem

$$\min_q \frac{1}{2} \|T(q) - T^{\text{obs}}\|_F^2. \quad (6.4)$$

Apart from the practical study of the above optimization problem (convexity, reconstruction), the theoretical study of this approach is interesting (existence of minimizers when adding regularization, optimality). Finally, it is interesting to examine ways to improve the already proposed ROM based FWI method when there is noise in the data, since as we observed, the reconstruction is affected.



# Chapter 7

## Summary

Inverse scattering problems arise in many applications, especially in imaging. In this thesis we studied frequency domain inverse scattering problems for the Helmholtz and the Schrödinger operators using both classical inverse scattering and modern reduced order model techniques.

We started by revisiting the classical Gelfand-Levitan-Marchenko (GLM) integral equation method for solving the inverse Schrödinger scattering problem in 1D. The inverse Schrödinger scattering problem is interesting for imaging purposes, since it is possible to transform the Helmholtz and the (frequency domain) acoustic wave equation to the Schrödinger equation using a coordinate transform. In particular, we considered the GLM method with noise in the data, where we contributed an error bound for the solution of the unregularised GLM equation. We also proposed a regularised total least squares formulation in the infinite dimensional setting and we showed well posedness. Moreover, we studied the 1D scattering problem for the Helmholtz operator and we developed a GLM theory exclusively for the Helmholtz problem. In particular, we derived a generalised GLM equation in the space of tempered distributions for reconstructing the Jost solutions of the Helmholtz operator. To do so, we had to examine the asymptotic behaviour of the Jost solutions of the Helmholtz operator in terms of the wavenumber.

After studying classical inverse scattering methods based on the GLM approach, we continued by studying inversion methods based on reduced order models (ROMs). We started with the inverse Schrödinger scattering problem of retrieving the scattering potential in 1D Schrödinger equation using boundary data. For that reason, we proposed a two-step approach inspired by a previously-published ROM-based method. We presented explicit expressions allowing the exact reconstruction of the ROM-matrices from boundary data and proposed a new data-assimilation approach for approximating the state from these matrices. Given the estimates of the states, the scattering potential is obtained by solving a Lippmann-Schwinger type integral equation. Finally, we combined the traditional FWI method with reduced order models and we proposed a new nonlinear inversion method for the inverse Helmholtz scattering problem. In particular,

the input of our misfit functional consisted of the stiffness matrix of the ROM projection. In this case, we studied the well posedness of the nonlinear optimization problem and we derived the optimality condition. We finally compared numerically the ROM based FWI method with the conventional FWI method.



# Chapter 8

## Samenvatting

Problemen binnen inverse scattering ontstaan op natuurlijke wijze in veel toepassingen, met name binnen de beeldvorming. In dit proefschrift hebben we problemen binnen inverse scattering in het frequentiedomein bestudeerd voor de Helmholtz- en de Schrödinger-operatoren, gebruikmakend van zowel klassieke inverse scattering als moderne model order reduction technieken.

We zijn begonnen met het herzien van de klassieke Gelfand-Levitan-Marchenko (GLM) integraalvergelijkingmethode voor het oplossen van het inverse Schrödinger-scattering probleem in 1D. Het inverse Schrödinger-scattering probleem is interessant voor beeldvormingsdoeleinden, aangezien het mogelijk is om de Helmholtz en de (frequentiedomein) akoestische golfvergelijking te transformeren naar de Schrödinger-vergelijking met behulp van een coördinatentransformatie. We hebben met name gekeken naar de GLM-methode met ruis in de gegevens, waar we een foutgrens hebben bijgedragen voor de oplossing van de niet-geregulariseerde GLM-vergelijking. We hebben ook een geregulariseerde kleinste kwadraten formulering in het oneindig dimensionale geval voorgesteld én goedgesteldheid aangetoond. Ook hebben we het 1D-scattering probleem voor de Helmholtz operator bestudeerd én een GLM-theorie direct voor het Helmholtz-probleem ontwikkeld. In het bijzonder hebben we een generaliseerde GLM vergelijking afgeleid in de ruimte van getempereerde distributies om Jostoplossingen van de Helmholtzoperator te reconstrueren. Om dit te doen, moesten we het asymptotische gedrag van de Jost-oplossingen van de Helmholtz-operator onderzoeken in termen van het golfgetal.

Na het bestuderen van klassieke inverse scattering methoden op basis van de GLM-benadering, zijn we verder gegaan met het bestuderen van inversiemethoden op basis van reduced order models (ROM's). We zijn begonnen met het inverse Schrödinger-scattering probleem van het ophalen van het scatteringpotentiaal 1D Schrödingervergelijking met behulp van grensgegevens. Om die reden hebben we een aanpak in twee stappen voorgesteld, geïnspireerd op een

eerder gepubliceerde op ROM gebaseerde methode. We hebben expliciete uitdrukkingen gepresenteerd die de exacte reconstructie van de ROM-matrices uit grensgegevens mogelijk maken en een nieuwe data-assimilatiebenadering voor het benaderen van de toestand van deze matrices voorgesteld. Gegeven de schattingen van de toestanden, wordt het scattering potentiaal verkregen door een integraalvergelijking van het type Lippmann-Schwinger op te lossen. Ten slotte hebben we de traditionele FWI-methode gecombineerd met reduced order models en hebben we een nieuwe niet-lineaire inversiemethode voorgesteld voor het inverse Helmholtz-scattering probleem. De input van onze misfit functional bestond met name uit de stijfheidsmatrix van de ROM-projectie. In dit geval hebben we de goedgesteldheid van het niet-lineaire optimalisatieprobleem bestudeerd en de optimaliteitsvoorwaarde afgeleid. We hebben uiteindelijk de op ROM gebaseerde FWI-methode numeriek vergeleken met de conventionele FWI-methode.

# Chapter 9

## Acknowledgements

First of all, I would like to thank my supervisor Tristan van Leeuwen for the support that he provided me during my PhD journey. He was always willing to help me with my research and to provide guidance for my PhD studies. Thanks Tristan for the collaboration! I also want to thank Sjoerd Verduyn Lunel for the support and all the productive discussions that we had on many mathematical concepts regarding my research. Thanks Sjoerd for the new things I learned and the inspiration that you gave me through our discussions! I am also thankful to Ivan Vasconcelos for our fruitful discussions and the support and the guidance he provided me during my PhD! Also, I want to thank Alex Mamonov for hosting me in the University of Houston during my research visit in the United States.

I also want to thank my fellow PhD students in the UCSI for all the discussions that we had, and of course, our consortium sponsors for funding our research. Thanks Leon for the discussions and the nice activities that we did. Thanks Haorui and David for all the fruitful discussions.

I also want to thank the fellow PhD students in the mathematical institute and especially my office mates and the people from the 5th floor of the mathematical institute, for all the nice discussions and the extracurricular activities we did together.

I would also like to thank the secretaries of the earth sciences department and of the mathematical institute for the support and the help in practical issues.

I would also like to thank my family and my friends, both in the Netherlands and in Greece, for the support that they provided me all these years of my PhD studies.



# Chapter 10

## Curriculum Vitae

Andreas Tataris was born on 16 December 1994 in Athens, Greece. After graduating from the Zanneio experimental high school and lyceum in Piraeus, he studied applied mathematics in the School of Applied Mathematical and Physical Sciences of the National Technical University of Athens. In July of 2019 he started his PhD in Utrecht University as a member of the Utrecht Consortium for Subsurface Imaging, under the supervision of Tristan van Leeuwen, Sjoerd Verduyn Lunel and Ivan Vasconcelos.



# Bibliography

- [1] Aktosun, T.: Stability of the marchenko inversion. *Inverse Problems* **3**(4), 555–563 (1987)
- [2] Aktosun, T., Papanicolaou, V.: Reconstruction of the wave speed from transmission eigenvalues for the spherically symmetric variable-speed wave equation. *Inverse Problems* **29**, 065007 (2013)
- [3] Alessandrini, G., de Hoop, M.V., Faucher, F., Gaburro, R., Sincich, E.: Inverse problem for the helmholtz equation with cauchy data: reconstruction with conditional well-posedness driven iterative regularization. *ESAIM: Mathematical Modelling and Numerical Analysis* (2019)
- [4] Bao, G., Li, P.: Inverse medium scattering for the helmholtz equation at fixed frequency. *Inverse Problems* **21**(5), 1621–1641 (sep 2005)
- [5] Bleistein, N., Cohen, J., Jr, J.: *Mathematics of Multidimensional Seismic Imaging, Migration, and Inversion*, vol. 13. Springer (2001)
- [6] Bleyer, I.R., Ramlau, R.: A double regularization approach for inverse problems with noisy data and inexact operator. *Inverse Problems* **29**(2), 025004 (2013)
- [7] Bleyer, I.R., Ramlau, R.: An alternating iterative minimisation algorithm for the double-regularised total least square functional. *Inverse Problems* **31**(7), 075004 (2015)
- [8] Borcea, L., Druskin, V., Mamonov, A., Moskow, S., Zaslavsky, M.: Reduced order models for spectral domain inversion: embedding into the continuous problem and generation of internal data. *Inverse Problems* **36**(5), 055010 (2020)
- [9] Borcea, L., Druskin, V., Mamonov, A.V., Moskow, S., Zaslavsky, M.: Reduced order models for spectral domain inversion: Embedding into the continuous problem and generation of internal data. *ArXiv* **abs/1909.06460** (2019)

- [10] Borcea, L., Garnier, J., Mamonov, A.V., Zimmerling, J.T.: Reduced order model approach for imaging with waves. *Inverse Problems* **38** (2021)
- [11] Borcea, L., Garnier, J., Mamonov, A.V., Zimmerling, J.T.: Waveform inversion via reduced order modeling. *ArXiv* **abs/2202.01824** (2022)
- [12] Brezis, H.: *Functional Analysis, Sobolev Spaces and Partial Differential Equations*. Springer (01 2010)
- [13] Brogгинi, F., Snieder, R.: Connection of scattering principles: a visual and mathematical tour. *European Journal of Physics* **33**(3), 593–613 (mar 2012)
- [14] Brogгинi, F., Wapenaar, K., van der Neut, J., Snieder, R.: Data-driven green’s function retrieval and application to imaging with multidimensional deconvolution. *Journal of Geophysical Research: Solid Earth* **119**(1), 425–441 (2014)
- [15] Burrige, R.: The gelfand-levitan, the marchenko, and the gopinath-sondhi integral equations of inverse scattering theory, regarded in the context of inverse impulse-response problems. *Wave Motion* **2**(4), 305 – 323 (1980)
- [16] Carroll, R., Santosa, F., Ortega, J.: Stability for the one dimensional inverse problem via the gel’fand-levitan equation. *Applicable Analysis* **13**(4), 271–277 (1982)
- [17] Chadan, K., Newton, R., Sabatier, P.: *Inverse Problems in Quantum Scattering Theory*. Theoretical and Mathematical Physics, Springer Berlin Heidelberg (2013)
- [18] Coen, S., Cheney, M., Weglein, A.: Velocity and density of a two-dimensional acoustic medium from point source surface data. *Journal of Mathematical Physics* **25**(6), 1857–1861 (1984)
- [19] Colton, D., Kress, R.: *Inverse acoustic and electromagnetic scattering theory*. Springer (2019)
- [20] Connolly, T.J., Wall, D.J.N.: On frechet differentiability of some nonlinear operators occurring in inverse problems: an implicit function theorem approach. *Inverse Problems* **6**(6), 949 (dec 1990)
- [21] Deift, P., Trubowitz, E.: Inverse scattering on the line. *Communications on Pure and Applied Mathematics* **32**(2), 121–251 (1979)
- [22] Diekmann, L., Vasconcelos, I.: Focusing and green’s function retrieval in three-dimensional inverse scattering revisited: A single-sided marchenko integral for the full wave field. *Physical Review Research* **3** (03 2021)



- [23] Diekmann, L., Vasconcelos, I., Cummings, D., Curtis, A.: Towards exact linearized full-waveform inversion via Marchenko redatuming, pp. 3380–3384 (2021)
- [24] Drazin, P.G., Johnson, R.S.: Solitons: An Introduction. Cambridge Texts in Applied Mathematics, Cambridge University Press, 2 edn. (1989)
- [25] Druskin, V., Moskow, S., Zaslavsky, M.: On extension of the data driven ROM inverse scattering framework to partially nonreciprocal arrays. *Inverse Problems* **38**(8), 084002 (jul 2022)
- [26] Druskin, V., Moskow, S., Zaslavsky, M.: Lippmann–schwinger–lanczos algorithm for inverse scattering problems. *Inverse Problems* **37** (2021)
- [27] Druskin, V., Moskow, S., Zaslavsky, M.: On extension of the data driven rom inverse scattering framework to partially nonreciprocal arrays. *Inverse Problems* (2022)
- [28] Eckhaus, W., van Harten, A.: The Inverse Scattering Transformation and The Theory of Solitons. ISSN, Elsevier Science (2011)
- [29] Feireisl, E., Karper, T.G., Pokorný, M.: Mathematical theory of compressible viscous fluids. Birkhäuser (2016)
- [30] Fink, J.P., Rheinboldt, W.C.: On the error behavior of the reduced basis technique for nonlinear finite element approximations. *Zamm-zeitschrift Fur Angewandte Mathematik Und Mechanik* **63**, 21–28 (1983)
- [31] Folland, G.B.: Fourier analysis and its applications, vol. 4. American Mathematical Soc. (2009)
- [32] Grubb, G.: Distributions and Operators, Graduate Texts in Mathematics, vol. 252. Springer (01 2009)
- [33] Hansen, P.C., O’Leary, D.P.: The use of the l-curve in the regularization of discrete ill-posed problems. *SIAM J. Sci. Comput.* **14**, 1487–1503 (1993)
- [34] von Harrach, B., Lee, E., Ullrich, M.: Combining frequency-difference and ultrasound modulated electrical impedance tomography. *Inverse Problems* **31**, 095003 (2015)
- [35] Hinze, M., Pinnau, R., Ulbrich, M., Ulbrich, S.: Optimization with PDE Constraints. Mathematical Modelling: Theory and Applications, Springer Netherlands (2008)
- [36] Hungerländer, P., Kaltenbacher, B., Rendl, F.: Regularization of inverse problems via box constrained minimization. *Inverse Problems and Imaging* **14**(3), 437–461 (2020)

- [37] Isakov, V.: Inverse problems for partial differential equations. Springer (2017)
- [38] Kärkkäinen, T.: An equation error method to recover diffusion from the distributed observation. *Inverse Problems* **13**(4), 1033 (1997)
- [39] Koelink, E.: Scattering Theory. Radboud University (2008)
- [40] Kouri, D.J., Vijay, A.: Inverse scattering theory: Renormalization of the lippmannschwinger equation for acoustic scattering in one dimension. *Physical Review E* **67**(4), 046614 (2003)
- [41] Kress, R.: Linear integral equations, vol. 82. Springer (2014)
- [42] van Leeuwen, T., Herrmann, F.: A penalty method for pde-constrained optimization in inverse problems. *Inverse Problems* **32** (04 2015)
- [43] van Leeuwen, T., Tataris, A.: A data-driven approach to solving a 1D inverse scattering problem. *AIP Advances* **13**(6) (06 2023), 065310
- [44] Lions, J., Seeliger, M., Mitter, S.: Optimal Control of Systems Governed by Partial Differential Equations: Die Grundlehren der mathematischen Wissenschaften in Einzeldarstellungen, Springer-Verlag (1971)
- [45] Lomas, A., Curtis, A.: An introduction to marchenko methods for imaging. *GEOPHYSICS* **84**(2), F35–F45 (2019)
- [46] Maday, Y., Patera, A.T., Turinici, G.: A priori convergence theory for reduced-basis approximations of single-parameter elliptic partial differential equations. *Journal of Scientific Computing* **17**, 437–446 (2002)
- [47] Mamonov, A.V., Borcea, L., Garnier, J., Zimmerling, J.: Velocity estimation via model order reduction, pp. 752–756 (2022)
- [48] McLean, W.: Strongly elliptic systems and boundary integral equations. Cambridge University Press (2000)
- [49] Mostafazadeh, A.: Transfer matrix in scattering theory: A survey of basic properties and recent developments (2020)
- [50] Natterer, F.: A discrete gelfand-levitan theory. *University of Muester* **3** (1989)
- [51] Pike, E.R., Sabatier, P.C.: Scattering, Two-Volume Set: Scattering and Inverse Scattering in Pure and Applied Science. Elsevier (2001)

- [52] Reed, M., Simon, B.: III: Scattering Theory. Methods of Modern Mathematical Physics, Elsevier Science (1979)
- [53] Rose, J.H.: 'single-sided' autofocusing of sound in layered materials. *Inverse Problems* **18**, 1923–1934 (2002)
- [54] Sen, S., Veroy, K., Huynh, D.B.P., Deparis, S., Nguyen, N.C., Patera, A.T.: "natural norm" a posteriori error estimators for reduced basis approximations. *J. Comput. Phys.* **217**, 37–62 (2006)
- [55] Silvia, M.T., Tacker, E.C.: Regularization of marchenko's integral equation by total least squares. *The Journal of the Acoustical Society of America* **72**(4), 1202–1207 (1982)
- [56] Symes, W.W.: The seismic reflection inverse problem. *Inverse Problems* **25**(12), 123008 (dec 2009)
- [57] Symes, W.W.: A differential semblance algorithm for the inverse problem of reflection seismology. *Computers & Mathematics with Applications* **22**(4), 147–178 (1991)
- [58] Tarantola, A.: Inversion of seismic reflection data in the acoustic approximation. *Geophysics* **49**(8), 1259–1266 (1984)
- [59] Tataris, A., van Leeuwen, T.: A distributional gelfand–levitan–marchenko equation for the helmholtz scattering problem on the line. *Journal of Mathematical Physics* **63**(10), 103507 (2022)
- [60] Tataris, A., van Leeuwen, T.: A regularised total least squares approach for 1d inverse scattering. *Mathematics* **10**(2) (2022)
- [61] Tröltzsch, F.: *Optimal Control of Partial Differential Equations: Theory, Methods, and Applications*. Graduate Studies in Mathematics (2010)
- [62] Vargas, D., Vasconcelos, I., Ravasi, M., Luiken, N.: Time-domain multidimensional deconvolution: A physically reliable and stable preconditioned implementation. *Remote Sensing* **13**(18) (2021)
- [63] Veroy, K., Prud'Homme, C., Rovas, D., Patera, A.: A posteriori error bounds for reduced-basis approximation of parametrized noncoercive and nonlinear elliptic partial differential equations. In: 16th AIAA Computational Fluid Dynamics Conference. p. 3847 (2003)
- [64] Virieux, J., Operto, S.: An overview of full-waveform inversion in exploration geophysics. *Geophysics* **74**, WCC1–WCC26 (2009)

- [65] Wald, A., Schuster, T.: Tomographic terahertz imaging using sequential subspace optimization. Springer (2018)
- [66] Ware, J.A., Aki, K.: Continuous and discrete inverse-scattering problems in a stratified elastic medium. i. plane waves at normal incidence. *The Journal of the Acoustical Society of America* **45**(4), 911–921 (1969)
- [67] Yagola, A., Leonov, A., Titarenko, V.: Data errors and an error estimation for ill-posed problems. *Inverse problems in engineering* **10**(2), 117–129 (2002)